

## **Plant Extract Counteracts Detimental Effects of Cellular Senescence in Human Skin Fibroblasts**

**André Dargen de Matos Branco**

Thesis to obtain the Master of Science Degree in

**Biological Engineering**

Supervisors:

Assoc. Prof. Dr. Johannes Grillari

Dr. Tiago Paulo Gonçalves Fernandes

**Examination Committee**

Chairperson: Prof. Jorge Humberto Gomes Leitão

Supervisor: Dr. Tiago Paulo Gonçalves Fernandes

Members of the Committee: Dr. Nuno Filipe Santos Bernardes

**November 2016**



## Acknowledgements

I would like to start by displaying gratitude towards the research group which accepted me without any constraints, Grillari Labs at the University of Natural Resources and Life Sciences, Vienna. I would like to thank its group leader, Assoc. Prof. Dr. Johannes Grillari, for his openness towards my request to perform the laboratorial work for my master thesis and for accepting to be my official supervisor. His guidance and support were a helping hand during the last six months. Also, I would like to express my gratitude towards Ingo Lämmermann. He has taught me all I have learned while in Vienna and I proudly consider him a mentor. Likewise, all the remaining colleagues who I also consider as good friends, from fellow students to post-docs, were essential for my development as a student and were the best company I could have wished for. Without any of them, this thesis wouldn't have been possible.

In a broader perspective, I would like to express gratitude towards Instituto Superior Técnico for allowing me to perform part of my course abroad. But more importantly, thanking its role in educating me over the course of these last five years.

Finally, I would like to thank my family and friends for their help and support during the process of completing this thesis.



## **Abstract**

Cellular senescence is an integrate part of aging, being one of the main promoters of age-related diseases. Senescence is responsible for encouraging dysfunction, atrophy and chronic inflammation that wear down any tissue with age. However, it exhibits essential benefits, such as suppressing tumor development, which make it more difficult to develop strategies to tackle senescence. When allied with the Papillary-to-Reticular Transition hypothesis, both these cellular events describe the human dermal fibroblast process of aging in skin.

A plant extract, named 1201, was evaluated in challenging fibroblast senescence, by several approaches. Also, more justification for the papillary-to-reticular transition hypothesis was searched.

1201 is the first reported concoction that can go against senescence in three different ways. Firstly, 1201 was shown to delay senescence by interfering in the papillary-to-reticular transition. Secondly, it was proven to cripple the secretory phenotype of senescent fibroblasts. Finally, abilities in selectively eliminating senescent cells were verified. Together, 1201 demonstrated considerable potential in being an all-round force against senescence in skin.

Keywords: cellular senescence; plant extract; senolytic; anti-SASP; papillary-to-reticular transition.



## **Resumo**

Sendo um dos impulsionadores das doenças relacionadas com a idade, senescência corresponde a uma parte indispensável do envelhecimento. Senescência celular é responsável por promover disfunção, atrofia e inflamação crónica, desgastando qualquer tecido com a idade. No entanto, por possuir vantagens fundamentais como impedir o desenvolvimento de cancro, torna-se mais difícil definir uma estratégia que impede artefactos da senescência sem comprometer este mecanismo de defesa contra tumores. Aliada à hipótese da transição papilar a reticular, ambos descrevem o processo de envelhecimento na pele.

Através de várias abordagens, um extrato vegetal, denominado 1201, foi avaliado pela sua possível capacidade de desafiar a senescência de fibroblastos. Ainda, maior fundamentação foi procurada para a hipótese da transição papilar a reticular.

1201 foi descoberto ser o primeiro em conseguir combater a senescência de três maneiras diferentes. Primeiramente, 1201 demonstrou atrasar a senescência, através da interferência na transição papilar a reticular. Em segundo lugar, o fenótipo secretório associado à senescência foi limitado pela sua ação. Finalmente, foram verificadas capacidades em remover, seletivamente, células senescentes. Em conjunto, 1201 comprovou ter um papel inédito contra a senescência em pele.

**Palavras-chave:** senescência celular; extracto vegetal; senolítico; anti-SASP; transição papilar a reticular.



# Contents

<b>1. Introduction.....</b>	<b>1</b>
<b>1.1 Aging.....</b>	<b>1</b>
1.1.1 Theories of Aging.....	1
1.1.2 The Machinery of Aging.....	3
<b>1.2 Cellular Senescence.....</b>	<b>5</b>
1.2.1 Triggers of Senescence.....	5
1.2.2 Senescence Pathways.....	6
1.2.2.1 p53/p21 Axis.....	6
1.2.2.2 p16/pRB Axis.....	7
1.2.3 Characteristics of Senescence.....	8
1.2.3.1 Irreversible Growth Arrest.....	8
1.2.3.2 Morphological Changes.....	8
1.2.3.3 Apoptosis Resistance.....	8
1.2.3.4 Senescence Associated $\beta$ -Galactosidase.....	9
1.2.3.5 Modified Gene Expression.....	9
1.2.3.6 Senescence Associated Secretory Phenotype.....	9
1.2.4 Impact of the SASP.....	10
1.2.5 Bonding Senescence and Aging.....	12
1.2.6 Struggle Against Senescence.....	14
<b>1.3 Skin Aging.....</b>	<b>16</b>
1.3.1 Skin Structure.....	16
1.3.1.1 Papillary vs. Reticular Fibroblasts.....	16
1.3.2 Skin Aging Phenotypes.....	18
1.3.2.1 Papillary-to-Reticular Transition.....	19
<b>2. Materials and Methods.....</b>	<b>21</b>
<b>2.1 Cell Culture.....</b>	<b>21</b>
2.1.1 Cell Lines.....	21
2.1.2 Culture Media.....	22
2.1.3 Cell Cultivation.....	22
2.1.3.1 Cell Thawing.....	22
2.1.3.2 Cell Passage.....	23

2.1.3.3	Cell Seeding.....	23
2.1.4	Stress-Induced Premature Senescence (SIPS) Treatment.....	23
2.1.5	Plant Extract Treatment.....	24
<b>2.2</b>	<b>Proliferation Assay.....</b>	<b>24</b>
<b>2.3</b>	<b>Senescence Associated <math>\beta</math>-Galactosidase Staining.....</b>	<b>24</b>
<b>2.4</b>	<b>BrdU Assay.....</b>	<b>25</b>
<b>2.5</b>	<b>Chemotaxis Assay.....</b>	<b>26</b>
<b>2.6</b>	<b>RNA Quantification.....</b>	<b>28</b>
2.6.1	RNA Isolation.....	28
2.6.2	cDNA Synthesis.....	29
2.6.3	Standard Preparation.....	29
2.6.4	Quantitative PCR (qPCR).....	30
<b>2.7</b>	<b>Protein Isolation.....</b>	<b>31</b>
<b>2.8</b>	<b>Statistical Analysis.....</b>	<b>32</b>
<b>3.</b>	<b>Results.....</b>	<b>33</b>
<b>3.1</b>	<b>1201 Intervenes in the Papillary-to-Reticular Transition.....</b>	<b>33</b>
3.1.1	Treatment Causes Fibroblasts to Maintain the Papillary State.....	33
3.1.1.1	1201 Induces Morphological Changes.....	33
3.1.1.2	Treatment Reduces Fibroblasts' Contact Inhibition.....	34
3.1.1.3	1201 Tips PRT Marker Expression Towards Papillary.....	35
3.1.1.4	Senescence Markers Are Influenced by 1201.....	36
3.1.2	Short-Term Acute Treatment Rules Out Papillary Selection.....	38
3.1.3	1201's Influence Corroborated By Site-Matched Fibroblasts.....	39
<b>3.2</b>	<b>1201 Disrupts Cellular Senescence Through SASP Mitigation.....</b>	<b>43</b>
3.2.1	HaCaT Growth Is Prevented With 1201 Treated Conditioned Media.....	43
3.2.2	Unclear Modulation of Cytokine Secretion by 1201 Treatment.....	46
3.2.3	Paracrine Senescence Wasn't Induced By SASP Conditioned Media.....	47
<b>3.3</b>	<b>1201 Demonstrates Signs of Senescence Eliminating Properties.....</b>	<b>48</b>
<b>3.4</b>	<b>PRT Validation With Site-Matched Fibroblasts.....</b>	<b>51</b>
3.4.1	Site-Matched Fibroblasts Display Distinct Marker Expression.....	51

3.4.2	Papillary and Reticular Fibroblasts Differ in Their Contact Inhibition.....	52
<b>4. Discussion.....</b>		<b>55</b>
<b>4.1 Delaying Cellular Senescence.....</b>		<b>55</b>
4.1.1	Thorough PRT Evaluation Shows 1201 Promotes Papillary Fitness.....	55
4.1.2	Not Only Papillary, But Reticular Fibroblasts Are Targets of 1201.....	58
4.1.3	Isolated Papillary and Reticular Fibroblasts Disperse any Doubt.....	58
<b>4.2 Mitigating Cellular Senescence.....</b>		<b>60</b>
4.2.1	Growth Factors Succumb to 1201's Sphere of Influence.....	60
4.2.2	Restriction of Cytokine Secretion by 1201 Is Uncertain.....	61
4.2.3	Lack of Paracrine Senescence Shrouds Possible 1201 Effect.....	62
<b>4.3 Eliminating Cellular Senescence.....</b>		<b>63</b>
<b>4.4 Confirming Papillary and Reticular Differences.....</b>		<b>63</b>
<b>4.5 1201's Place Towards Senescence.....</b>		<b>64</b>
<b>5. Bibliography.....</b>		<b>65</b>
<b>6. Appendix I.....</b>		<b>73</b>
<b>7. Appendix II.....</b>		<b>74</b>

## Figure and Table Index

<b>Figure 1 –</b> Overview of the pathways that give rise to senescence, their promoters and stimuli. Both senescence axis are represented leading to the irreversible cell cycle arrest. Adapted from van Deursen, J. (2014) <sup>1</sup> .....	7
<b>Figure 2 –</b> Acute vs. chronic senescence. Characterization and consequences of each senescence state. Positive and negative effect of the senescence associated secretory phenotype. Adapted from Childs, B. et al (2015) <sup>2</sup> .....	11
<b>Figure 3 –</b> Key manifestations of senescence that contribute to aging. Destabilization of their surrounding environment is the means senescence uses to promote age-related deterioration. Adapted from van Deursen (2014) <sup>1</sup> .....	13
<b>Figure 4 –</b> Cross-sections of young, middle-aged and old skin (from top to bottom). Hematoxylin and eosin staining facilitates visualization of both the epidermis and the dermis. Aging related changes are noticeable, especially flattening of the rete ridges. Scale bar = 100 µm. Adapted from Giangreco, A. et al (2010) <sup>3</sup> .....	17
<b>Figure 5 –</b> Proposed model for skin aging. Thinning and flattening of the dermis, along with changes in the dermis compartments are some of the reported age-related observations. Adapted from Mine, S. et al (2008) <sup>4</sup> .....	19
<b>Figure 6 –</b> Schematic describing the papillary-to-reticular transition. Age-dependent morphological changes are demonstrated with <i>in vitro</i> images. Scale bar = 100 µm.....	20
<b>Figure 7 –</b> (A) Top view of the ibidi chemotaxis slide, which possesses space for 3 different assays. Each one consists of a central chamber flanked by two reservoirs. (B) Scheme displaying which ports to use when trying to fill each component of the assay. (C) Overall perspective showing the concept of the assay and a cross-section which demonstrates how the chemotaxis is achieved.....	27
<b>Figure 8 –</b> Representative microscopic capture of 1201's morphological effect over the course of five cell passages. Treated and non-treated fibroblasts from donor 2 are shown paired from 3 different time-points. Cells from the 1 <sup>st</sup> passage (left), 3 <sup>rd</sup> passage (middle) and 5 <sup>th</sup> passage (right) display the cumulative influence of 1201. Scale bar = 100 µm.....	34
<b>Figure 9 –</b> Growth curves resulting from proliferation assays. (A) Fibroblasts from donor 1 at PD 38.5, except replicative young at PD 10. (B) Donor 2 derived fibroblasts at PD 24, while the replicative young fibroblasts were at PD 12. Significance is relative to differences between the 1201 treated and the non-treated cells. Data shown as mean ± standard deviation. *p < 0.05; **p < 0.01; ***p < 0.001.....	35
<b>Figure 10 –</b> PRT marker expression levels for both donors. Papillary markers (■) and reticular markers (□) were quantified for cells from donor 1 at PD 36 (A) and from donor 2 at PD 24 (C). For each marker, the 1201 treated sample was normalized by its respective non-treated, represented by a dashed line. Data shown as mean ± standard deviation. n.s. p > 0.05; *p < 0.05; **p < 0.01; ***p < 0.001. ....	36

- Figure 11** – p21 and SNEV expression was quantified for cells from donor 1 at PD 36 (A) and from donor 2 at PD 24 (C). For each marker, the 1201 treated sample was normalized by its respective non-treated, represented by a dashed line. Data shown as mean ± standard deviation. n.s. p > 0.05; \*p < 0.05; \*\*p < 0.01; \*\*\*p < 0.001. ....37
- Figure 12** – Bar graphs quantifying the percentages of β-galactosidase positive cells. (A) Fibroblasts from donor 1 at PD 38.5 and (B) from donor 2 at PD 24. Data shown as mean ± standard deviation. \*\*p < 0.01.....37
- Figure 13** – mRNA levels of reticular and papillary markers of acute 1201 treated and non-treated fibroblasts. (A) HDF Donor 1 at PD 34 and (B) HDF Donor 2 at PD 17 were tested for expression of papillary markers (■), PDPN and NTN1, and reticular markers (□), PPP1R14A and A2M. For each marker, the 1201 treated sample was normalized by its respective non-treated, represented by a dashed line. Data shown as mean ± standard deviation. n.s. p > 0.05; \*p < 0.05; \*\*p < 0.01; \*\*\*p < 0.001.....38
- Figure 14** – Representative images of the visual effects of 48 hours of 1201 treatment on both donors. (Left) – Fibroblasts from donor 1 at PD 34 before 1201 treatment and the post-treatment scenario made up by treated and non-treated cells. (Right) – Similar arrangement, but with cells from donor 2 at PD17. Scale bar = 100 µm.....39
- Figure 15** – Representative microscopic images depicting the effect of 1201 on site-matched fibroblasts from donor A. Scale bar = 100 µm.....40
- Figure 16** – (A) Proliferation assay performed at the 3<sup>rd</sup> passage using 1201 treated and non-treated cells from the papillary cell line of donor A at PD 10. (B) Same assay, except with cells from the reticular population of donor A at PD 8. Data shown as mean ± standard deviation. n.s. p > 0.05; \*p < 0.05.....41
- Figure 17** – Expression levels of papillary (A) and reticular (B) markers. (□) Non-treated and (■) 1201 treated reticular fibroblasts from donor A at PD 8. Both 1201 treated and non-treated reticular samples were normalized by its respective site-matched papillary fibroblast population at PD 5, represented by a dashed line. Data shown as mean ± standard deviation. n.s. p > 0.05; \*p < 0.05; \*\*p < 0.01; \*\*\*p < 0.001.....42
- Figure 18** – Senescence marker expression levels. (A) p21 and SNEV relative mRNA levels. Both 1201 treated and non-treated reticular samples were normalized by its respective site-matched papillary fibroblast population at PD 5, represented by a dashed line. (B) Percentage of positive cells resulting from the β-galactosidase staining procedure of reticular fibroblasts from donor A at PD 8. Data shown as mean ± standard deviation. n.s. p > 0.05.....42
- Figure 19** – (A) HaCaT cell number determination after 8 culture using conditioned media from donor 1 at PD 24. (B) Representative images of the same HaCaT culture at P40 during day 0 and of HaCaT cultured with both conditioned media prepared from non-treated and 1201 treated senescent cells during day 8. (SIPS CM) – Conditioned media from non-treated

senescent cells. (SIPS+1201 CM) – Conditioned media from 1201 treated senescent cells.	
Data shown as mean ± standard deviation. *p < 0.05. Scale bar = 100 µm.....	44
<b>Figure 20 –</b> (A) HaCaT growth cell numbers using conditioned media from donor 2 at PD 15. (B) Representative images of the HaCaT culture at P41 during day 8 under the three conditions for donor 2. (unCM) – Unconditioned Media. Data shown as mean ± standard deviation. n.s. p > 0.05. Scale bar = 100 µm.....	44
<b>Figure 21 –</b> Determination of fibroblast cell number from donor 2 after media conditioning for the first repetition (A) and the second (C). HaCaT cell numbers from the first repetition (B) and the second (D). Data shown as mean ± standard deviation. n.s. p > 0.05.....	45
<b>Figure 22 –</b> Migration profile of three chemotaxis assays. (unCM) – Unconditioned Media (SIPS CM) – Conditioned media from non-treated senescent cells. (SIPS+1201 CM) – Conditioned media from 1201 treated senescent cells. Black paths correspond to cells whose migration ended in the top half of the graph, while grey paths display cells whose tracking finished in the lower half of the graph.....	46
<b>Figure 23 –</b> Representative quantification of BrdU positive cells through flow cytometry. Dark cluster represents BrdU negative events, while grey is associated with BrdU positive events.....	47
<b>Figure 24 –</b> Cell density levels of quiescent (Q0) and senescent (SIPS) cells from donor 1 with and without 1201 treatment. Data shown as mean ± standard deviation. n.s. p > 0.05; *p < 0.05.....	48
<b>Figure 25 –</b> (A) Quantification of cellular density of quiescent (Q0) and senescent (SIPS) fibroblasts from donor 2 treated with 1201 and 1201's solvent, ZEMEA. (B) Representative depictions of the morphological cellular state of the various tested conditions. Data shown as mean ± standard deviation. n.s. p > 0.05. Scale bar = 100 µm.....	49
<b>Figure 26 –</b> Cell density of two repetition trials from quiescent (Q0) and senescent (SIPS) fibroblasts from donor 2 treated with 1201 and 1201's solvent, ZEMEA. Data shown as mean ± standard deviation. n.s. p > 0.05; *p < 0.05; **p < 0.01; ***p < 0.001.....	50
<b>Figure 27 –</b> Determination of mRNA expression levels of papillary (PDPN and NTN1) (A), reticular (PPP1R14A and A2M) (B) and senescent markers (SNEV and p21) (C). Site-matched papillary cell lines (□) and reticular cell lines (■) from three donors were tested. All samples were normalized by donor A's papillary cell line levels. Data shown as mean ± standard deviation. n.s. p > 0.05; *p < 0.05; **p < 0.01; ***p < 0.001.....	52
<b>Figure 28 –</b> Representation of growth curves from every site-matched donor, giving rise to six lifespans.....	53
<b>Figure 29 –</b> Additional migration profiles from two other biological replicates. (unCM) – Unconditioned Media (SIPS CM) – Conditioned media from non-treated senescent cells. (SIPS+1201 CM) – Conditioned media from 1201 treated senescent cells.....	73
<b>Figure 30 –</b> Gradual depicting of the morphological effect of 1201 on cells from donor 2 over 5 passages. Scale bar = 100 µm.....	74
<b>Table I –</b> Primer list of selected genes.....	31

## Abbreviation List

A2M	Alpha-2-macroglobulin
ATM	Ataxia telangiectasia mutated
ARF	Tumor suppressor ARF
BCL-2	Apoptosis Regulator BCL-2
BrdU	Bromodeoxyuridine
CCL	C-C motif chemokine
CCN1	CCN family member 1
CDK1	Checkpoint kinase 1
cDNA	Complementary DNA
CXCL	C-X-C motif chemokine
DDR	DNA damage response
DMEM	Dulbecco's modified eagle medium
dNTP	Deoxynucleoside triphosphate
E2F	Transcription factor E2F
ECM	Extracellular matrix
EDTA	Ethylenediamine tetraacetic acid
ERM	Ezrin/Radixin/Moesin
FBS	Fetal bovine serum
FITC	Fluorescein isothiocyanate
GAPDH	Glyceraldehyde-3-phosphate dehydrogenase
HDM2	E3 ubiquitin-protein ligase
IGF	Insulin growth factor
IGFBP	Insulin growth factor binding protein
IL-1 $\alpha$	Interleukin-1 $\alpha$
IL-2	Interleukin-2
IL-6	Interleukin-6
KBM	Keratinocyte basal medium
KGF	Keratinocyte growth factor
KGM	Keratinocyte growth medium
MMP	Matrix metalloproteinases
mTOR	Mammalian target of rapamycin
NF- $\kappa$ B	Nuclear factor kappa-B
NFW	Nuclease free water
NGS	Next generation sequencing
NTN1	Netrin-1
p16 <sup>INK4a</sup>	Cyclin-dependent kinase inhibitor 2A

p21	Cyclin-dependent kinase inhibitor 1
p53	Cellular tumor antigen p53
pRB	Retinoblastoma protein
PAI-1	Plasminogen activation inhibitor 1
PBMC	Peripheral blood mononuclear cells
PBS	Phosphate buffer saline
PCA	Principle component analysis
PCR	Polymerase chain reaction
PD	Population doubling
PDPN	Podoplanin
PI	Propidium iodine
PPP1R14A	Protein phosphatase 1 regulatory subunit 14A
PRT	Papillary-to-reticular transition
PTEN	Phosphatase and tensin homolog
qPCR	Quantitative PCR
ROS	Reactive oxygen species
SA- $\beta$ -gal	Senescence associated $\beta$ -galactosidase
SAHF	Senescence associated heterochromatin foci
SASP	Senescence associated secretory phenotype
SESC	Selective elimination of senescent cells
SIPS	Stress induced premature senescence
SNEV	Pre-mRNA processing factor 19
TERT	Telomerase reverse transcriptase
TIMP	Tissue inhibitor of metalloproteinase
UV	Ultraviolet
X-Gal	5-bromo-4-chloro-3-indolyl- $\beta$ -D-galactopyranoside

# 1. Introduction

## 1.1 Aging

### 1.1.1 Theories of Aging

All living species seem to be characterized by a limited lifespan. Sources of this constraint normally involve harmful interactions with our environment. Hostile associations between different organisms, such as infections, are one of the numerous nefarious phenomena that seemed to be denying living beings immortality.

However, even with advances in medicine and technology to surpass most environmental risks, aging still persists, apparently creating a boundary to one's lifetime. Many theories have been formulated in an attempt to explain or question the inevitability of the aging process.

A recent attempt was made to organize all the aging theories and to categorize them in a rational way<sup>5</sup>. Altogether more than 300 theories were identified and systematically classified. However, modern theories of aging are typically branded into two of the main categories, the evolutionary theory of aging and programmed aging.

With the formulation of the evolution theory, the concept of natural selection became the cornerstone of biological changes, optimizing species for reproduction and survival. Consequently, aging as a temporal modification was said to be the result of natural selection by Alfred Russel Wallace<sup>6</sup>. August Weismann shared this idea and hypothesized that it supposedly served the purpose of cleansing worn out individuals from a population, after surpassing their peak, so as to not become a burden<sup>7</sup>. This postulation, known as *wear-and-tear*, gave birth to the programmed aging theory, a deterministic model.

The main idea behind this theory states that through natural selection a programmed aging pathway is present in every organism, limiting their lifespan. A semelparous species is the ideal example of this concept, as they experience unavoidable death after reproduction<sup>8</sup>. With the development of modern molecular biology and genetics, more advanced techniques were generated that made it possible to identify and discern different genes, signaling pathways and regulation mechanisms apparently related to aging. One of the model organisms in this field is the nematode *C. elegans*, as most of its genes are homologs of human. While having a mean lifespan of approximately 20 days, which is compatible with research purposes, it seems to be affected by similar aging phenotypes as humans<sup>9</sup>. *C. elegans* is relevant to programmed aging, since many life-extending mutations in different genes have been reported, some of which have doubled their lifespan<sup>10</sup>. Although these observations seem to put this theory on solid ground, there are flaws that have blocked it being accepted over others. Firstly, it's rare for species to reach timepoints where age-related deterioration becomes the cause of death. Thus, the initial argument of the necessity of natural selection to pressure the removal of worn out individuals is void, as it only seems to be applied to an exceptionally low cases of species that actually suffer from age-related decline. Also, the whole foundation of the theory is based on a circular argument. While asserting that the existence of exhausted individuals and their negative influence on

the population is the cause of aging, the origin of this “exhaustion” would also be attributed to aging and so aging becomes both the cause and the consequence in this argument<sup>11</sup>. The need for another approach to this issue is therefore clear.

The evolutionary theory of aging begins to be shaped at the same event as before, the evolution principle. The main difference to programmed aging starts with the definition of natural selection itself. Peter Medawar argued that the pressure from natural selection actually decreases with age, after surpassing the peak of Darwinian fitness<sup>12</sup>. It therefore does not go against evolution itself, by not rejecting claims that natural selection works to promote reproduction and survivability of a species. As natural selection does not have an influencing part in this theory, it is typically classified as a stochastic theory.

All the following developments of the evolutionary theory of aging are based on this lack of natural selection pressure. Medawar contributed to the field with the development of the mutation accumulation theory<sup>6,11</sup>. He stated that mutations in the germ line that have adverse manifestations only later with age would not be efficiently eliminated by natural selection, as its action decreases with age. Affecting the germ line, they would then be allowed to be passed on through generations. Thus, without the regulatory action of natural selection, age-causing mutations would accumulate and manifest in the known aging process. Only until more organisms begin to reach older age, would the peak of an individual move to higher ages and cause natural selection to widen its effect and henceforth remove the negative mutations. Another expansion to this stochastic theory was made by Denham Harman. He attributed the blame of aging to chronic toxic levels of reactive oxygen species (ROS) in later periods of life<sup>13</sup>. To some extent the equilibrium of ROS production and elimination is altered and consequently their excess causes oxidative stress and damage. Although oxidative stress isn't the cause of all age-related phenotypes, it is definitely an important piece to the global theory. Recently, the free radical theory has been questioned, given the observations that while the increase of ROS is correlated with age, deletion or overexpression of enzymes that control ROS levels, such as peroxidases, catalases or superoxide dismutases, don't cause the expected extension or reduction of the lifespan<sup>14,15</sup>. Thomas Kirkwood also added his own extension to this theory called Disposable Soma<sup>16</sup>. He hypothesized that an organism will optimize the distribution of available energy between different areas of cell activity depending on its priorities. By allocating more energy into germ cells to ensure that high-energetic processes like DNA repair and proofreading are well kept and saving energy in somatic cells by not energetically funding these to the same degree, mutation-free reproduction is guaranteed<sup>6,11</sup>. The obvious disadvantage that arises is the accumulation of mutations that surpassed the under-funded DNA repair mechanisms with time, thus leading to a cumulative aging phenotype. A last branch of the evolutionary theory to be mentioned here is the Antagonistic Pleiotropy, formulated by George Williams<sup>17</sup>. It describes the existence of genes that have effects depending on the age of the organism. They start by having a beneficial effect in younger time periods, while the natural selection pressure is strong, but then become adverse once the organism reaches an advancing age<sup>6,11</sup>. These specific genes would then be responsible for the aging phenotype and its associated diseases, being able to cause harm without the consequence of being selected and removed.

All the above mentioned branches of both the evolutionary theory of aging and the programmed aging theory are not able to explain the concept of aging to a full extent, but simply describe a piece of the puzzle. Combining these pieces to achieve a joined and united theory of aging would be an ambitious but important goal for this field.

### **1.1.2 The Machinery of Aging**

Studying and understanding aging are pivotal to someday achieve in preventing or delaying it. All the macroscopic effects and consequences of aging, categorized as age-related diseases, should be able to be broken down to the building blocks of any organism, the cellular level. Any dysfunction found at this tier ought to explain higher and more complex aging phenotypes, such as osteoarthritis or Alzheimer's disease.

All cellular processes can suffer from aging-related alterations. This all-around sphere of influence is the characteristic which makes aging so apparently inevitable and so difficult to stand against. Proof of this can be shown by observing main cellular tasks such as protein synthesis, metabolism and replication.

Division of cells, be it through mitosis or meiosis, can become either a cause or a victim of aging. This occurrence deals greatly with the genome, as it needs to replicate the DNA and successfully segregate it to the rightful daughter cell. Consequently, random genomic mutations occurring over time are spread through cellular generations if the respective repair mechanisms are bypassed. Also, these same mutations can eventually alter the replication process itself, if affecting genes encoding proteins responsible for this process, such as DNA polymerases or helicases. Here replication falls victim to age-deterioration, through genomic instability. However, replication can also become an aging accomplice. The DNA duplication stage of replication, or the S phase, has an intrinsic fault. The end-points of each chromosome cannot be replicated due to problems that arise when duplicating the end of the lagging DNA strand. Therefore a limited part of each chromosome is truncated with each replication. Thus, the existence of repetitive and non-coding sequences, named telomeres, at the end of each chromosome is required. These have been found to be shortened throughout the lifespan<sup>18</sup>. If telomeres aren't elongated, once a certain age has been reached, the replication process will start truncating critical and encoded sequences of DNA, leading again to age-deterioration<sup>19</sup>. This corresponds to the other perspective, where the division of cells itself fosters aging.

Cell metabolism has been early on connected with aging. Mitochondria, who are responsible for cellular respiration, are the organelles with the most contact with reactive oxygen species. Following the original logic behind the free radical theory, eventual mitochondria dysfunction due to cumulative oxidative stress over time demonstrates how changes in metabolism can bring about aging. Although the role of ROS is now being questioned, the relevance of the state of mitochondria towards aging is clear<sup>20</sup>. Mitochondria integrity has been compromised with mutations in its corresponding mitochondrial DNA, resulting in an accelerated aging phenotype<sup>21,22</sup>. Another link between metabolism and aging is

present in the nutrient sensing pathways. Variations in networks such as the insulin growth factor 1 (IGF-1) or the insulin signaling pathway tend to influence the lifespan<sup>20</sup>. By knocking out a downstream target of IGF-1, namely the insulin growth factor type 1 receptor, lifespan in mice was extended<sup>23</sup>. This demonstrates that similarly to replication, cellular metabolism has inherent issues that intrinsically and without external stimuli promote aging.

Finally, the clutches of aging can also reach the protein synthesis. Like an assembly line, the biosynthesis of proteins is long and dependent on various types of cellular equipment, such as polymerases, ribosomes, and chaperones. This characteristic makes it especially vulnerable, considering that any sort of problem at any stage will compromise the mainly linear chain of protein bioproduction. Yet again, genetic mutations are the common culprit and their occurrence will cripple any newly formed proteins in the future. Thus, transcription and translation will highly depend on good DNA repair mechanisms. However, proteostasis also includes a functional post-synthesis and maintenance program for formed proteins. From folding to proteasomal degradation, even after translation proteins need to be overseen. Owing to several layers of protein structure and possible future denaturing stresses, folding is necessary and conducted by chaperones. Overexpression of these proteins was shown to increase the lifespan over several different animal models<sup>24,25</sup>. After proteins have done their job or have suffered denaturing, proteolysis has to prevail and remove these unwanted by-products. May it be through autophagy or the ubiquitin-mediated proteasome pathway, misfolded or denatured proteins are removed. These have been found to degrade with age and their modulation, be it inhibition or overexpression, has respectively increased or diminished the lifespan<sup>26,27</sup>.

Merely by observing some main cellular functions the permeability of aging is visible. Nevertheless, the building blocks of aging have also shown themselves. Telomere attrition, genomic mutations and the loss of protein homeostasis are just some of the perpetrators previously discussed. Each can be traced or be held accountable for at least one age-related disease. Certain mutations have given rise to an earlier manifestation of aging phenotypes, leading to premature aging<sup>28</sup>. These disorders are termed progeroid syndromes and were essential for human studies of aging. One of the most known syndromes is the Hutchinson-Gilford progeria syndrome and is caused by a point mutation of the gene encoding a protein called prelamin A. This mutation hinders the maturation of prelamin A to lamin A, which is normally part of the nuclear lamina<sup>29</sup>. This leads to abnormal nuclear structure and accelerated aging. Protein aggregates that form due to failed proteolysis can be also linked to age-related disorders. Both Alzheimer's and Huntington's disease are consequences of accumulation of their respective protein aggregates<sup>30,31</sup>. Bearing in mind that age-related disease is just a combination of these simpler cellular manifestations, these cellular hallmarks of aging are key to discerning, preventing and curing their more complex and downstream counterparts.

One hallmark that hasn't been mentioned until now is cellular senescence. Being the main aging hallmark dealt here, it will be discussed next in detail.

## 1.2 Cellular Senescence

On a simple note, cellular senescence was described as being an irreversible growth arrest. This definition arose from observing that normal cells don't proliferate indefinitely *in vitro*, also termed the Hayflick limit<sup>32</sup>. This humble description, by itself, had considerable implications at the time. Firstly, it meant the existence of a terminal end-point for cellular replication. Thus, it went against the previous paradigm, developed by Alexis Carrel, that cells cultured *in vitro* were immortal<sup>33</sup>. Secondly, with knowledge about cancer, another implication for senescence was hypothesized. If compared, cancerous and senescent cells are both abnormal cellular states, but are on different ends concerning cell proliferation. Therefore, cellular senescence was insinuated and later proven to have the role of a tumor-suppressor<sup>34</sup>. Whenever a cell would be on the brink of transforming into an indefinitely dividing cancer cell, the senescence program would be activated and thus halt any further replication and growth. Finally, by following the rationale that each cell will eventually suffer from senescence, any mechanism related with renewal of tissue in a multicellular organism would be crippled with time, a characteristic of aging.

Only with the first formal definition of senescence, a connection between it, cancer and aging is already to be seen. Nonetheless, cellular senescence has currently a more robust and extensive description, which will begin here with its sources<sup>35</sup>.

### 1.2.1 Triggers of Senescence

The first type to be mentioned here is the replicative senescence<sup>36</sup>. This kind was demonstrated by Hayflick's experiment, where the consecutive population doublings force the cells to gradually degrade their telomeres until critical DNA is reached<sup>20</sup>. This cause and effect was proven when the telomere attrition problem was shown to be sidestepped with the help of telomerase reverse transcriptase (TERT)<sup>37</sup>. This enzyme, when overexpressed in normal human cells, prevented telomere shortening and accordingly its effect, the replicative senescence. Besides protecting chromosomes against the end-replication problem, telomeres also avoid unwanted DNA damage response (DDR) as chromosome ends resemble double stranded breaks. They achieve this by their inherent cap structure, called T-loop<sup>38</sup>. This latter function, if disrupted, can be the source of replicative senescence. When telomeres are shortened past their capabilities to avoid the DDR, DNA damage checkpoint kinases, such as ATM or CDK1 and 2, cause cell-cycle arrest<sup>39,40</sup>. If this signaling is permanent, the cell has reached replicative senescence.

Another category of senescence is the DNA-damage induced senescence<sup>41</sup>. Based on the same DDR network, this type of senescence is triggered by actual damage to the genome. Instead of resembling DNA damage, external stresses cause real harm and result in this kind of senescence. From ionizing radiation to reactive oxygen species, these agents have been even shown to cause premature senescence when used in excess<sup>42,43</sup>.

The final type to be presented here is oncogene-induced senescence<sup>44</sup>. As a general tumor-suppressive mechanism, this form of senescence serves as a barrier against cancer and is therefore induced by early signs of it. Oncogenes are genes that if mutated have the ability to transform normal cells into their hyperproliferative counterparts. Numerous oncogenes are made up of participants of mitogenic signaling pathways. Any irregular high or chronic mitogenic signal prompts this senescence. This was first demonstrated by expression of the oncogenic state of RAS, a transducer of mitogenic signals, in human fibroblasts<sup>45</sup>. Any excess of downstream targets from the RAS signaling pathway or loss of mitogenic signal dampeners, such as PTEN, have been proven to be responsible for activating this type of senescence<sup>46,47</sup>.

Having identified the triggers of senescence, the mechanistic pathways that are behind this new cellular state should be elucidated.

## 1.2.2 Senescence Pathways

Two main pathways are normally acknowledged when discussing senescence, the p53/p21 and the p16<sup>INK4a</sup>/pRB<sup>48</sup>. Each type of senescence will, depending on its causing signaling effectors, converge and eventually promote one of these pathways.

### 1.2.2.1 p53/p21 Axis

The p53/p21 axis revolves mainly around the tumor-suppression protein and transcription factor p53. Depending on the state of p53, either phosphorylated, degraded, inhibited or promoted, senescence can be either promoted or avoided. In ordinary cellular conditions, p53 levels are controlled by the E3 ubiquitin-protein ligase (HDM2). As its nomenclature infers, HDM2 binds to p53 and promotes ubiquitination, causing the activation of the ubiquitin-proteasome pathway and p53's subsequent degradation<sup>49</sup>. However, the binding event by itself is enough to inhibit p53's transcriptional activity<sup>50</sup>. To activate this pathway, the aim is always to achieve stable levels of activated p53. One way to accomplish this is through the induction of the tumor-suppressive protein ARF. Unusual mitogenic signals, one of the causes of senescence, is responsible for ARF promotion<sup>50</sup>. The gain in ARF levels results in a sequestration of HDM2 and its blocking activity towards p53, allowing p53's stabilization and activation. ARF binds directly to HDM2 and localizes it to the nucleolus<sup>51</sup>. Another option exists in response to another source of senescence, DNA damage. DNA double strand breaks, consequences of telomere attrition or exogenous DNA damage, activate Ataxia telangiectasia mutated (ATM). Functional ATM causes phosphorylation of p53, releasing p53 from HDM2's grip<sup>52</sup>. With p53 free, activated and stabilized, targets of its transcriptional activity are affected. One of these includes p21, a crucial cyclin-dependent kinase inhibitor<sup>53</sup>. By hindering the cyclin-dependent kinases, which are determinant cell cycle regulators, senescence is consequently induced.

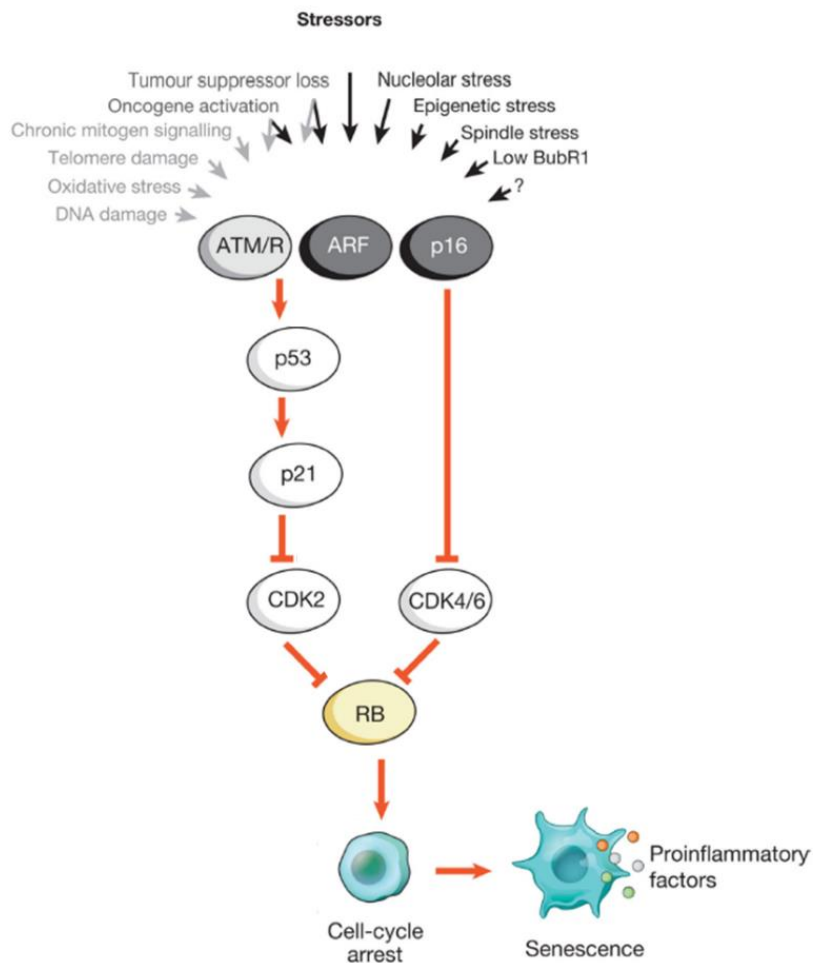


**Fig. 1** – Overview of the pathways that give rise to senescence, their promoters and stimuli. Both senescence axis are represented leading to the irreversible cell cycle arrest. Adapted from van Deursen, J. (2014)<sup>1</sup>.

### 1.2.2.2 p16/pRB Axis

The other side of the coin is the p16<sup>INK4a</sup>/pRB axis. Here the main focus goes to the retinoblastoma protein (pRB), also a tumor suppressor protein. Similarly to the former pathway, the state of pRB controls the outcome of the axis. When the cell is acting normally, pRB is in its phosphorylated and deactivated condition<sup>54</sup>. This post-translational modification is imbued by cyclin-dependent kinases. To keep this from happening and promote senescence, another cyclin-dependent kinase inhibitor has to be recruited, namely the cyclin-dependent kinase inhibitor 2a or p16<sup>INK4a</sup>. Activation of pRB prevents cell proliferation by halting the action of E2F, a transcriptional factor responsible for enlisting genes that control cell-cycle progression<sup>36</sup>. This is achieved by pRB with its ability of creating senescence associated heterochromatin foci (SAHF)S<sup>55</sup>. These foci are structures of tightly packed DNA that silence genes, in this case those associated with growth and proliferation. A considerable difference between this and the p53/p21 pathway is the irreversibility of each respective senescent state. While senescence induced by the p53/p21 pathway can be reversed if the network is inactivated, the same cannot be said for the p16<sup>INK4a</sup>/pRB axis. Disruption of any element of the

p16<sup>INK4a</sup>/pRB pathway does not rescue cellular growth and proliferation<sup>56</sup>. The irreversibility is due to the SAHFs, as they become independent and self-maintaining after their formation<sup>55</sup>.

Both apparently independent pathways are actually intertwined to a certain extend. As both p21 and p16<sup>INK4a</sup> are cyclin-dependent kinases inhibitors, they have the same effect towards pRB activation. Although both these pathways are considered to be the main culprits of senescence, there are reports of possible independent pathways that culminate in senescence<sup>57</sup>.

With both the causes and subsequent pathways explored, a full characterization of senescence is missing.

### **1.2.3 Characteristics of Senescence**

#### **1.2.3.1 Irreversible Growth Arrest**

Irreversible growth arrest maintains its position as the main feature of senescence. It is the consequence of both main pathways and ensures its assumed role of a tumor-suppressive mechanism. The interruption of the cell cycle causes stagnation in the G1 phase, thus not entering the DNA replication phase, but the cell still remains metabolically active<sup>42</sup>.

#### **1.2.3.2 Morphological Changes**

Besides not growing, senescent cells usually suffer from morphological changes. An increase of volume, occasionally even a twofold rise, is observed when comparing certain senescent cells to their proliferative counterparts<sup>58</sup>. Cytoskeleton reorganization is also promoted with age, giving rise to flattened and irregular shapes, characteristic properties of senescent cells<sup>59</sup>.

#### **1.2.3.3 Apoptosis Resistance**

The relationship of senescence with another terminal cell stage, apoptosis, is another characteristic to be pointed out. Senescent cells tend to express some gained apoptotic resistance<sup>60</sup>. This was shown when a fibroblast cell line was exposed to apoptotic stimuli, such as actinomycin D, cisplatin or UVB irradiation. Replicative young cells underwent, as expected, apoptosis. On the other hand, the senescent cells didn't, falling later victim to necrosis<sup>61</sup>. This resistance was shown to be possibly related to an up-regulation of the anti-apoptotic protein BCL-2<sup>62</sup>. Here, instead of altering the mean of cell death, senescent cells were actually encouraged to survive when facing apoptotic agents<sup>63</sup>. Apoptosis and senescence have the same intrinsic objective, to prevent damaged cells from being detrimental to their organism, such as cancer development. However, the means they use to achieve this protection differ. Apoptosis leads to cell death, whereas senescence keeps cells alive, mainly by inflicting growth arrest. Each approach can be preferable depending on the conditions of each issue. Considerable apoptosis or cell death would lead to tissue voids, while considerable senescence would

still keep the tissue structure intact, although dysfunctional. Many other arguments can be given to justify one over the other. In the end, senescence and apoptosis seem to complete their objectives and could even be considered complementary cell fates<sup>60</sup>. Nonetheless, when one avenue is chosen, namely senescence, it becomes difficult to trigger the other, thus displaying apoptotic resistance.

#### **1.2.3.4 Senescence-Associated β-Galactosidase**

Senescent cells were discovered to express considerable amounts of β-galactosidase<sup>64</sup>. This specific characteristic was taken advantage of and turned into one of the most known markers for senescence. While being an enzyme with an optimal pH of 4.0-4.5, its detection is usually done at pH 6.0, with the use of a substrate named X-gal<sup>65</sup>. This constricted detection condition, pH 6, ensures that only β-galactosidase activity exclusive to senescent cells is determined. Currently, it is known that this senescence associated β-galactosidase (SA-β-gal) is actually lysosomal β-galactosidase<sup>66</sup>. Consequently, it follows an increase of lysosomal activity. Unfortunately, a surge in lysosomal activity is not restricted to senescence. High levels of β-galactosidase are also present in normal osteoclasts<sup>67</sup>. Quiescent cells kept in culture for longer periods of time can also suffer an increase in lysosomal β-galactosidase<sup>68</sup>. Yet its ease of detection and the possibility to perform histochemical staining make it very desirable. Improvements can also be implemented to avoid some β-galactosidase detection that is not related with senescence, such as performing the staining in non-confluent conditions. Although being an accepted and routine marker, at the present time, results from SA-β-gal staining should be processed with care as the implications taken from it might not represent reality<sup>68</sup>.

#### **1.2.3.5 Modified Gene Expression**

Somewhat implied by the existence of senescence-activating pathways, is that senescent cells suffer from altered gene expression. As a consequence of the transformation to the senescent state, the senescence-causing stimuli force cells to change their normal gene patterns. However, modifications don't occur only with genes related to cell cycle progression. A number of attempts were successful in identifying other deviations in gene expression of senescence cells<sup>69,70</sup>. A considerable portion of these changes that are unrelated with cell cycle progression are responsible for another characteristic of senescent cells, the senescence associated secretory phenotype (SASP).

#### **1.2.3.6 Senescence-Associated Secretory Phenotype**

Consequence of altered gene expression, is the gain of a novel secretory front. With this feature, senescent cells acquire a powerful influence on their surroundings. The elements of the SASP, termed SASP factors, include a mixture of cytokines, chemokines and growth factors<sup>71,72</sup>. Organization of these can be done in three different categories, soluble signaling elements, secreted proteases and secreted insoluble components<sup>73,74</sup>.

Some of the soluble signaling elements include some of the members of the interleukin family. Interleukins are cytokines with numerous functions, depending on the interleukin element considered.

Both, IL-1 and IL-6, are upregulated in the secretome of senescent cells<sup>71,75</sup>. These signaling elements are proinflammatory cytokines and their chronic secretion due to the senescent state will overstimulate the immune system and contribute to an excessive inflammatory environment<sup>76</sup>. One highlight to be mentioned is IL-1 $\alpha$ , since it aggravates and reinforces the SASP due to a positive feedback loop. The feedback network depends on activation of NF- $\kappa$ B, a transcription factor involved in cellular responses, such as cytokine production<sup>77</sup>. These SASP factors can also influence one another. IL-1 $\alpha$  can also positively affect IL-6 levels, as was shown when interference in IL-1 $\alpha$  expression in senescent cells considerably reduced IL-6<sup>78</sup>. Many chemokines are also part of this category, of which the CCL and CXCL families are to be emphasized<sup>73</sup>. Chemokines are a type of cytokine, which can generate chemotaxis, a movement of a cell in response to a chemical stimulus. Thereby these SASP factors strengthen the chronic immune stimulation, by luring and attracting members of the immune system. The last significant group of soluble signaling elements to be stated here are a number growth factors. The IGF pathway is very much part of the SASP, represented in senescent cells by the insulin growth factor binding proteins (IGFBPs)<sup>71</sup>. These proteins augment or repress the activity of insulin growth factors (IGFs), depending on the IGFBP in question. More representative growth factors include connective tissue growth factor and the colony-stimulating growth factors<sup>71</sup>.

The next class of SASP factors, named secreted proteases, is significantly responsible for the SASP's ability to alter the surrounding ECM and have influence over tissue organization. A number of matrix metalloproteinases (MMPs) are part of the SASP, being able to degrade a considerable amount of extracellular matrix proteins<sup>73,79</sup>. Elements of the plasminogen activation pathway are also present in the SASP. Tissue plasminogen activation is a protein with an ability to breakdown clots. Both this protein and its respective inhibitor (PAI-1) have altered expression profiles in senescent cells<sup>80</sup>. Considering its function, the destabilization of the plasminogen activation pathway through development of the SASP would surely have implications in wound healing.

The remaining of SASP factors coalesce into the extracellular insoluble molecules. Fibronectin, an ECM modulator, can interact with integrins and so intervene in cellular adhesion, migration and growth<sup>81</sup>. Its expression was found increased in senescent cells, showing once again the SASP's capacity of influencing their surrounding environment<sup>82</sup>.

With these factors, a cell expressing the SASP has the all tools to exert a significant impact over its extracellular surroundings. Yet, the SASP is not universal in its expression, as it tends to be cell-type specific<sup>44</sup>. But when thinking overall of senescence, the main notions that surround it are usually related with crippling deterioration, gradual weakening, loss of function and atrophy. The SASP seems to be the only characteristic of senescent cells which transmits the idea of a more active state of being.

#### 1.2.4 Impact of the SASP

Considering the signaling nature of the SASP, with cytokines and chemokines at its disposal, senescence should be a target of the immune system. This strengthens the idea that the SASP has an

actual purpose, serving as a lighthouse for immune cells to converge and remove senescence cells. The attraction of immune elements by senescent cells have been shown, due to the SASP's inflammatory ability<sup>83</sup>. Its clearance has been also observed to be achieved by several participants of the immune system, from natural killer cells to T cells<sup>84,85</sup>. So the SASP, at least partly, actually contributes to the removal of senescent cells after they have prevented neoplastic transformation. Nevertheless, the immune system is also known to suffer from age-related deterioration and therefore the immunoclearance of senescent cells will decline<sup>86</sup>. This allied to the very self-sustainable nature of senescence, makes accumulation of senescent cells with age very probable.

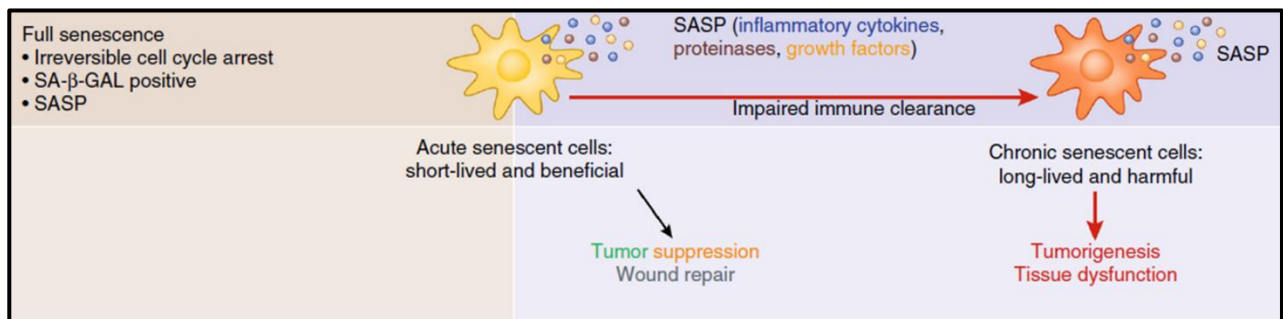


**Fig. 2** – Acute vs. chronic senescence. Characterization and consequences of each senescence state. Positive and negative effect of the senescence associated secretory phenotype. Adapted from Childs, B. et al (2015)<sup>2</sup>.

Wound healing has an odd response when affected by aging. Older individuals suffer only from a delay, whereas no deterioration is observable<sup>87</sup>. Nevertheless, delayed wound healing is an aging phenotype. Senescence and wound healing have a suspected link, the SASP. Integrated in the SASP are most of the components required for wound healing, spearheaded by elements such as matrix metalloproteinases (MMPs). Surprisingly, senescence was found to actually to be part of the normal wound healing mechanism<sup>88,89</sup>. This discovery provided a new function for senescence and to some extent justified the existence of the SASP, a phenotype that previously seemingly possessed only adverse effects. On the other hand, this senescence is moderately different than what has been previously described. Specifically, myofibroblasts were found out to suffer from senescence when an injury occurred. An extracellular matrix protein, CCN1, through integrin signaling, gave rise to ROS-mediated senescent cells<sup>88</sup>. These would then make use of their matrix altering and growth SASP factors to, at the same time, prevent fibrosis in the wake of tissue renewal and promote growth for wound healing. After completing their job, these senescent myofibroblasts would then be cleared, using the chemoattractants to signal the immunoclearance. This event has been termed, acute senescence, as only a small number of specified cells become senescent for a short period of time until there are cleared by the immune system<sup>1</sup>. An organized, queued and limited form senescence is what acute senescence represents.

A powerful ability of the SASP is called paracrine senescence or bystander senescence. Using the SASP, a senescent cell has also the capability to induce senescence onto others. This isn't a new source by definition, since to be able to encourage this kind of senescence, at least one senescent element must have already formed. Two studies performed similar experiments, but reached different

conclusions. One stated that merely a coculture led to bystander senescence and therefore it was assumed to be a cell-to-cell contact event<sup>90</sup>. This paradigm was shifted when the other study demonstrated the success of an experiment involving only conditioned media from senescent cells. It showed that no cell-to-cell contact was actually needed, but simply the secreted SASP factors<sup>91</sup>. Thus another positive feedback loop is developed, reinforcing senescence after its appearance. It seems senescence can be very self-supporting once it's established.

A contradictory finding related to the SASP has linked senescence to tumor-promotion. This goes against the main purpose of senescence, tumor-suppression. It sounds more predictable after, noticing that some SASP factors belonging to the CXCL chemokine family, such as CXCL1, are also known as growth-regulated proteins or growth-related oncogenes. These have been implicated in tumor growth and metastasis<sup>92</sup>. Tumorigenesis and hyperproliferation were induced in epithelial cells by senescent cells. Between direct senescent cell contact and the SASP itself, half of the stimulation was attributed to the latter<sup>93</sup>. Other cancer characteristics, such as cell migration and invasion have been also traced back to the action of SASP factors<sup>94</sup>. Although fighting against malignant transformation of itself, senescence cells in truth encourage neighboring pre-malignant cells to grow, gain aggressiveness and form tumors. Although a clashing concept against the general idea of senescence, this side-effect only solidifies its presence in the Antagonistic Pleiotropy dogma. Only in an aged organism, who passed natural selection pressure, is the scenario of senescent cells neighboring pre-neoplastic cells possible. Merely in this case, is this adverse SASP effect to be observed.

### **1.2.5 Bonding Senescence and Aging**

Now with a more comprehensive description and characterization of senescence, its connection with aging should be reviewed. Previously, some minor associations were implied, but although senescence seems to naturally fit into an aging hallmark, it should be rightfully justified.

From the theoretical point of view, for senescence to be part of aging, it should have a place inside the theories of aging. An initial approach would seem that due to its pre-defined pathways senescence would belong to the programmed aging field, especially when considering telomere attrition, a biological and molecular clock. However, the remaining triggers of senescence are related to a more sporadic and stochastic decay over time, which is more distinctive of the evolutionary theory of aging. Senescence's rightful place seems to be clear when observing some of the consequences of its characteristics. While contemplating its features, senescence seems to have both detrimental and beneficial effects to an organism. These contrary effects are not randomized over the timescale, but follow an order. Initially, senescence is stimulated to fulfill its role as a tumor-suppressive mechanism, functioning for the benefit of the organism. Then, adverse consequences of senescence appear, such as dysfunction, atrophy and chronic inflammation. The side-effects succeed the initial positive value of senescence. This behavior follows the premises of the Antagonistic Pleiotropy and therefore senescence is one of the main examples given for this branch of the evolutionary theory of aging<sup>44</sup>.

In the practical perspective, numerous steps have been made to solidify senescence as a mechanism of aging. However, senescence started with a step backwards towards this goal. Initially, several studies demonstrated an inverse correlation between the onset of senescence *in vitro* and the donor age, working in favor of linking replicative senescence and aging<sup>95,96</sup>. But based on the argument that the cell culture and biopsy conditions were not controlled and the donor health state was hardly specified, an extensive study was conducted with 124 donors, where no significant correlation was found between donor age and the replicative lifespan *in vitro*<sup>97</sup>. In contrast, the approving evidence for the association between senescence and aging, both in *in vitro* and *in vivo* conditions, is growing.

With senescence-related markers such as p16<sup>INK4a</sup> levels and SA- $\beta$ -gal, the existence of senescent cells could be tracked in all kinds of tissue<sup>98</sup>. Thus temporal studies could be conducted to monitor the senescent population with age. After surveying several tissues, accumulation of senescent cells through aging is clear<sup>99,100</sup>. This does not establish a causal relationship between senescence and aging. However, a positive correlation between the two, means that an accumulation of the adverse effects of senescence happens with age, which suggests an involvement of senescence with age-related diseases.

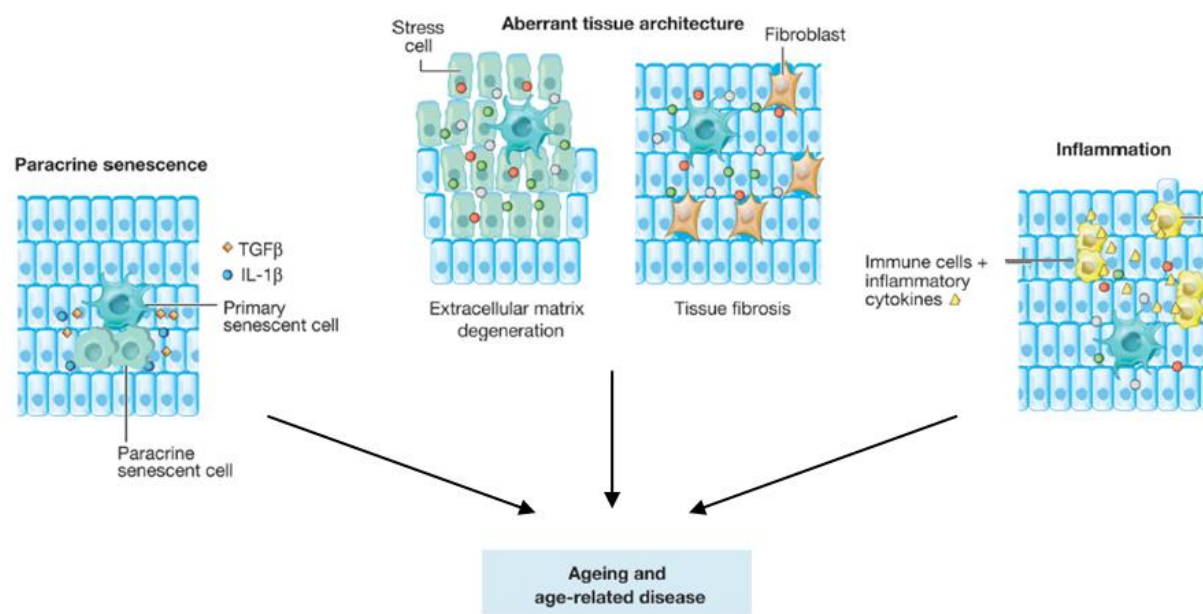


**Fig. 3 – Key manifestations of senescence that contribute to aging. Destabilization of their surrounding environment is the means senescence uses to promote age-related deterioration. Adapted from van Deursen (2014)<sup>1</sup>.**

One of the drivers of aging and age-related diseases is chronic inflammation and this association has brought about the term “inflammaging”<sup>101</sup>. The constant lingering of proinflammatory signals causes chronic strain on the immune system. Nevertheless, in chronic inflammation the actual level of the signals is never as high as in acute inflammation<sup>102</sup>. The comparison of centenarians has revealed that both frail and healthy centenarians have greater pro-inflammatory signals than young individuals, correlating increased inflammatory profile with age<sup>103</sup>. But the difference between both centenarians was a higher amount of anti-inflammatory elements in healthy than in frail<sup>104</sup>. It seems that

what really drives inflamming is actually the surplus of proinflammatory signals in the balance of both sides. This aging phenotype is connected with several age-related diseases, including Alzheimer's, atherosclerosis and diabetes<sup>105</sup>. An important and chronic source of proinflammatory signals is the SASP<sup>102,106</sup>. With numerous cytokines and chemokines at their disposal, the secretome of senescent cells fulfills the requisites of being a significant contributor of inflamming<sup>73</sup>.

An overall approach to connect aging with senescence was tried using a transgenic mouse model. A BubR1 deficient mouse was developed as a model for premature aging. BubR1 is a mitotic checkpoint protein required for cell-cycle progression, and thus its absence causes a progeroid mouse model. With this model, the role of senescence was observed through manipulation of the p16<sup>INK4a</sup> encoding gene. After p16<sup>INK4a</sup> inactivation, substantial and overall enhancements were verified. Lifespan increase, sarcopenia attenuation, maintenance of the subdermal adipose tissue are some of the benefits reaped from inhibiting p16<sup>INK4a</sup>-dependent senescence<sup>107</sup>. A posterior improvement to this experimental design was made to assess a different tactic. Firstly, natural aging mice were used instead of a premature progeroid model. Secondly, the effect of clearance of p16<sup>INK4a</sup>-positive cells after accumulation was studied, using a transgene named INK-ATTAC. This approach was based on a similar transgene used for a different purpose, termed FAT-ATTAC<sup>108</sup>. INK-ATTAC, when in contact with a synthetic drug called AP20187 causes the dimerization of a membrane-bound myristoylated FK506-binding-protein-caspase 8 fusion protein (FKBP-Cas8). Consequently, caspase-mediated apoptosis is triggered. As it is also fused with the minimal fragment of the promoter of the *Ink4a* locus, this transgene is only expressed in p16<sup>INK4a</sup>-positive cells<sup>109</sup>. Multi-organ improvement was observed after removal of p16<sup>INK4a</sup>-positive cells, attributing the blame of age-related deterioration to these type of cells<sup>110</sup>. However, one issue to point out is the need for caution when assessing these results, as p16<sup>INK4a</sup>-positive cells aren't necessarily senescent cells. While being a marker, although an important one, it doesn't fully amount to a senescent state. Nevertheless, these series of studies shed no doubt over an involvement of senescence in aging, while possibly even demonstrating it to be a major part of the aging process. Its clearance was likewise proven to be a formidable method for a potential anti-aging therapy.

### 1.2.6 Struggle Against Senescence

With senescence having earned its place in the field of aging, its prevention, delay or removal has made it a novel aging therapeutic target<sup>111</sup>. Multiple fronts exist when trying to tackle senescence. While there might be multiple paths for this purpose, the true therapies will need to survive the funnel that separates the theoretically conceivable from the practically possible.

A thinkable approach could be to challenge senescence at the beginning of the network, before the senescence state has been reached. It would involve either inhibiting or knocking down the senescence pathways or delaying the journey to senescence. Gene therapy to disrupt senescent pathways is a theoretical avenue of avoiding senescence. However, this type of approach has several issues. Gene altering therapies have considerable potential and already some success. Nevertheless,

after undesirable side-effects from the used vector shaped into a form of leukemia in some patients, gene therapy was stained with distrust<sup>112</sup>. Also, the concept of inactivating a senescent pathway would cost the organism an evolutionary conserved tumor-suppressive mechanism. The consequences are shown by the embodiment of this concept, the study involving p16<sup>INK4a</sup> inactivation in BubR1 progeroid mice. Although age-related phenotypes were attenuated, more tumors were found in mice who had suffered the p16<sup>INK4a</sup> inactivation<sup>107</sup>. So to develop an effective anti-senescence therapy, its antagonistic pleiotropy should be considered. An alternative tactic consists in delaying the onset of senescence, meaning the maintenance of cellular health and fitness. Dietary restriction has shown to be an important strategy to hinder the appearance of senescence, by reducing metabolic stress<sup>113</sup>. Also certain compounds have been reported to improve cellular well-being, thus delaying the reach to senescence<sup>114</sup>. Overall, senescence seems to be unavoidable, as evading it opens the door to another nefarious disease, cancer.

With the senescence-preceding options exhausted, the tide turns towards a post-senescence scenario. Senescence cells have their dark side mostly represented by the SASP<sup>73</sup>. It seems reasonable to have SASP-oriented strategies. A screening of compounds led to the discovery of glucocorticoids as SASP suppressors. These were observed to act over the transcriptome and consequently reduced mRNA levels of numerous SASP factors<sup>115</sup>. An additional SASP-modulating therapy was found, revolving around the mammalian target of rapamycin (mTOR)<sup>116</sup>. mTOR has been linked to the SASP's network through IL-1α, thus gaining control over NF-κB, a significant regulator of a considerable amount of SASP factors<sup>78</sup>. Consequently, mTOR's known inhibitor, rapamycin, has the possibility to disrupt the SASP<sup>117</sup>. Following this line of thought, other mTOR inhibitors or analogs demonstrate a similar effect and as a result this group of compounds has much relevance to the anti-SASP field<sup>118</sup>. The remaining approach to be taken would be the selective elimination of senescent cells (SESC). Clear benefits are associated with preferring this kind of choice. The tumor-suppressive component of senescence is assured, as only after their formation do senescent cells become a target for the therapy. Any negative influence from its SASP is eliminated at the root, which is probably the best result for an anti-SASP strategy. Accumulation of senescent cells doesn't occur, nor do any of its consequences, such as cumulative tissue dysfunction. Finally, there is the risk of damaged cells eventually escaping their senescence and becoming possibly malignant<sup>119</sup>. Senescent cell clearance would remove that risk of cancer development. However, one important factor to take notice is the existence of acute senescence. Any treatment involving senescent cell removal, would have to take care and avoid affecting wound healing-associated senescent cells. The proof-of-concept study mentioned above, using the transgene INK-ATTAC, demonstrated significant success with this approach. Many compounds of several types have been found to target senescent cells. Specifically, advantage of the survival promoting networks was taken, since they correspond to the main barrier against apoptosis. Drugs, such as dasatinib, quercetin and navitoclax, and even siRNA targeting these pro-survival networks were successfully responsible for selectively killing senescent cells<sup>120,121</sup>. A final benefit gained from these senolytics is connected with the aftermath of their use. As senescent cells are non-dividing, drug resistance due to adaptive mutations is nonexistent, avoiding therefore any possible expiration date of the senescence-eliminating drugs<sup>2</sup>.

## **1.3 Skin Aging**

### **1.3.1 Skin Structure**

One of the most visual aging transformations that can be observed affects the skin. When looking at the skin, a layered and hierarchical organization can be found. Two main layers compartmentalize the skin, each with their own characteristics.

The epidermis corresponds to the outermost layer of skin. Although usually the thinnest of all skin tiers, it's the most structured and stratified. The beginning of the epidermis is made up by the stratum basale, a cell thick continuous layer. It is populated by keratinocyte stem cells, the source of the epidermis itself. These will proliferate and differentiate, giving rise to mature keratinocytes, the main cell-type of the epidermis. This progressive differentiation process, occurs through the stratum spinosum and granulosum, layers that are located over the stratum basale. Keratin filaments are formed during this time, providing keratinocytes with their brick-like structure. Before reaching the last tier, the stratum corneum, keratinocytes release lamellar bodies containing several lipids, which have the objective of helping create the skin's valuable barrier function. The end-point for keratinocytes is the stratum corneum, the most upper part of the epidermis and thus the skin. Here keratinocytes have lost their nuclei and cellular organelles, transforming into corneocytes. These form thick layers, which allied to an insoluble and cornified envelope establish an efficient barrier function<sup>122</sup>.

The dermis is located between the epidermis and the hypodermis, a subcutaneous fat layer. The dermis' existence is coupled with responsibilities of being the main foundation and physical support of skin. Extracellular matrix (ECM) components help reach that objective. A web of fibrous elements, made up of elastin and various collagens, in conjunction with proteoglycans regulate the mechanical properties of the skin<sup>122</sup>. Fibroblasts are the main cell-type that populate the dermis. Two distinguishable compartments cover the dermis, the papillary and the reticular dermis<sup>123</sup>. According to the layer of dermis, a characteristic subpopulation of fibroblasts exists and consequently, they are respectively named after their specific layer. As these cell-types have great prominence in this thesis, a more detailed description is in order.

#### **1.3.1.1 Papillary vs. Reticular Fibroblasts**

As to understand the heterogeneity of both kinds of fibroblasts, a comparative analysis is a pertinent approach.

Papillary fibroblasts reside in the dermal layer closest to the epidermis, whereas the reticular are located closer to the subcutaneous adipose layer. Morphologically, both subpopulations diverge greatly. Papillary fibroblasts possess a spindle-like shape, while reticular fibroblasts are flattened and expanded<sup>124</sup>. Proliferation rates from both subpopulations are also different, as the papillary fibroblasts can grow at a much faster pace than their reticular counterparts<sup>125</sup>. In cell culture, reticular fibroblast

reach a lower cell density, which implies larger contact inhibition than papillary fibroblasts<sup>124</sup>. If they are allowed to reach confluence, papillary fibroblasts can accomplish multilayers, while reticular fibroblasts remain in a monolayer conformation<sup>126</sup>. In accordance with the dermis' role in supporting the epidermis, the relationship between its populating cell-types was studied. Coculture of papillary fibroblasts with keratinocytes gave origin to keratinocyte masses, which displayed all stages of keratinocyte differentiation. This proved that papillary fibroblasts assist correct differentiation. However, when cocultured with reticular fibroblasts, dysfunctional masses with irregular shapes formed, lacking terminal differentiated cells<sup>126</sup>. As fibroblasts and keratinocytes are not located in the same skin layer *in vivo*, their secretions were observed. As expected, papillary and reticular fibroblasts diverged considerably in cytokine and growth factor release. Keratinocyte growth factor (KGF), important for keratinocyte proliferation, was secreted in higher amounts in papillary fibroblasts, when compared to reticular<sup>126</sup>.

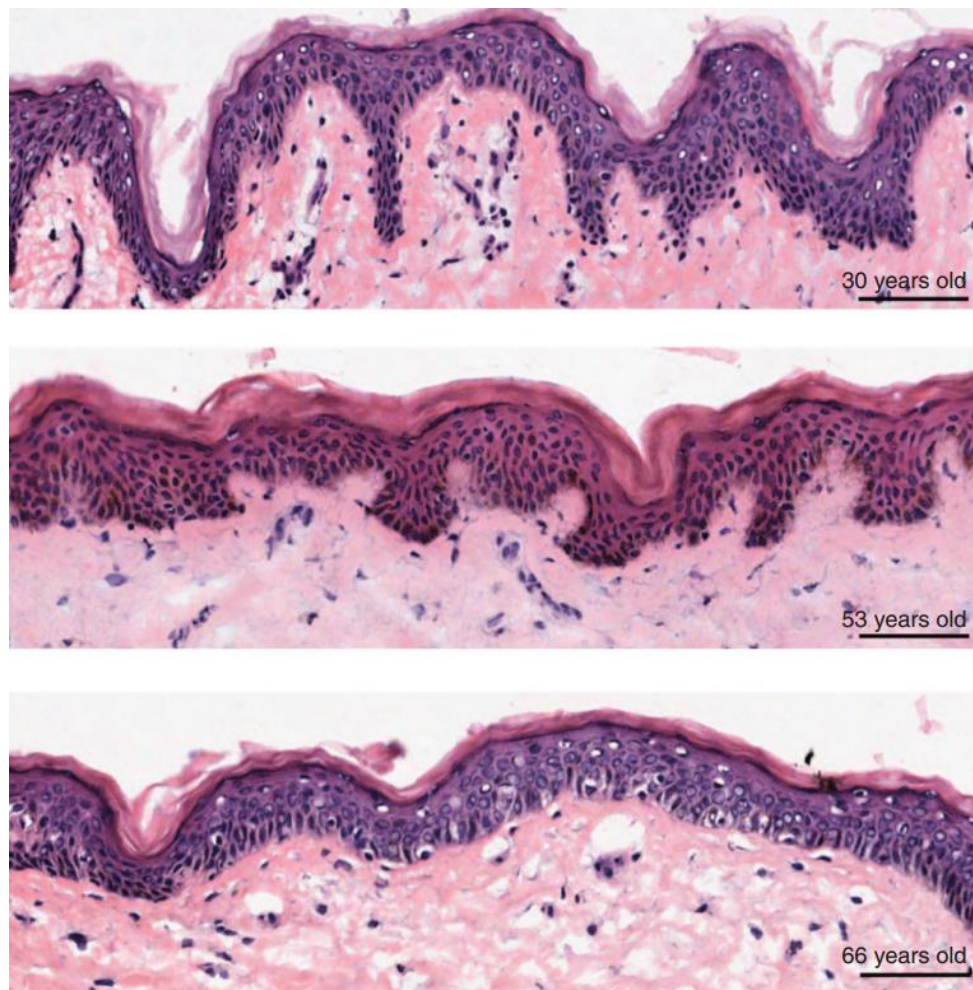


**Fig. 4** – Cross-sections of young, middle-aged and old skin (from top to bottom). Hematoxylin and eosin staining facilitates visualization of both the epidermis and the dermis. Aging related changes are noticeable, especially flattening of the rete ridges. Scale bar = 100  $\mu\text{m}$ . Adapted from Giangreco, A. et al (2010)<sup>3</sup>.

Also ECM production, an important role of the dermis, is distributed and not similar between papillary and reticular fibroblasts<sup>127</sup>. These observations correlate with results in experiments performed with the *in vitro* skin model, termed human skin equivalents. Skin equivalents differ from usual coculture, since they are organized and layered to resemble the skin. An air-liquid interface is present to stimulate epidermal differentiation and mimic *in vivo* conditions. Reticular fibroblasts were unable to support the formation of a successful skin equivalent, when seeded under keratinocytes. In contrast, similar aged papillary fibroblasts originated better skin equivalents, with increased thickness and a correctly layered epidermis<sup>4</sup>.

With this significant divergence between papillary and reticular fibroblasts, gene expression profiles were created to assess the existence of possible molecular markers. Several genes were found, facilitating future studies using these cell-types<sup>128</sup>.

### 1.3.2 Skin Aging Phenotypes

Skin has an important protective role, shielding the rest of the body from exterior harm. Therefore, it is also really susceptible to external stresses and to age-related attrition.

The loss of the epidermal rete ridges is a distinct morphological trace of skin aging. The interdigitated dermis retracts, resulting in a complete loss of the wavy-like structure<sup>129</sup>. Cell density and thickness of the dermis decrease with age<sup>130</sup>. Chronic UV exposure alters the elastic fibers, causing them to become amorphous and dysfunctional. Collagen polymers and glycosaminoglycans also change with age, interfering with correct fibrillogenesis and bundle formation<sup>131,132</sup>. This event gives rise to a reduction in skin elasticity and thus wrinkling<sup>133</sup>. Atrophy seems to describe well the age-related changes that affect the skin. From morphological changes to modifications of the ECM, aging punishes the skin for being the first line of defense. Senescence also integrates the skin aging phenotype, where its microenvironment-altering abilities have a big impact<sup>134</sup>. Its accumulation was highlighted in primates, revealing that more than 15% of skin cells in old individuals correspond to senescent cells<sup>135</sup>. One considerable source of senescence in skin is photoaging, resulting from UV exposure.

One final occurrence in skin aging to be mentioned is the balance between dermal compartments and their respective fibroblasts. The papillary dermis has been observed to diminish with age, linked to a vanishing papillary fibroblast population<sup>136</sup>.

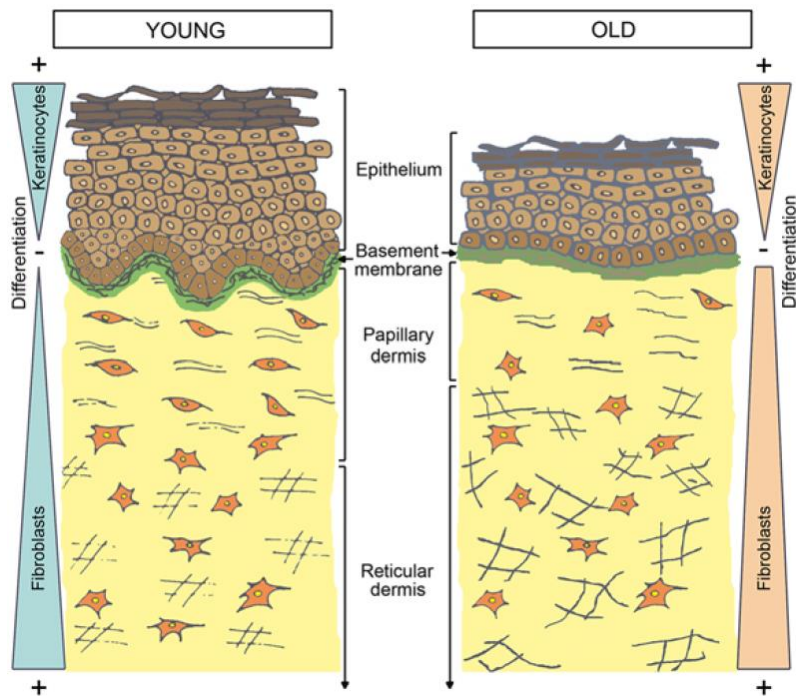


**Fig. 5** – Proposed model for skin aging. Thinning and flattening of the dermis, along with changes in the dermis compartments are some of the reported age-related observations. Adapted from Mine, S. et al (2008)<sup>4</sup>.

### 1.3.2.1 Papillary to Reticular Transition

Papillary and reticular fibroblasts are both important for skin homeostasis. Promotion of skin aging is achieved with a loss of equilibrium due to either side. Aging has a different effect on each kind of dermal fibroblast. Papillary fibroblasts seem to suffer a significant age-dependent transformation, whereas reticular appear to be mostly unaffected.

Papillary fibroblasts have, with increasing age, a more active secretion profile, with more MMPs and tissue inhibitor of metalloproteinase (TIMPs). Curiously, the divergent proliferative profile of the two kinds of fibroblasts changed. Papillary fibroblasts, through aging, lose some of their growth potential and resemble more their slower reticular counterparts<sup>4</sup>. The same repeats itself with their capacity to support an epidermal layer in a skin equivalent model<sup>137</sup>. Whilst young papillary fibroblasts performed well in supporting keratinocyte differentiation and forming a well-rounded epidermis, older papillary fibroblasts' performance bundled with the poor ability of reticular fibroblasts in creating reconstructed skin. A thin and incomplete epidermis was the result of both young and old reticular fibroblasts and old papillary fibroblasts<sup>4</sup>.

From an age perspective papillary and reticular fibroblasts, once completely different cell types, seem to converge to similar ground. However, it seems that only papillary fibroblasts suffer from aging modifications and thus come closer a more reticular-like phenotype.

Gene expression changes accompany this age-related change. Older papillary fibroblasts lose expression from papillary biomarkers and gain reticular biomarkers instead. All these observations justify the existence of a differentiation process, where papillary fibroblasts differentiate into reticular fibroblasts<sup>136</sup>. This process was termed papillary to reticular transition.

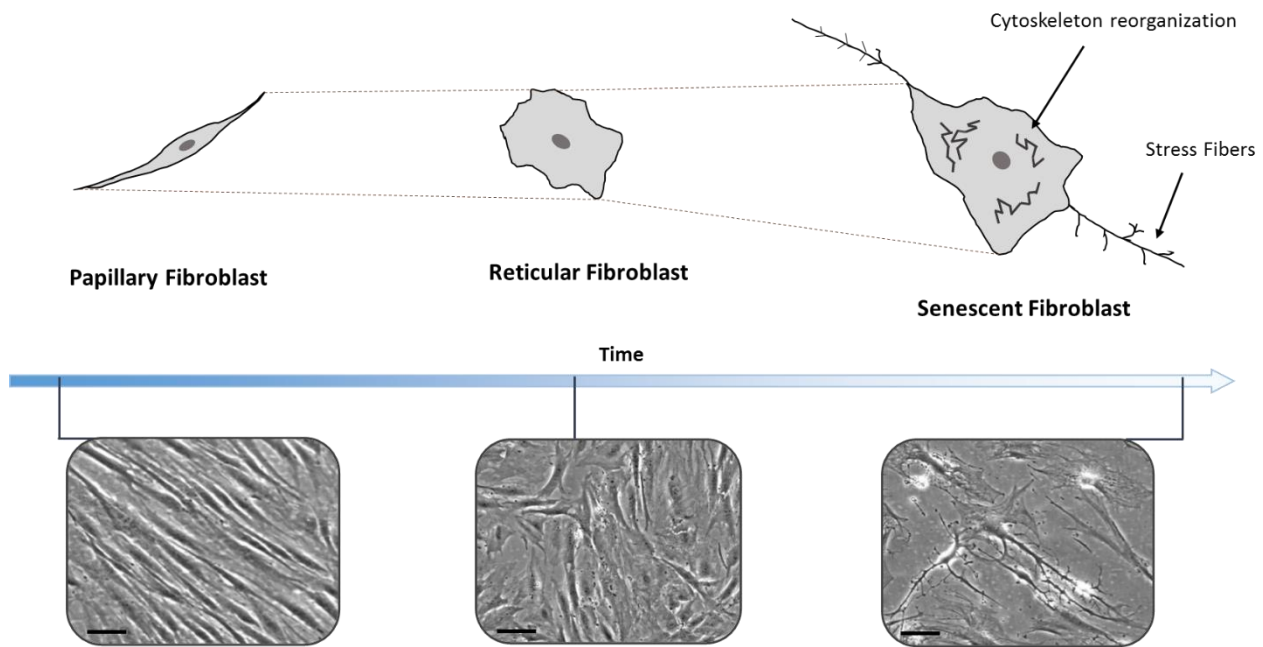


**Fig. 6** – Schematic describing the papillary-to-reticular transition. Age-dependent morphological changes are demonstrated with *in vitro* images. Scale bar = 100 µm.

## **2. Materials and Methods**

### **2.1. Cell Culture**

#### **2.1.1. Cell Lines**

##### **HDF Donor 1**

Human Dermal Fibroblasts retrieved from an abdominoplasty of a 58 year old donor. Information of diversity of fibroblast populations wasn't available.

##### **HDF Donor 2**

Human Dermal Fibroblasts retrieved from an abdominoplasty of a 65 year old donor. Lack of knowledge over the distribution of fibroblasts populations. Possesses a more reticular-like behavior.

##### **HDF Donor A Pap**

Human Dermal Fibroblasts originated from skin of a 33 year old Caucasian female. Isolated from an upper portion of the dermis, the papillary dermis. High expression of papillary biomarkers and low of reticular<sup>128</sup>. Kindly provided by A. El Ghalbzouri.

##### **HDF Donor A Ret**

Human Dermal Fibroblasts originated from skin of a 33 year old Caucasian female. Site-matched retrieval from the lower part of the dermis, the reticular dermis. Low expression of papillary biomarkers and high of reticular<sup>128</sup>. Kindly provided by A. El Ghalbzouri.

##### **HDF Donor B Pap**

Human Dermal Fibroblasts originated from skin of a 49 year old Caucasian female. Isolated from an upper portion of the dermis, the papillary dermis. High expression of papillary biomarkers and low of reticular<sup>128</sup>. Kindly provided by A. El Ghalbzouri.

##### **HDF Donor B Ret**

Human Dermal Fibroblasts originated from the same 49 year old Caucasian female's skin. Site-matched retrieval from the lower part of the dermis, the reticular dermis. Low expression of papillary biomarkers, with PDPN showing a low positive, and high of reticular<sup>128</sup>. Kindly provided by A. El Ghalbzouri.

### **HDF Donor C Pap**

Human Dermal Fibroblasts originated from skin of a 37 year old Caucasian female. Originated from the papillary dermis. High expression of papillary biomarkers and low of reticular<sup>128</sup>. Kindly provided by A. El Ghalbzouri.

### **HDF Donor C Ret**

Human Dermal Fibroblasts originated from the same respective skin of a 37 year old Caucasian female. Site-matched cells isolated from the reticular dermis. Low expression of papillary biomarkers and high of reticular<sup>128</sup>. Kindly provided by A. El Ghalbzouri.

### **HaCaT**

Spontaneously transformed aneuploid immortal keratinocyte cell line from adult human skin.

## **2.1.1 Culture Media**

### **Fibroblast Media**

In routine cell culture, every fibroblasts cell line was cultured in DMEM/HAM's F-12 (F4815 Biochrom) or a mixture of 1:1 DMEM (F0435 Biochrom) and HAM's F-12 (F0815 Biochrom). These commercial media were supplemented with 4 mM of L-Glutamine (G7513 Sigma-Aldrich) and 10% Fetal Bovine Serum (F7524 Sigma-Aldrich).

### **Keratinocyte Media**

The HaCaT cell line was maintained in culture with routine culture fibroblast media. Occasionally, HaCaT cells were cultured in KBM Clonetechs (CC-3101 Lonza) supplemented with only two KGM SingleQuots (CC-4131 Lonza), insulin (CC-4021E Lonza) and hydrocortisone (CC-4031E Lonza).

## **2.1.2 Cell Cultivation**

All cell cultivation followed good laboratory practice (GLP).

### **2.1.2.1 Cell Thawing**

Desired cells were stored in liquid nitrogen inside cryotubes (374081 Thermo Scientific) containing cell suspension in the usual growth media supplemented with 10% DMSO (D2650 Sigma-

Aldrich). Cells were thawed at room temperature, submerged in 70% ethanol. The cryotubes' content was transferred into a 15 ml falcon tube half filled with media, which was then inserted into a centrifuge (5810 R Eppendorf) for 5 minutes at 170g. Following the recovery of the tubes, the supernatant was discarded and the cell pellet was resuspended in the chosen volume and transferred to its rightful T-flask. Finally, the thawed cells inside their flasks were inserted into the incubator (HERAcell 150i Thermo Scientific), where they were normally incubated at 37°C and with 7% CO<sub>2</sub>.

#### **2.1.2.2 Cell Passage**

All cell lines, except peripheral blood mononuclear cells (PMBCs), were adherent in nature and as such were cultivated in T-flasks or wells (Greiner Bio-One). To passage and expand, cells were retrieved from their incubator. The medium was removed and cells were washed twice with phosphate buffer saline (PBS) (L1820 Biochrom) to remove any remnants of media which could inhibited future trypsin. Afterwards, trypsinization was performed with a 0.1% Trypsin (27250-018 Gibco)/EDTA (E6511 Sigma-Aldrich) solution for fibroblasts and with a 0.25% Trypsin/EDTA solution for keratinocytes. Following an incubation of 5-10 minutes inside the incubator, cells were detached from the surface and could be harvested. When the media contained fetal bovine serum (FBS), no trypsin inhibitor was needed. Otherwise, as in the case for HaCaT cells, trypsin inhibitor (T6416 Sigma-Aldrich) was added to neutralize the trypsinization. While respecting the appropriate ratios, new media was added. Then, the cell suspension was distributed into their new corresponding T-flasks and returned to the incubator.

#### **2.1.2.3 Cell Seeding**

Seeding a known fixed number of cells began with detaching the cells from their surface as before. Afterwards, cells were diluted with new media and stored in the appropriate falcon tube. 1 mL was appropriated for cell counting using an automated cell counter (Vi-CELL XR Beckman Coulter). Following the determination of the cell suspension's cell concentration, the right amount needed for seeding was calculated. This cell suspension volume was then diluted with fresh media until fulfilling the total volume, equivalent to the amount of flasks or wells wanted. Finally, it was distributed through respective flasks or wells and introduced into the incubator.

#### **2.1.2.4 Stress-Induced Premature Senescence (SIPS) Treatment**

Since senescence is an aging process, its study can be complicated due to its slow manifestation rate. Therefore, from a practical perspective it became very important to develop methods to trigger senescence in an acceptable timescale. Thus stress-induced premature senescence was discovered and explored as a source of aging models. Provoking premature senescence in cells was performed using initial aliquots of 30% H<sub>2</sub>O<sub>2</sub> (216763 Sigma-Aldrich), resulting in oxidative stress. Cells

were initially seeded with a cell density of 3500 cells/cm<sup>2</sup> and were inserted inside the incubator for 24 hours. Afterwards, their media was supplemented with 100-60 µM of H<sub>2</sub>O<sub>2</sub>, optimized for the FBS batch in use, and an incubation time of 1 hour at 37°C and with 7% CO<sub>2</sub> followed. Afterwards, H<sub>2</sub>O<sub>2</sub> containing media was removed and fresh media was added. Cells were then returned to their incubator. This process was performed nine times over the course of two weeks.

#### **2.1.2.5 Plant Extract Treatment**

A plant extract, termed 1201, was used as an active supplement throughout several experiments. Several treatment regimes existed and each was performed in specific situations. Concentrations ranging from 0.006% to 0.1% were used as media supplements. Duration of treatment also varied, extending from 48 hours to 39 days. Occasionally, its solvent, ZEMEA® Propanediol (DuPont), was also used by itself as a treatment condition to serve as a control.

### **2.2 Proliferation Assay**

Cells to be surveyed for their proliferation rates were seeded in 6-well plates with a cell density of 40 000 cells/well. The number of wells seeded was dependent on the number of different conditions and days to be tested. At each chosen time-point, after aspirating its media, the particular well was subjected to 0.5 ml of trypsin. Following detachment, cells were diluted with fresh media to a total volume of 1 ml. This volume was transferred to the Vi-CELL container and counted. The cell density was monitored at several time-points, originating a growth profile.

### **2.3 Senescence Associated β-Galactosidase Staining**

This assay had the objective of determining β-Galactosidase activity at pH 6, a marker of senescent cells. It revolved around one reagent, 5-bromo-4-chloro-3-indolyl-β-D-galactopyranoside (X-Gal), which is hydrolyzed when the enzyme is present and releases galactose and an indole. The indole will afterwards dimerize and form a visible and insoluble blue product. Before staining, cells were seeded into 6-well plates with a seeding density of 40 000 cells/well. After 3 days of incubation, cells had their media aspirated and were washed twice with PBS. Afterwards, they were fixed by adding 2 ml of a 2% formaldehyde (Sigma)/0.2% glutaraldehyde (Sigma) in PBS fixating solution per well. Wells were incubated at room temperature during 10 minutes. While the incubation proceeded, a staining solution of 5 mM potassium ferricyanide, 5 mM potassium ferrocyanide, 2 mM MgCl<sub>2</sub>, 10 mg/L of X-Gal (B1690 Life Technologies) in a staining buffer of pH 6 (37 mM Citrate and 126 mM NaHPO<sub>4</sub>) was prepared. The fixating solution was removed and cells were again washed twice with PBS. Due to the light-sensitive nature of the X-Gal reagent, subsequent steps were performed hidden from any light

source, including the preparation of the staining solution. Desired wells, were washed with 2 ml of staining buffer. Then, 1 ml per well was added of staining solution, followed by an incubation time of 24 hours at 37°C and with 7% CO<sub>2</sub>. The result was observed under the microscope (Leica) in phase-contrast mode. Ten photographs were taken for each tested well with 100x magnification in randomly throughout the well. Blinded visualization and counting of all photographs was made to avoid biased quantifications.

## 2.4 BrdU Assay

Bromodeoxyuridine (BrdU) and propidium iodine (PI) staining were performed and analyzed by flow cytometry to assess the existence of proliferating cells and cell-cycle progression, respectfully. BrdU is an analogue of thymidine and thus gets incorporated when DNA is replicated. Proliferating cells will, as a consequence, be able to be quantified through anti-BrdU antibodies. However, not only cells which are proliferating can incorporate BrdU. DNA damage repair can be responsible for introducing BrdU in the DNA, although limited to a small amount. Other cells, which have stalled in S phase of cell cycle, also perform DNA replication, assimilating BrdU, but do not progress through the cell cycle. Consequently, incorporated BrdU quantification by itself cannot assure the detection of only proliferating cells. PI is used to clarify the identity of the BrdU positive cell population. Propidium iodine stains DNA, giving information about the amount of DNA in each cell. Depending on a cell's location in its cell cycle, the quantity of DNA will vary. Therefore, a cell cycle distribution will arise from PI staining. It will discern if BrdU positive cells correspond to proliferating cells, by verifying if any abnormal cell behavior is present.

Cells to be assayed present in their respective wells, had their media supplemented with 10 µM BrdU (B5002 Sigma-Aldrich) for 24 hours. Afterwards, they were harvested by trypsinization and diluted with enough fresh media to have a total volume of 5 ml. They were then transferred to a 15 ml falcon tube and centrifuged for 10 minutes at 170g. All subsequent centrifugations were executed with these conditions. The supernatant was discarded and the cell pellet was vortexed (Janke & Kunkel IKA) at low speed, to avoid clumping, while cells were fixed by adding, dropwise, 1ml of ice-cold (-20°C) 70% ethanol (1009832500 Merck). When finished, fixed cells were incubated overnight at 4°C. After incubation, cells were forced through another centrifugation step. Their respective supernatant was removed and 1 ml of 2M HCl/1% Triton X (X100 Sigma-Aldrich) was added with the same care as the fixating step, drop by drop with low vortexing. This DNA denaturing step required an incubation time of 30 minutes at room temperature, followed by a third centrifugation. After discarding the supernatant the pellet was resuspended in 1 ml 0.1 M sodium tetraborate (S9640 Sigma-Aldrich), for neutralization. Following an additional centrifugation step, the pellet was resuspended in 300 µl of a 0.5% Tween 20 (P2287 Sigma-Aldrich)/1% Bovine Serum Albumin (A7906 Sigma-Aldrich) in PBS solution and 6 µl of a mouse anti-BrdU antibody (347580 BD Biosciences). 30 minutes incubation time at room temperature were necessary for the antibody to bind to the incorporated BrdU, now sterically available due to the denaturing step. A succeeding centrifugation removed the excess antibody solution. Unspecific binding

antibodies were eliminated with a washing step with 5 ml of 0.5% Tween 20/1% Bovine Serum Albumin in PBS. A centrifugation step followed, removing its respective supernatant. The following stages were performed in the dark as the reagents used from this point are light-sensitive. Cell pellet was resuspended in 200 µl of the previous washing solution with a 1:100 stock dilution of the anti-mouse secondary antibody, which is conjugated with fluorescein isothiocyanate (FITC) (F8264 Sigma-Aldrich). Subsequently, a binding incubation time of 30 minutes at room temperature was needed. Afterwards, a final washing step was executed with 9 ml of PBS. Centrifugation removed the supernatant, and cleared the cell pellet from another unspecific binding. Finally, the pellet was resuspended in 200 µl of PBS supplemented with 2.5 µg/ml of PI (P4864 Sigma-Aldrich) and transferred to flow cytometry tubes.

The tubes were then brought to the flow cytometer (Gallios B43620 Beckman Coulter) where the corresponding lasers were used. Data retrieved was analyzed with Kaluza Analysis Software (Beckman Coulter).

## 2.5 Chemotaxis Assay

There were three main elements to this assay, the chemotaxis slide (80326 ibidi), the conditioned media and the immune cells. Altogether, they created the need for a preparation phase.

The chemotaxis slides had space for three different assays. Each assay comprised of 2 reservoirs separated by 1 central channel. They came with plugs used to seal all the ports, keeping the environment inside the slide sterile. One of the reservoirs will receive the corresponding conditioned media while the other is filled with unconditioned media, thus creating the chemical gradient. Cells embedded in a 3D matrix will be inserted into the central chamber. One day before the assay was performed, the slides were introduced into the incubator for equilibration. As the plastic is gas-permeable, it should be introduced previously into the assay's environment to prevent air bubbles from emerging during the assay. For this equilibration, the slides were introduced into sterile Petri dishes, which contain sterile PBS-humidified tissues. Then, a batch of conditioned media needed to be conveniently prepared beforehand, from the respective target cells. Each reservoir had a volume of 60 µl and the total amount of conditioned media needed was foreseen. If any unconditioned media was also chosen for an assay, it would also be subjected to the equilibration step.

After preparing all the necessary reagents, the first task at hand was the preparation of the 3D matrix containing the cells and inserting it into the central channel. Desired immune cells were isolated from a healthy donor. Retrieved blood was diluted with an amount of PBS equivalent to the blood volume. This diluted solution was inserted slowly over a defined volume of Biocoll (L6115 Biochrom) equal to the initial amount of blood. Centrifugation followed at 400g during 40 minutes at room temperature, originating the density gradient. Phase separation created 3 different segments. The erythrocytes constituted the lowest layer, followed by the Biocoll. Between the plasma phase located at the top and the Biocoll phase, a ring of mononuclear cells was present. The ring was aspirated with caution, so as to isolate a relatively pure population of PBMCs. Addition of erythrocyte lysis buffer to the PBMCs followed, incapacitating any red blood cells potentially present in the PBMCs solution.

Afterwards, centrifugation at 400g for 10 minutes at room temperature was executed and its subsequent supernatant discarded.

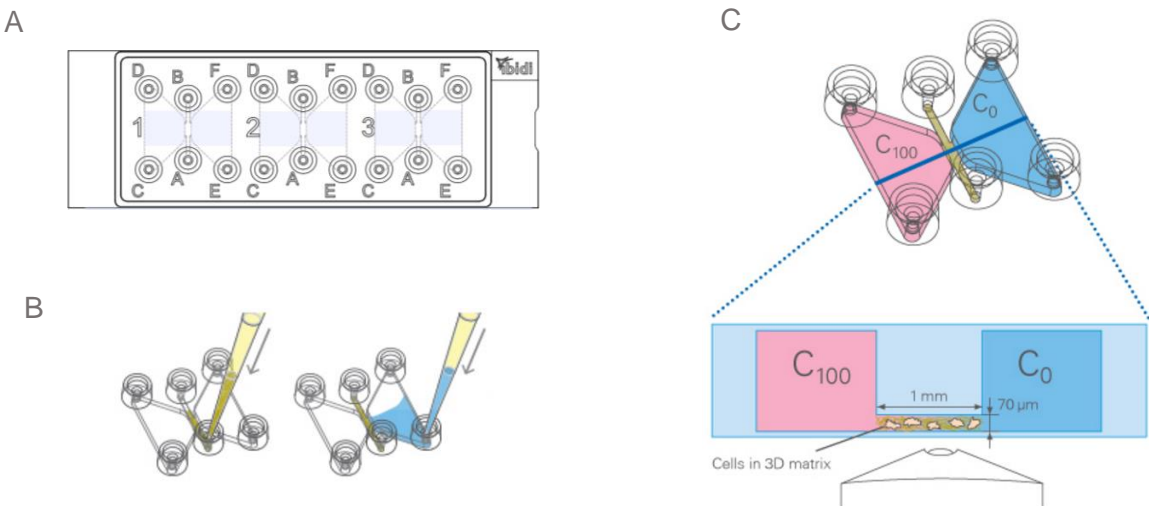


**Fig. 7** – (A) Top view of the ibidi chemotaxis slide, which possesses space for 3 different assays. Each one consists of a central chamber flanked by two reservoirs. (B) Scheme displaying which ports to use when trying to fill each component of the assay. (C) Overall perspective showing the concept of the assay and a cross-section which demonstrates how the chemotaxis is achieved.

A wash step with PBS was performed, trailed by another similar centrifugation step. When the last supernatant was discarded, the PBMCs were resuspended in RPMI 1640 media (FG1215 Biochrom), making them ready to be used.

After isolating PBMCs, the cell suspension concentration was determined. Cells were then embedded in a supporting matrix. The 3D matrix was based on collagen G (L7213 Biodine). 300  $\mu$ l of matrix solution was made up of 4  $\mu$ l L-Glutamine, 20  $\mu$ l 10x MEM (MO275 Sigma-Aldrich), 10  $\mu$ l of bicarbonate sodium (S8761 Sigma-Aldrich), 50  $\mu$ l RPMI 1640, 53.2  $\mu$ l of nuclease free water (NFW) (Gibco), 112.5  $\mu$ l of collagen G and 50  $\mu$ l of cell suspension, so as to reach a final desired number of cells of  $3 \times 10^6$ /ml. After mixing all the reagents, the slides were retrieved from the incubator and 6  $\mu$ l of cell containing matrix was slowly added into the entry port of the central chamber. To help the flow in the central chamber create a uniform and solid 3D matrix channel, careful aspiration from the end port was done. Afterwards, a 1 hour incubation time at 37°C and 7% CO<sub>2</sub> followed until the matrix was solidified. With the cells in place, the reservoirs were each filled with their respective conditioned media. With all the components ready, the assay began. The central chamber was observed under the microscope with capabilities of maintaining a cell culture and photos were taken every 2 and a half minutes for 12 hours.

With the whole data recovered, analysis of the results was done using the software ImageJ (National Institutes of Health). 289 frames from each assay were compiled into a multilayered image, which could afterwards be opened with ImageJ. Using an ImageJ plugin, Manual Tracking, a cell migration path could be traced through the 289 frames. 30 cells were tracked per condition, creating a

migration profile. Blinded quantification of cell paths was done to ensure unbiased tracking. To visualize the profile, another plugin, Chemotaxis Tool (Ibidi), was used. When plotting the migration result, the beginning of each cell path was joined together at the axes origin, forcing them to start from the same point. The plot displayed each individual cell path and determined the profile's center of mass.

## 2.6 RNA Quantification

### 2.6.1 RNA Isolation

To begin RNA isolation, cultured cells must be prepared and lysed properly. After removing the cells from their incubator, their media was aspirated. Following a wash with PBS, cells were then subjected to a chemical lysis reaction. TRIzol reagent (T9424 Sigma-Aldrich) was introduced onto the cells and after covering all surfaces newly produced lysates were recovered into nuclease-free tubes (72.692 Sarstedt). The next step involved a few seconds of vortexing, homogenizing the lysates, followed by an incubation of 5 minutes at room temperature. Afterwards, they could either directly progress to an RNA isolation or get stored at -80°C. The procedure continued with these RNA lysates extracted from cells. The microcentrifuge (5415R Eppendorf) was configured to have an operating temperature of 4°C during the whole protocol. Due to the toxic nature of the TRI reagent and to avoid contamination with RNase, all steps were performed inside a fume hood. Firstly, chloroform (C2432 Sigma-Aldrich) was added to induce a phase separation into an organic layer and aqueous layer. 200 µl of chloroform was used per milliliter of lysate. The solution was then mixed with the vortex, during 15 seconds, followed by an incubation time of 3 minutes at room temperature. Centrifugation to thoroughly separate the phases was next, for 15 minutes at 12 000g. Afterwards, the tubes were carefully removed from the centrifuge to avoid disturbing the phases. With the same caution, 400 µl of aqueous phase per milliliter initial lysate was removed and transferred to a new nuclease free tube. Addition of 500 µl of isopropanol (20922.394 VWR Chemicals Prolabo) per milliliter initial lysate followed, to cause RNA precipitation. The solution was mixed using a micropipette and later incubated for 10 minutes at room temperature. Another centrifugation was needed to aggregate the RNA precipitates, at 12 000g for 10 minutes. After removing the tubes, their supernatant was aspirated slowly and the pellet was washed with 1 ml of 70% ethanol. The samples were then centrifuged for 5 minutes at 7600g. Once more, the supernatant was discarded carefully, maintaining the RNA pellet undisturbed. A final centrifugation at 7600g for 2 minutes was executed to later meticulously remove any supernatant left. The pellet was left to dry for 10 minutes to completely eliminate any remaining ethanol. Resuspension of the dry pellet in 30 µl NFW was done before heating the samples for 10 minutes at 57°C. Finally, the isolated RNA samples were stored at -80°C.

## **2.6.2 cDNA Synthesis**

High Capacity cDNA Reverse Transcriptase Kit (4368814 Applied Biosystems) was used to achieve conversion of RNA to complementary DNA (cDNA). Kit instructions were followed, with the reaction volume totaling 20  $\mu$ l. By mixing 2  $\mu$ l of 10x RT Buffer, 0.8  $\mu$ l of 25x dNTP Mix, 2  $\mu$ l 10x RT Random Primers, 1  $\mu$ l of RNase Inhibitor (N2115 Promega), 1  $\mu$ l of Multiscribe Reverse Transcriptase, 10  $\mu$ l of template and 3.2  $\mu$ l of NFW the equivalent of one reaction was established. 500 ng of RNA template were used in each reaction. To have templates with that specific final concentration, they had to initially be quantified at the NanoDrop One and diluted correspondingly. The mastermix and the template were mixed and introduced into the thermocycler. The sequence of steps was developed as stated by the manufacturer. Initially, the thermocycler performed a step 25°C during 10 minutes to activate the polymerase, followed by a reaction phase of 2 hours at 37°C. To end the cycle, an 85°C step was performed during 5 minutes, denaturing the enzyme. The newly synthesized cDNA was then diluted with 80  $\mu$ l of NFW to a final concentration of 5 ng/ $\mu$ l and used immediately in a quantitative PCR (qPCR) or stored at -20°C.

## **2.6.3 Standard Preparation**

After cDNA synthesis, the samples were ready to be subjected to a qPCR quantification. This method uses an intercalating fluorescent DNA dye to follow the amplification of the desired PCR product. In each cycle step the dye binds to the newly formed strands, causing the fluorescence signal to increase. A cumulative signal is measured, which is proportional to the initial amount of product present in the sample. The signal is quantified by determining the threshold cycle. This variable represents the cycle step at which the signal intensity overcomes the threshold limit, defined to rule out noise effects. However, to translate this threshold cycle into product copy number a standard curve is necessary, creating the need to prepare standards of known concentration for each PCR product tested.

The first step involved amplifying the desired PCR product. For this, a DNA template was needed, one that possessed the required gene. To amplify the gene, a polymerase chain reaction (PCR) was executed. GoTaq DNA Polymerase Kit (M300 Promega) was used and its manufacturer's instructions were followed. For each reaction, 10  $\mu$ l of 5X Green GoTaq Reaction Buffer, 1  $\mu$ l of deoxynucleoside triphosphate (dNTP) (10 mM), 0.25  $\mu$ l of GoTaq DNA Polymerase (5u/ $\mu$ l), 1  $\mu$ l of both the forward (10  $\mu$ M) and the reverse primer (10  $\mu$ M), 2  $\mu$ l of DNA template and 34.75  $\mu$ l of NFW were mixed to a total volume of 50  $\mu$ l. Both forward and reverse primers (Integrated DNA Technologies), were designed to amplify a sequence of desired mRNA of 70-300bp length separated by an intron with at least 1000bp to avoid amplifying genomic DNA. After producing the reaction mix inside each corresponding PCR tube, they were introduced into the thermocycler (T3 Biometra). The lid was preheated up 104°C and an initial denaturation step was performed at 95°C during 5 minutes. A sequence of three steps, denaturation, annealing and extension, was repeated 39 times. The

denaturation step was executed at 95°C for 30 seconds, followed by an annealing step at 55°C for 30 seconds. Finally, an extension at 72°C for 20 seconds completed the cycle, which then restarted. The proceeding step involved a final extension at 72°C during 5 minutes. The program finished with a cooling until 15°C.

With amplification complete, the PCR products were checked for the correct size and intensity through a gel electrophoresis. A 2% agarose gel was prepared, by mixing LE Agarose (840004 Biozym) with the respective amount of the buffer solution containing Tris base, acetic acid and EDTA (50x TAE buffer). After solubilizing the agarose, the solution was cooled down and a drop of Midori Green DNA stain (MG02-MP Biocat) was added before pouring it into a gel mold. Following gel solidification, the gel was retrieved and placed inside the gel box, previously filled with TAE buffer. Gel chambers were rinsed with buffer and both the samples and the 100 kb DNA ladder (Generuler SM0241 Thermo Scientific) were loaded onto the gel. 5µl of Midori Green DNA stain were added to the running buffer at the positive pole reservoir as well. Then, the gel was run at 130 V during approximately 30 minutes. A visualization of the finished gel was done inside the imaging docking apparatus (Gel Doc XR+ Bio-Rad). Through UV irradiation, DNA strands became visible and the PCR results could be assessed. With approval of the amplified products, their purification from the gel was next.

With a scalpel under UV light, the desired DNA band was cut out of the gel and transferred into an Eppendorf tube. Its subsequent purification was achieved with use of the FavorPrep Gel Purification Mini Kit (FAGCK001 Favorgen Biotech Corp), following its instructions. Purified, the DNA standard was quantified using a UV/Vis spectrophotometer (NanoDrop One Thermo Scientific). Knowing their concentration and their size in base pairs, DNA standards were diluted to reach a final concentration of  $1 \times 10^9$  fragment copies/µl. With the standards completed, they were ready to be used or could be stored at -20°C.

#### 2.6.4 Quantitative PCR (qPCR)

Preparation for this method was facilitated through the use of the 5x HOT FIREPol™ EvaGreen™ qPCR Mix Plus (ROX) (08-24-00020 Solis Biodyne). 2 µl of 5x HOT FIREPol™ EvaGreen™ qPCR Mix Plus, 0.25 µl of each primer, 1 µl template and 6.5 µl of NFW composed one qPCR reaction of a total volume of 10 µl. However, before preparing the desired sample's reaction, the target gene's previously prepared standard was needed to produce a 6 element standard curve. Each element was a 1:10 dilution of the previous, starting with the initial prepared standard of  $1 \times 10^9$  copies/µl. Consequently, the range of diluted standards ranged from  $1 \times 10^8$  copies/µl to  $1 \times 10^3$  copies/µl. Each diluted standard was prepared to be enough to have two technical replicates for the qPCR run. Each sample desired to be tested had to have their qPCR reaction repeated in technical quadruplicates.

Initially, the standard dilutions were performed, after thawing the original standard of  $1 \times 10^9$  copies/µl. Afterwards, the necessary mastermix was created, using all the mentioned reagents except the templates and diluted standards. The equivalent of one reaction of mastermix without template was distributed over all qPCR tubes. Finally each individual diluted standard and sample was introduced

into its respective qPCR tube and mixed with the micropipette. When finished, all tubes were sealed with caps and every single one was brought into the qPCR thermocycler (Rotor-GenQ Qiagen).

Table I – Primer list of selected genes.

Gene	Forward Sequence	Reverse Sequence	Product Length
A2M	AGAGCAGCATAAAGCCCAGT	TCTCAGTGGTCTCAGTGTGGA	243 bp
GAPDH	CGACCACTTGTCAAGCTCA	TGTGAGGAGGGGAGATTCAAG	210 bp
NTN1	TGCCATTACTGCAAGGAGGG	TTGCAGGTGATACCCGTCAC	167 bp
p21	GGCGGCAGACCAGCATGACAGATT	GCAGGGGGCGGCCAGGGTAT	222 bp
PDPN	GCATCGAGGATCTGCCAACT	CCCTTCAGCTTTAGGGCG	266 bp
PPP1R14A	GTGGAGAAGTGGATCGACGG	CCCTGGATTTCCGGCTTCT	131 bp
SNEV	TCATTGCCGTCTCACCAAG	GGCACAGTCTTCCCTCTCTTC	238 bp

The cycle began with a denaturation step for 10 minutes at 95°C, followed by a repetitive sequence of stages. A denaturation step began the sequence for 15 seconds at 95°C. Annealing for 30 seconds at 60°C corresponded to the next stage. The elongation stage that followed, 72°C for 15 seconds, was also taken advantage of by using it as measurement opportunity. To finish the cycle, another measurement acquisition was executed at 80°C for 2 seconds. This sequence was repeated between 45 and 55 times, until a final melt curve, which corresponded to a linear heating from 65°C until 99°C, completed the qPCR run. The assimilated data was analyzed with the Rotor-Gene Q software. All samples were normalized by their respective GAPDH expression for relative comparisons.

## 2.7 Protein Isolation

Initially, desired cells were detached through trypsinization, diluted with enough media to be recovered into a 15 ml falcon tube. A pre-cooled centrifuge at 4°C was the next destination for the cells, where they were centrifuged for 10 minutes at 600g. After retrieving the cells and discarding their supernatant, they were resuspended in 1 ml of PBS and transferred to their own Sarstedt tube. Once again, the tubes were taken to a pre-cooled microcentrifuge at 4°C and centrifuged for 10 minutes at 600g. While the microcentrifuge was working, a lysis solution was prepared. Depending on the amount of lysates anticipated, the right amount of volume was prepared. For 500 µl of lysis solution, 250 µl of 2x TNE buffer, 205 µl of NFW, 25 µl of phosphatase inhibitor (PhosSTOP 4906837001 Roche) and 20 µl of protease inhibitor (4693132001 Roche) were mixed. After lysis solution preparation, the tubes

could be recovered from the microcentrifuge and their supernatant discarded. The cell pellet was resuspended in 60 µl of lysis solution and incubated on ice for 15 minutes. After their incubation, samples were vortexed for a few seconds and subsequently centrifuged at 6000g and 4°C for 10 minutes. After causing cellular lysis and centrifuging them, samples were removed and their supernatant was aspirated away from the cellular debris pellet and transferred to a QIAshredder spin column (79656 Qiagen), causing DNA fragmentation. The columns were inserted into the cooled microcentrifuge to perform at 16 000 g for 2 minutes. The flow-through of the column was recovered and transferred to the same QIAshredder filter column again. The same centrifugation step was repeated and 60 µl of the flow-through was relocated into a new tube. 20 µl of 4x loading dye SDS was added to these tubes containing purified protein lysates, which were then subjected to 95°C on a heatblock (Eppendorf) for 10 minutes. After cooling down, the protein lysates were stored at -20°C.

## 2.8 Statistical Analysis

An unpaired two tailed t test was the hypothesis test used to calculate the p-value for determination of the significance of comparisons.

### **3. Results**

With the objective of uncovering compounds that could benefit skin and retard its aging, an initial screening of several actives was performed. 1201 was a plant extract, which outperformed the remaining actives in inducing positive changes in fibroblasts, without having toxic consequences. Early signs of delaying the PRT were found, with considerable morphological changes towards a more papillary state. Other preliminary experiments showed signs that 1201 was more successful than the other extracts in reducing fibroblast contact inhibition and causing some variations in papillary and reticular marker expression. Concerns of 1201 being able to reverse the PRT appeared, which following the PRT hypothesis could imply that 1201 would probably also reverse cellular senescence. As avoiding senescence altogether is unsafe due to its role as a tumor-suppressive mechanism, a lifespan was performed with this candidate plant extract, to rule out this scenario. 1201 was shown to slightly increase the lifespan, although it wasn't able to avoid senescence (data not shown). A considerable effect was observed concerning the healthspan of the cells. Instead of showing a gradual decline to senescence, 1201 maintained papillary-like behavior causing, at a later stage, a rapid drop to the senescent state. As a result, 1201 became an interesting target to investigate.

Following its suspected role in the PRT, fibroblasts were firstly subjected to different 1201 treatments to thoroughly determine its connection with the PRT.

#### **3.1. 1201 Intervenes in the Papillary-to-Reticular Transition**

##### **3.1.1. Treatment Causes Fibroblasts to Preserve Papillary State**

Fibroblasts were followed throughout 3-5 passages, to assess if 1201 could reverse, halt or delay differentiation from papillary to reticular fibroblasts. Plant extract treatment was coupled to each completed cell passage, simply by using standard fibroblast media supplemented with 0.006% 1201 in half of the fibroblast population. Cells commenced each trial after having been already passaged in T-25 flasks to escape from thawing stress. After 3 or 5 passages, several assays were conducted to evaluate possible effects over morphology, proliferation and marker expression. Biological replicates varied between 3 and 4 for both donors.

###### **3.1.1.1. 1201 Induces Morphological Changes**

Substantial morphological changes were observed after 1201 treatment. Both donors experienced the same effects. Fibroblasts retained or gained a spindle-like shape (Fig. 8 & Appendix II). They became more elongated whereas their width decreased. This description matches a papillary-

type phenotype. Non-treated cells maintained or aggravated their more rounded and flattened shape, displaying a more reticular morphology. 1201 treatment delays and, to some extent, reverses morphological changes that are characteristic of the PRT. Furthermore, evolution of cell density through the passages was different between treated and non-treated cells. 1201 treatment allowed for a visually decreased contact inhibition and thus a higher cell density when compared to the non-treated.

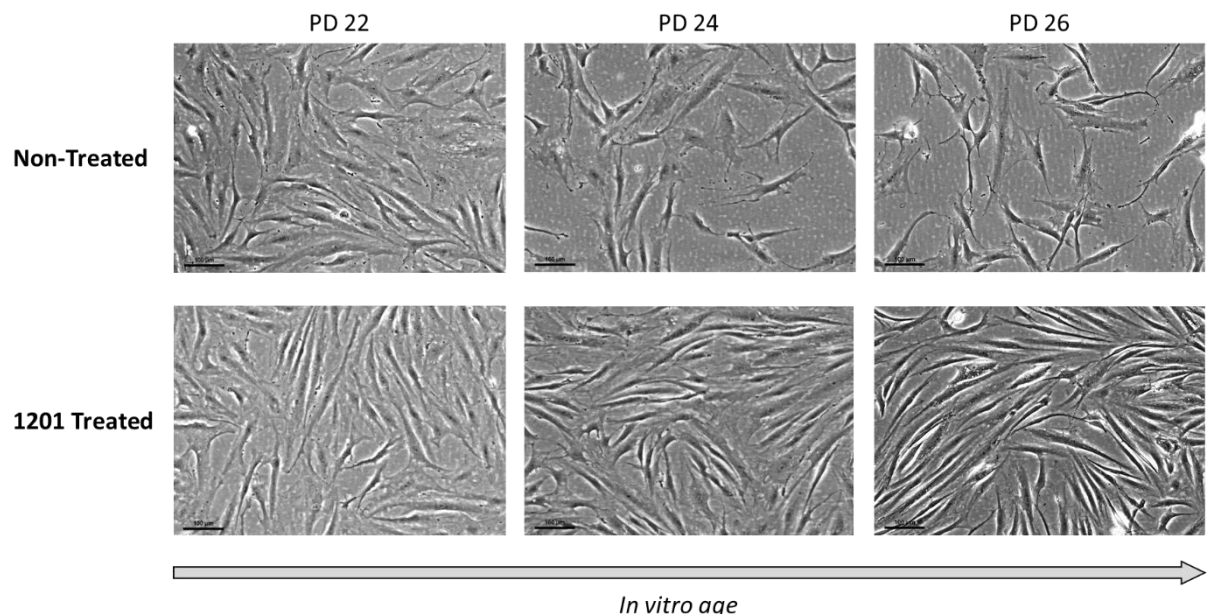


**Fig. 8** – Representative microscopic capture of 1201's morphological effect over the course of five cell passages. Treated and non-treated fibroblasts from donor 2 are shown paired from 3 different time-points. Cells from the 1<sup>st</sup> passage (left), 3<sup>rd</sup> passage (middle) and 5<sup>th</sup> passage (right) display the cumulative influence of 1201. Scale bar = 100 µm.

### 3.1.1.2. Treatment Reduces Fibroblasts' Contact Inhibition

Proliferation of treated and non-treated was monitored over several days while maintaining their culture conditions. A replicative young fibroblast population was also included for comparison.

For the first donor, the assay was performed after the 5<sup>th</sup> passage at population doubling (PD) 38.5 (Fig. 9A). Treated cells showed an initial lack of proliferation potential and trailed the other two populations at day 3. However, measures performed at day 7 and 10 demonstrated a significant higher cell number of 1201 treated cells when compared to the non-treated. Nevertheless, the replicative young fibroblasts had the best performance between the three, showing the highest confluent cell density and proliferation rate. These results were previously established and are only present here to maintain interdonor comparison consistency.

The other donor, had its proliferation assay executed after the 3<sup>rd</sup> passage at PD 24, while its replicative young counterpart was at PD 12 (Fig. 9B). Just after 3 cell passages with 1201 treatment, treated cells displayed a much higher growth rate through most of the proliferation assay than both the replicative young and the non-treated fibroblasts. Significantly higher cell numbers for treated cells

showed an enhanced growth curve and greater confluent cell density than the remaining two populations.

The results were consistent throughout all donors and differed only in the degree of improvement. 1201 treatment enhanced fibroblasts' ability to proliferate by reducing contact inhibition.

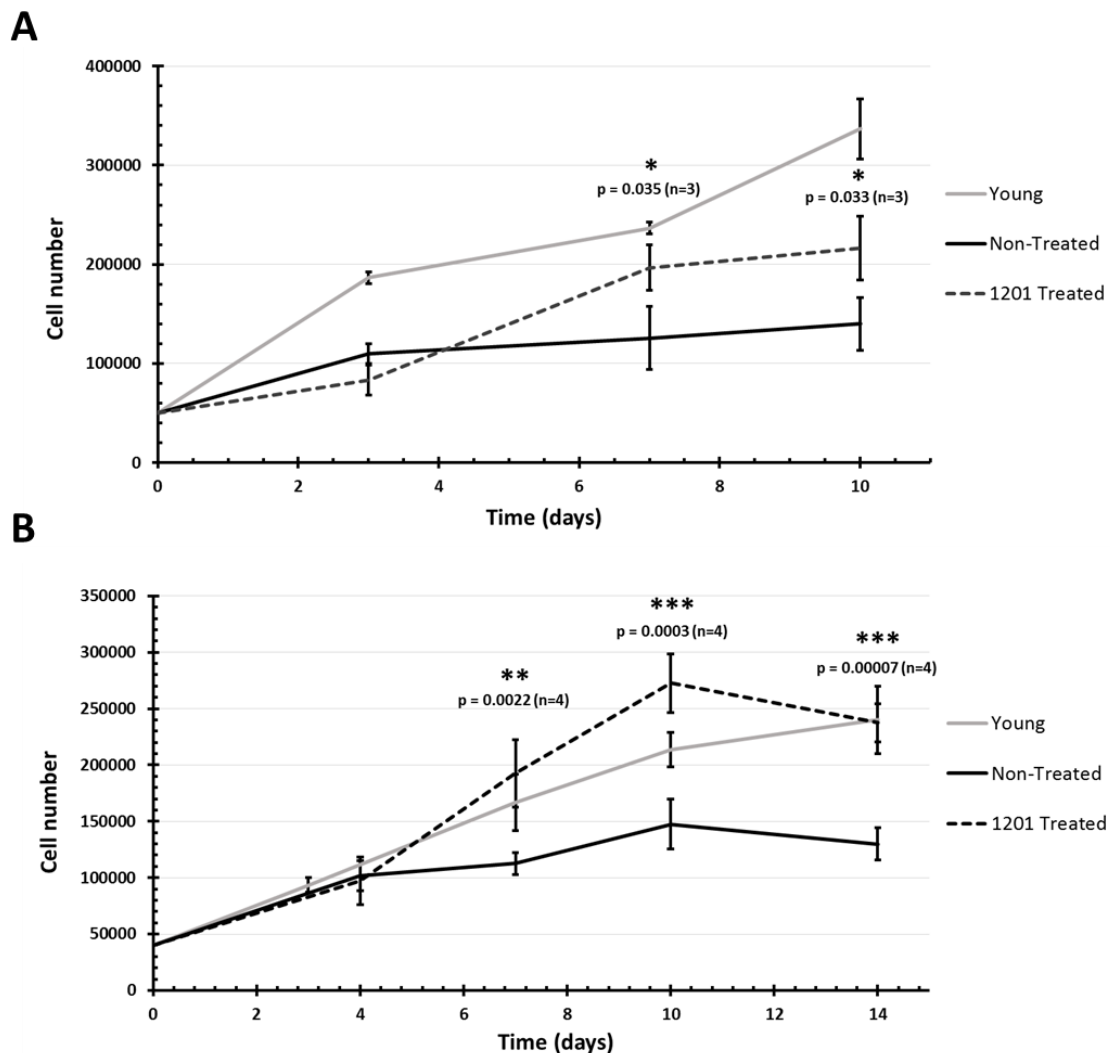


**Fig. 9** – Growth curves resulting from proliferation assays. (A) Fibroblasts from donor 1 at PD 38.5, except replicative young at PD 10. (B) Donor 2 derived fibroblasts at PD 24, while the replicative young fibroblasts were at PD 12. Significance is relative to differences between the 1201 treated and the non-treated cells. Data shown as mean  $\pm$  standard deviation. \* $p < 0.05$ ; \*\* $p < 0.01$ ; \*\*\* $p < 0.001$ .

### 3.1.1.3. 1201 Tips PRT Marker Expression Towards Papillary

Papillary and reticular marker levels were investigated to track gene expression changes due to 1201. Both RNA and protein were isolated after repeat of the experiment, but only protein was stored. RNA was isolated, transcribed and used for qPCR analysis. Netrin-1 (NTN1) and podoplanin (PDPN)

were chosen as papillary markers, while protein phosphatase 1 regulatory subunit 14A (PPP1R14A) and alpha-2-macroglobulin (A2M) were used as reticular markers<sup>128</sup>.

For the first donor, treated cells displayed a substantially different marker profile, in comparison to the non-treated (Fig. 10A). Fibroblasts exposed to 1201 showed a significantly higher expression of papillary markers, while having a lower expression of reticular. Overall, a consensus of markers infers that treated cells were more papillary and less reticular than their non-treated counterparts.

Similar behavior was verified in the second donor (Fig. 10B). However, a mixed result was obtained in the papillary markers. Whereas PDPN was increased in 1201 treated cells, NTN1 was significantly down-regulated. Still, reticular marker levels were much higher in non-treated cells than 1201 exposed fibroblasts, with the difference amid both populations being more considerable in this donor.

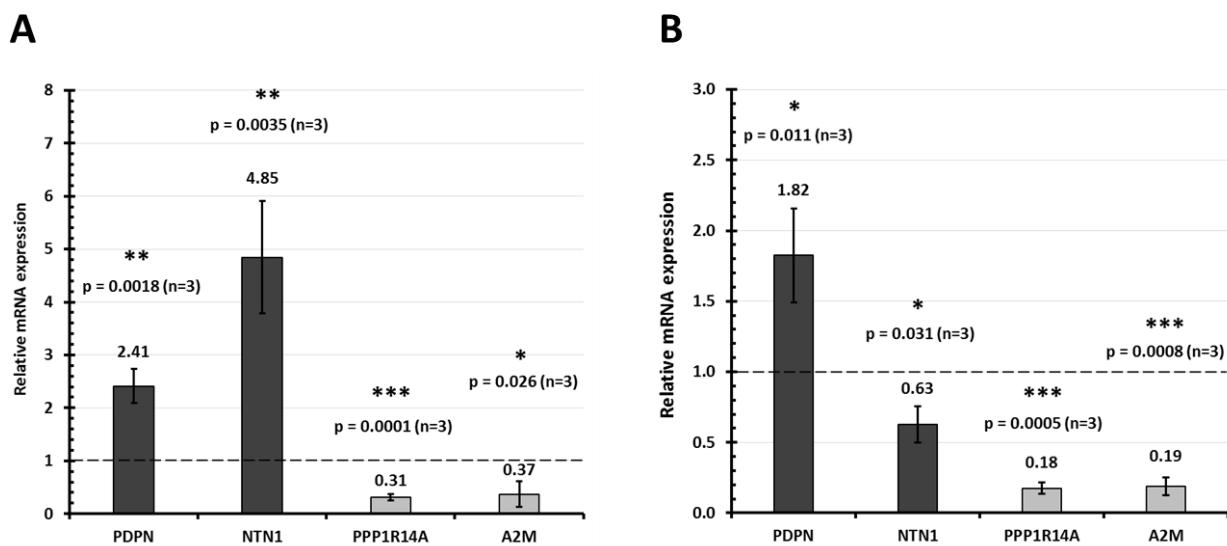


**Fig. 10** – PRT marker expression levels for both donors. Papillary markers (■) and reticular markers (□) were quantified for cells from donor 1 at PD 36 (A) and from donor 2 at PD 24 (C). For each marker, the 1201 treated sample was normalized by its respective non-treated, represented by a dashed line. Data shown as mean ± standard deviation. n.s. p > 0.05; \*p < 0.05; \*\*p < 0.01; \*\*\*p < 0.001.

### 3.1.1.4. Senescence Markers Are Influenced by 1201

As senescence is hypothesized to be the end-point of the PRT, influence on senescence markers was also observed. Cyclin-dependent kinase inhibitor 1 (p21) and SA-β-galactosidase were chosen as senescence markers, given their common usage for this matter. However, pre-mRNA-processing factor 19 (SNEV) was additionally used. Its connection with senescence was highlighted with overexpression and knockdown experiments, which were respectively able to extend the replicative lifespan and promote senescence in different organisms<sup>138,139</sup>.

In terms of gene expression, no variation between both populations was observed in p21 expression. However, SNEV was higher expressed in 1201 treated cells. In contrast to the previous

donor, an almost mirrored profile between donors is shown with p21 and SNEV expression levels (Fig. 11). Merely, the significance of higher levels of SNEV in treated cells versus non-treated cells was greater.

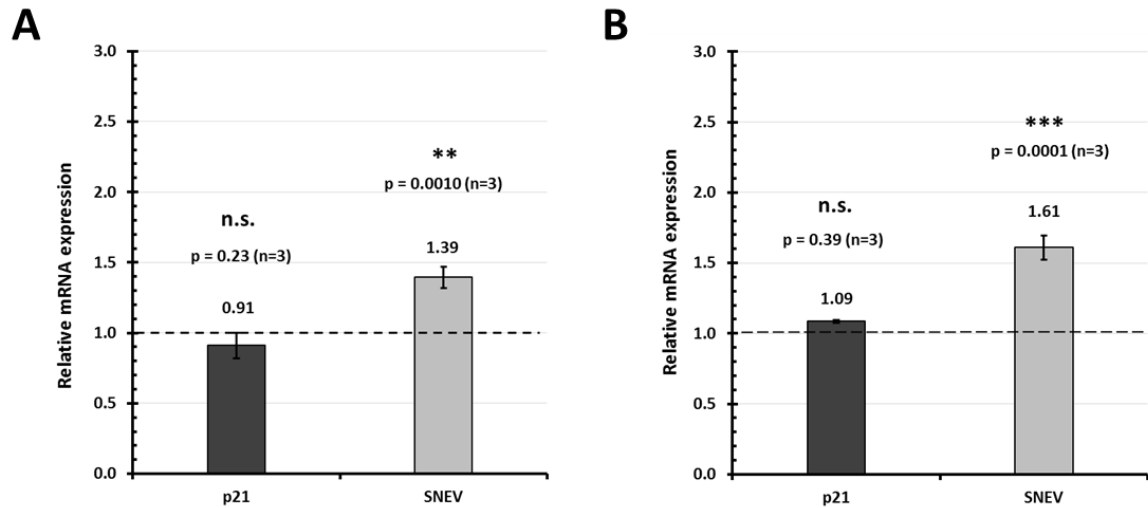


**Fig. 11** – p21 and SNEV expression was quantified for cells from donor 1 at PD 36 (A) and from donor 2 at PD 24 (C). For each marker, the 1201 treated sample was normalized by its respective non-treated, represented by a dashed line. Data shown as mean  $\pm$  standard deviation. n.s. p > 0.05; \*p < 0.05; \*\*p < 0.01; \*\*\*p < 0.001.

Afterwards, equivalent cells were subjected to a  $\beta$ -galactosidase staining, to visualize any 1201 influence on this senescent marker.

For the first donor, an increase of  $\beta$ -galactosidase positive cells is seen between replicative old non-treated cells and young (Fig. 12A). The low expression of  $\beta$ -galactosidase is rescued, justified by a significant reduction of positive cells in the 1201 treated fibroblasts of around 50%.

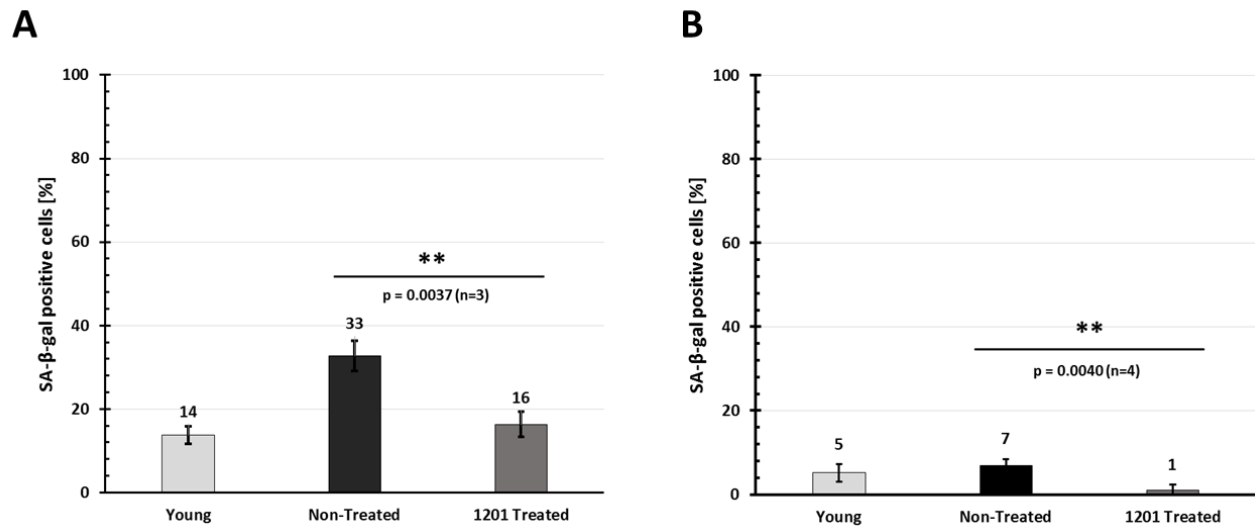


**Fig. 12** – Bar graphs quantifying the percentages of  $\beta$ -galactosidase positive cells. (A) Fibroblasts from donor 1 at PD 38.5 and (B) from donor 2 at PD 24. Data shown as mean  $\pm$  standard deviation. \*\*p < 0.01.

In the second donor, young cells' level of SA- $\beta$ -galactosidase is comparable to the older non-treated cells (Fig. 12B). However, a reduction can also be seen in 1201 treated fibroblasts when compared to the non-treated population. The treated population even showed a level inferior to the replicative young control.

Overall, low percentages of positive cells are observed, especially in the second donor. A clear positive effect toward decreasing the SA- $\beta$ -galactosidase is verified with 1201 treatment in both donors.

### 3.1.2. Short-Term Acute Treatment Rules Out Papillary Selection

Both donors possess a mixed population of papillary and reticular fibroblasts. Considering the proliferative differences between both subpopulations, papillary fibroblasts could have unintentionally been selected through consecutive passaging. Thus, the previously verified effects could have only manifested in papillary fibroblasts. As a way of assuring reticular fibroblasts also respond to 1201, a short-term acute treatment during 48 hours of the two donors was performed. After undergoing cell passage fibroblasts were treated with 0.1% 1201. After 48 hours, RNA was isolated and transcribed into cDNA. qPCR was performed to assess 1201's effect on papillary and reticular markers.

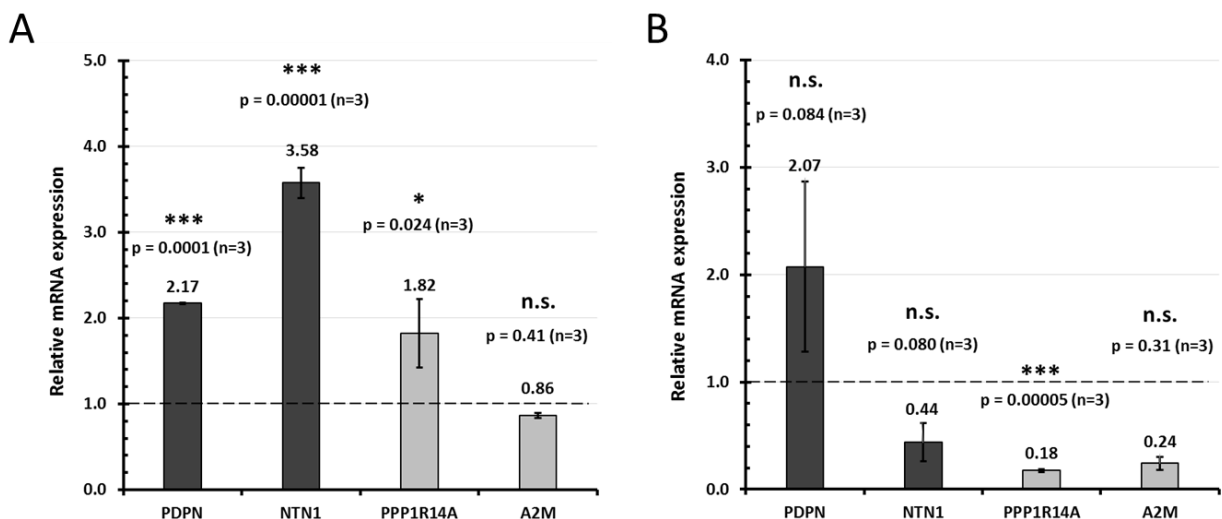


**Fig. 13 –** mRNA levels of reticular and papillary markers of acute 1201 treated and non-treated fibroblasts. (A) HDF Donor 1 at PD 34 and (B) HDF Donor 2 at PD 17 were tested for expression of papillary markers (■), PDPN and NTN1, and reticular markers (□), PPP1R14A and A2M. For each marker, the 1201 treated sample was normalized by its respective non-treated, represented by a dashed line. Data shown as mean  $\pm$  standard deviation. n.s. p > 0.05; \*p < 0.05; \*\*p < 0.01; \*\*\*p < 0.001.

After only 48 hours, considerable variations were noticeable between treated and non-treated (Fig.13). In the first donor, papillary markers were significantly more expressed in cells treated with 1201. Reticular markers had a mixed performance, with PPP1R14A also being more expressed in treated cells and A2M having no significant change amid both populations. In addition, visual alterations were present between treated and non-treated (Fig. 14). Fibroblasts appeared to gain a papillary-like

shape, displaying a thinner and elongated structure. In terms of cell density, 1201 treated cells appeared denser than the non-treated.

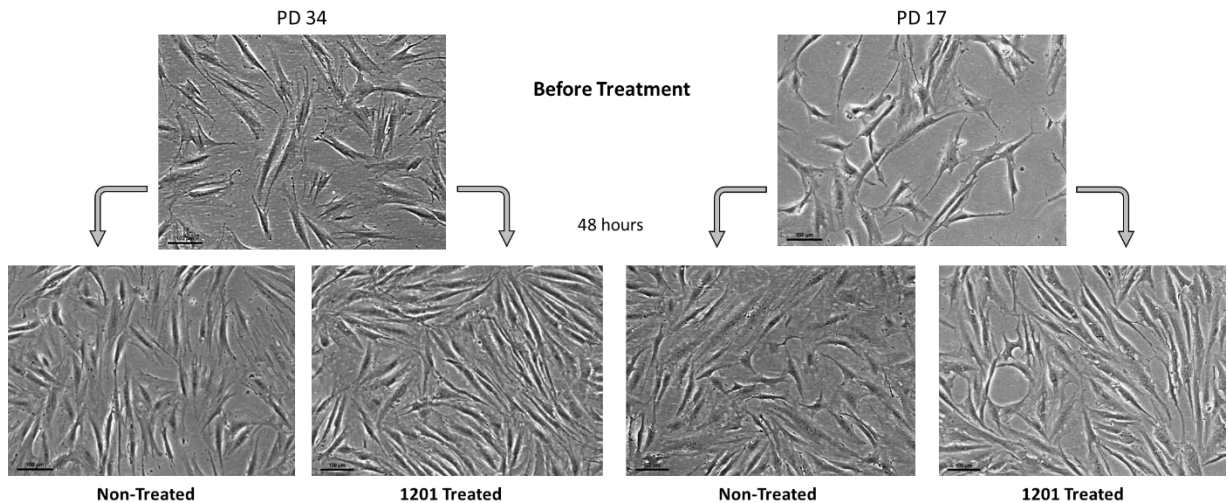


**Fig. 14** – Representative images of the visual effects of 48 hours of 1201 treatment on both donors. (Left) – Fibroblasts from donor 1 at PD 34 before 1201 treatment and the post-treatment scenario made up by treated and non-treated cells. (Right) – Similar arrangement, but with cells from donor 2 at PD17. Scale bar = 100 µm.

The acute treatment also had an effect in the second donor. PDPN expression in treated cells was higher but not significant, whereas NTN1 was lower and also not significant. Nonetheless, the levels of reticular markers were both reduced in treated cells, although A2M's difference was not significant. Similar morphological effects were observable after 48 hours of treatment with this donor (Fig. 14). Cell density effects were comparable between donors, but for donor 2 they were mitigated to a certain extent. Effects on the second donor appear to take more time to develop, although being clearly present after just 48 hours.

1201 didn't merely influence papillary, but also had an effect on reticular fibroblasts in both donors.

### 3.1.3. 1201's Influence Corroborated by Site-Matched Fibroblasts

Fibroblasts isolated from the same tissue, only from different dermal compartments, termed site-matched, were used to solidify previous results. By having separated treatments of the two kinds of fibroblast populations, 1201's relationship with each one could be clearly characterized without doubt.

Donor A was subjected to the PRT experimental design starting at PD 6 for the reticular cell line and PD 8 for the papillary cell line. Assays were performed at the 3<sup>rd</sup> passage.

Treatment with 1201 was responsible for causing morphological changes in site-matched fibroblasts with the same characteristics as mentioned before (Fig. 15). Both papillary and reticular cells became more elongated and thinner compared to non-treated. Therefore, 1201 has the unquestionable

ability of influencing both papillary and reticular fibroblasts, confirming results from the short-term treatment.

Proliferation assays resulted in mixed results between both types of fibroblasts. 1201 treated papillary fibroblasts had similar proliferation rates as non-treated, however cell numbers were slightly inferior to the non-treated papillary fibroblasts (Fig. 16A). Non-treated cells were significantly higher at time-point day 10.

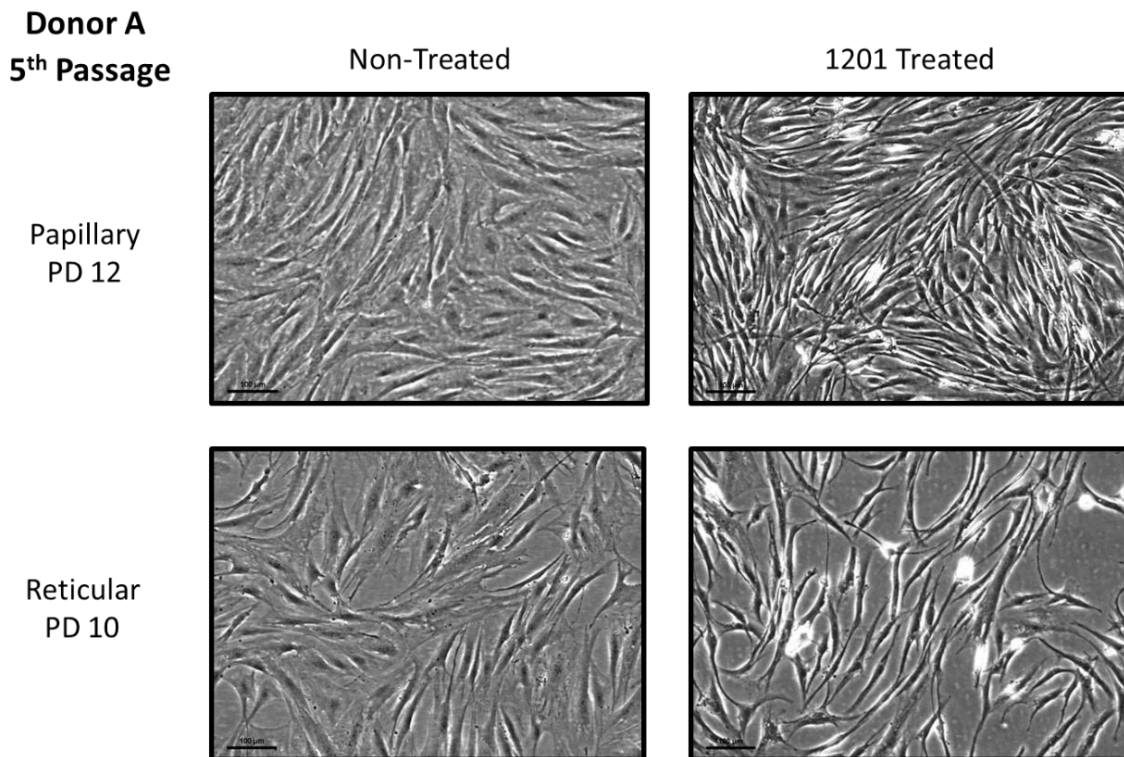


**Fig. 15** – Representative microscopic images depicting the effect of 1201 on site-matched fibroblasts from donor A. Scale bar = 100  $\mu$ m.

For reticular cells, treated and non-treated displayed an almost equivalent growth curve until time-point day 7 (Fig. 16B). After day 7, non-treated cell number stabilized, while 1201 treated fibroblasts continued to grow. This resulted in a significantly increased cell number at time-point day 10. The remaining assays that followed were pursued with only the reticular populations as the interest in 1201 laid with reversing or halting the PRT.

Thus, PRT marker expression was analyzed only in the reticular cell line from donor A and non-treated papillary fibroblasts were used as an early PRT control. Both papillary markers were significantly increased in treated fibroblasts (Fig. 17A). Surprisingly, PDPN expression levels of the treated and non-treated reticular cells were higher than the papillary fibroblasts. However, this didn't propagate to the NTN1 levels, since papillary expression was the highest, followed by treated cells and trailed by non-treated fibroblasts, showing a rescue of expression by 1201. With reticular markers, considerable variations were detected in the different populations (Fig. 17B). Non-treated cells demonstrated much higher expression of both PPP1R14A and A2M than their papillary counterparts, reaching increases of almost 70 fold.

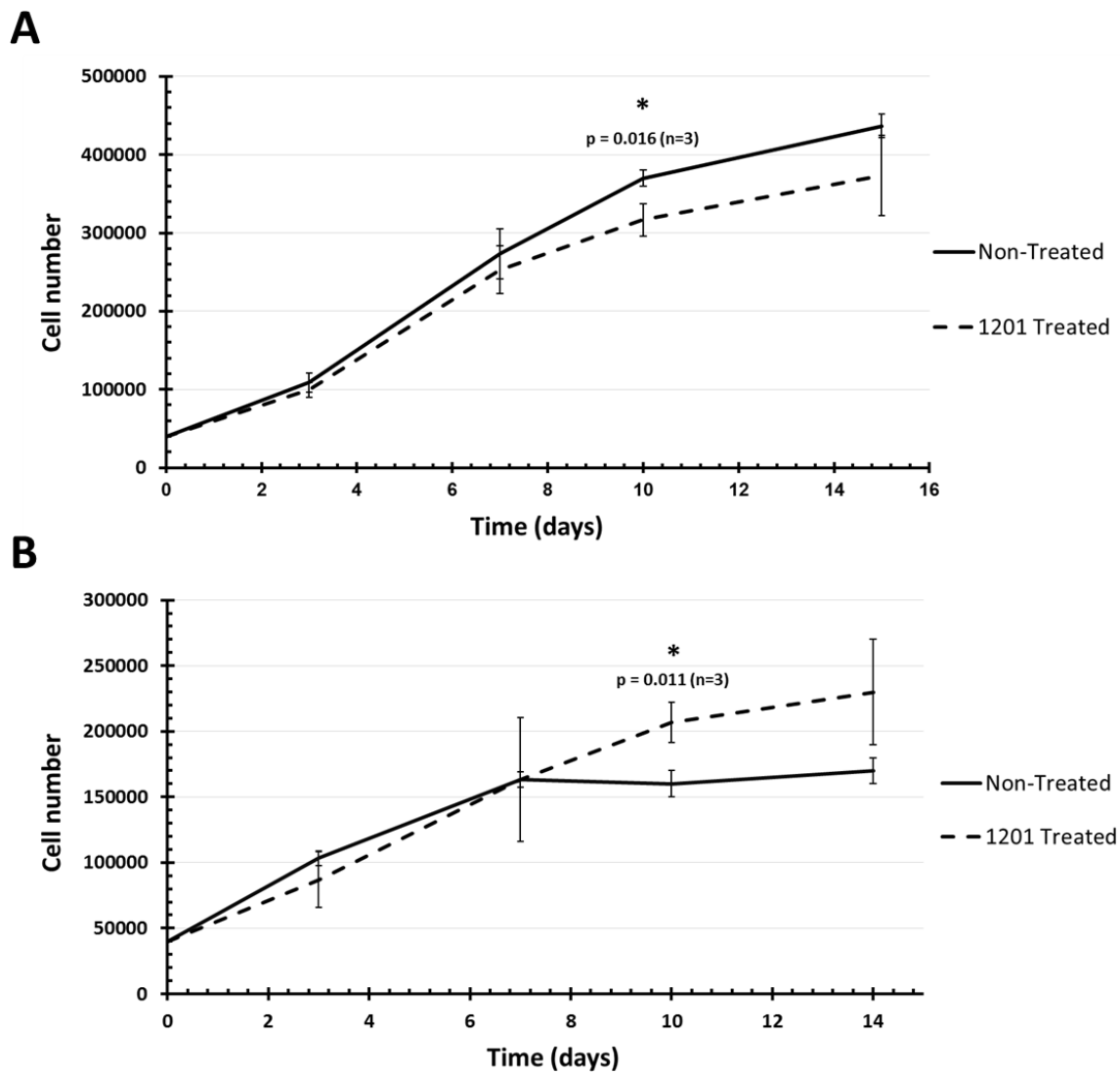


**Fig. 16 –** (A) Proliferation assay performed at the 3<sup>rd</sup> passage using 1201 treated and non-treated cells from the papillary cell line of donor A at PD 10. (B) Same assay, except with cells from the reticular population of donor A at PD 8. Data shown as mean  $\pm$  standard deviation. n.s.  $p > 0.05$ ; \* $p < 0.05$ .

1201 treatment reduced reticular marker levels by a similar substantial degree, returning the expression very close to the papillary levels.

In terms of senescence markers, 1201 didn't have any significant effect over gene expression levels (Fig. 18A). Both treated and non-treated reticular levels of p21 were 2-fold increased when compared to papillary levels. SNEV expression showed a decreasing trend from papillary to non-treated reticular, which was inverted with 1201 treatment to a certain extent.

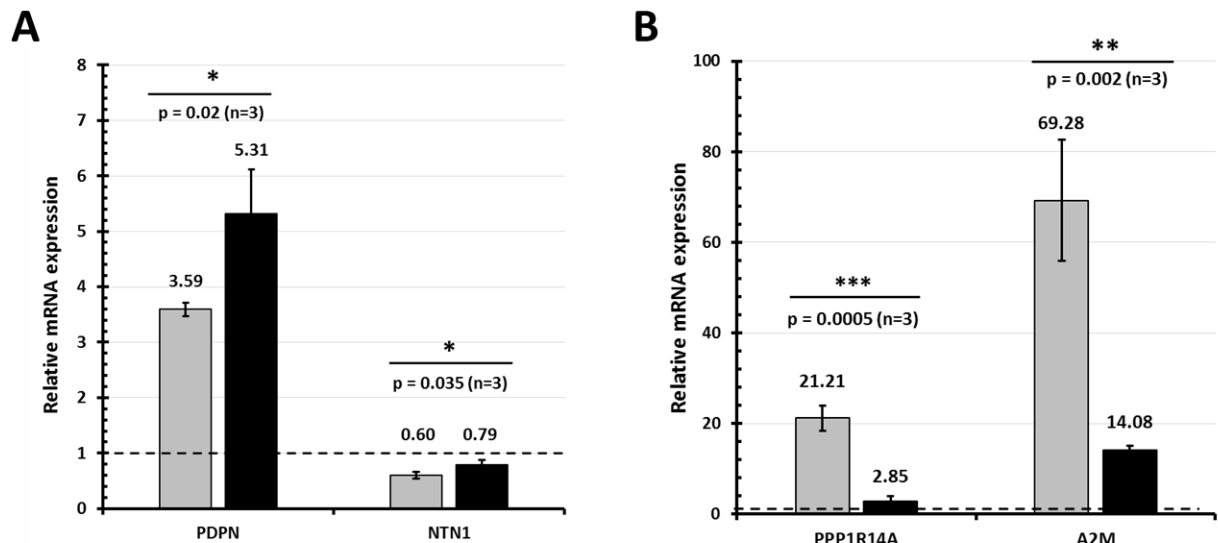


**Fig. 17** – Expression levels of papillary (A) and reticular (B) markers. (■) Non-treated and (■) 1201 treated reticular fibroblasts from donor A at PD 8. Both 1201 treated and non-treated reticular samples were normalized by its respective site-matched papillary fibroblast population at PD 5, represented by a dashed line. Data shown as mean  $\pm$  standard deviation. n.s.  $p > 0.05$ ; \* $p < 0.05$ ; \*\* $p < 0.01$ ; \*\*\* $p < 0.001$ .

SA- $\beta$ -galactosidase staining was performed to ascertain any possible influence of 1201 on this senescence marker. Equivalent number of SA- $\beta$ -gal positive cells were counted in both treated and non-treated (Fig. 18B). However, such extremely low percentages of positive cells prevented any evaluation of 1201 treatment, since a reduction wouldn't be discernable.

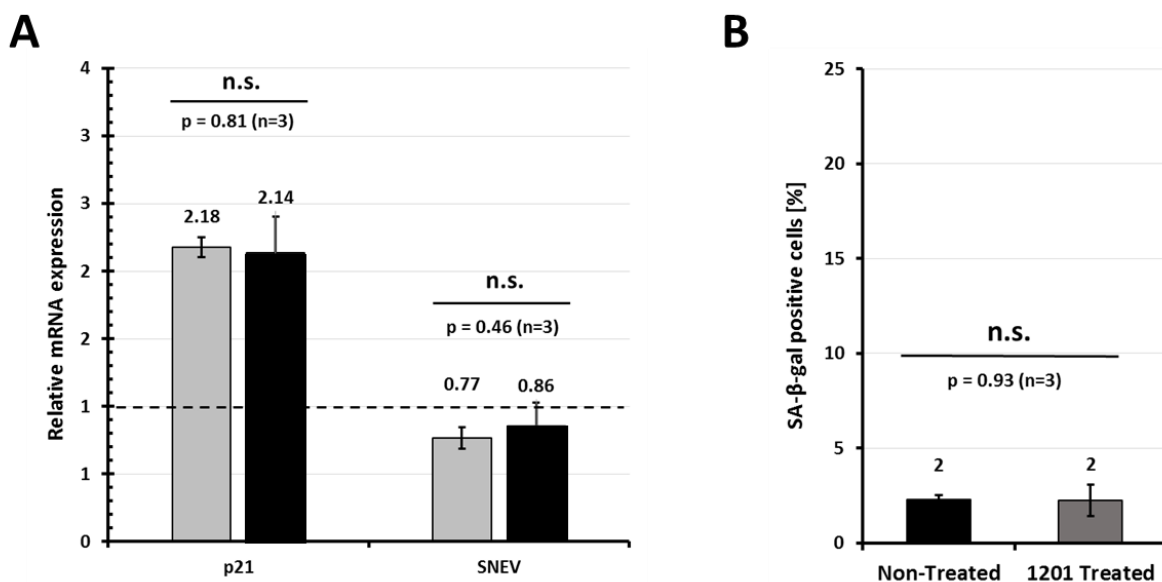


**Fig. 18** – Senescence marker expression levels. (A) p21 and SNEV relative mRNA levels. Both 1201 treated and non-treated reticular samples were normalized by its respective site-matched papillary fibroblast population at PD 5, represented by a dashed line. (B) Percentage of positive cells resulting from the  $\beta$ -galactosidase staining procedure of reticular fibroblasts from donor A at PD 8. Data shown as mean  $\pm$  standard deviation. n.s.  $p > 0.05$

When working with donors with a mixed population, 1201's overall effect couldn't be distinguished between delaying the PRT and reversing it. With the two subpopulations separated, 1201 was shown to be able to do both. Reticular fibroblasts' exposure to 1201 demonstrated a clear reversal of the normal PRT direction.

### **3.2.1201 Disrupts Cellular Senescence Through SASP Mitigation**

After defining 1201's ability in intervening with the balance between papillary and reticular fibroblasts, its relationship with cellular senescence, the end-point of the PRT, was assessed. The possibility of 1201 being able to attenuate the senescent phenotype was the first approach chosen to follow. Next generation sequencing (NGS) of 1201 treated and non-treated senescent and quiescent fibroblasts, was performed to visualize differences in overall transcript expression levels. This comparison was cross-checked with all known members of the SASP, showing a down-regulation by 1201 treatment of numerous factors (data not shown). Principal component analysis (PCA) of all four sequenced conditions revealed that 1201 treated senescent cells had a global expression level more similar to both quiescent populations than to the non-treated senescent. This led to several assays focused on discovering 1201's potential in causing SASP attenuation.

#### **3.2.1. HaCaT Growth Is Prevented With 1201 Treated Conditioned Media**

Previous work with a coculture of HaCaT cells and senescent fibroblasts resulted in HaCaT growth promotion by non-treated senescent cells. 1201 treatment managed to reduce HaCaT proliferation, displaying the first signs of influencing the SASP. As a means of assuring the secretions as the culprit of HaCaT growth stimulation and to exclude cell-to-cell contact effects, a variant of this experiment was planned. Based on production of conditioned media, HaCaT growth was exposed only to secretions from treated and non-treated premature senescent fibroblasts. Also, with this experimental setup, the plant extract didn't come into contact with the HaCaT cells, eliminating any possible direct effect of 1201 towards them.

Effect of 1201 on the SASP of premature senescent human dermal fibroblasts was investigated. Fibroblasts were subjected to the two week SIPS treatment, to originate stable premature senescent cells. A four day treatment with 0.01% 1201 of half of the senescent population followed. Fresh supplemented KBM was then added to the treated and non-treated fibroblasts and 24 hours was given for cells to express their SASP and give rise to conditioned media due to secreted factors. At the same time, 20 000 HaCaT cells were seeded into each desired well of the 6-well plate. These were grown in supplemented KBM for 2 days before adding conditioned media to have the culture deprived of growth factors. The next day, conditioned media from fibroblasts was harnessed and transferred to the HaCaT wells. Unconditioned KBM was also added onto HaCaT cells as a negative control. Enough conditioned

media was produced to be able to perform a media change at the half time-point of HaCaT culture. HaCaT cells were cultured with conditioned media for a time period that ranged from 6 to 8 days.

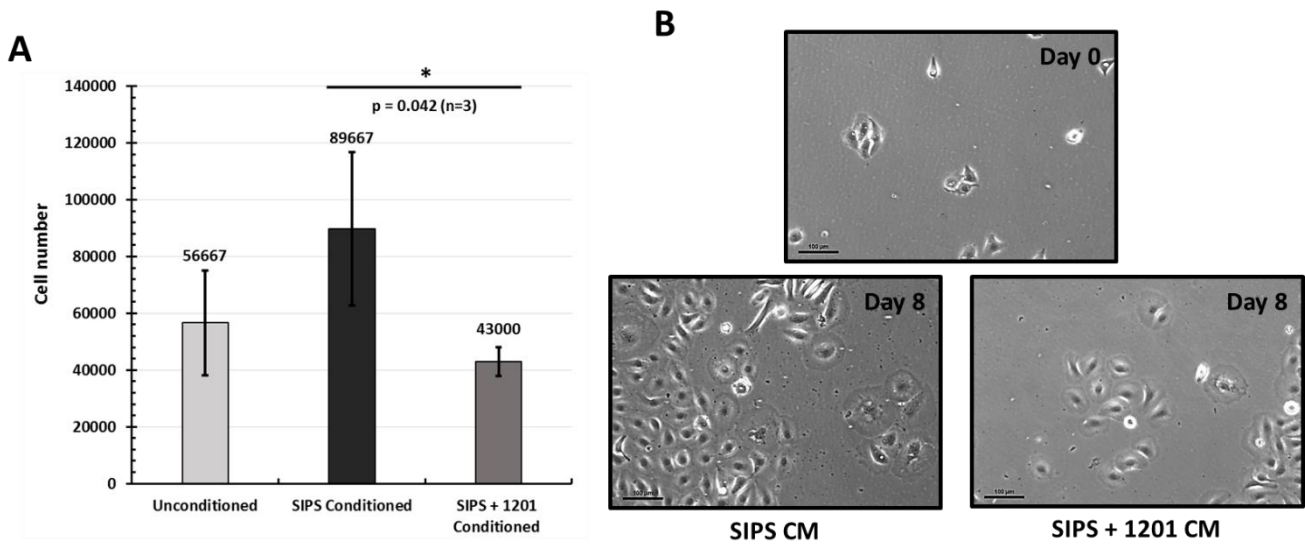


**Fig. 19** – (A) HaCaT cell number determination after 8 culture using conditioned media from donor 1 at PD 24. (B) Representative images of the same HaCaT culture at P40 during day 0 and of HaCaT cultured with both conditioned media prepared from non-treated and 1201 treated senescent cells during day 8. (SIPS CM) – Conditioned media from non-treated senescent cells. (SIPS+1201 CM) – Conditioned media from 1201 treated senescent cells. Data shown as mean  $\pm$  standard deviation. \* $p < 0.05$ . Scale bar = 100  $\mu$ m.

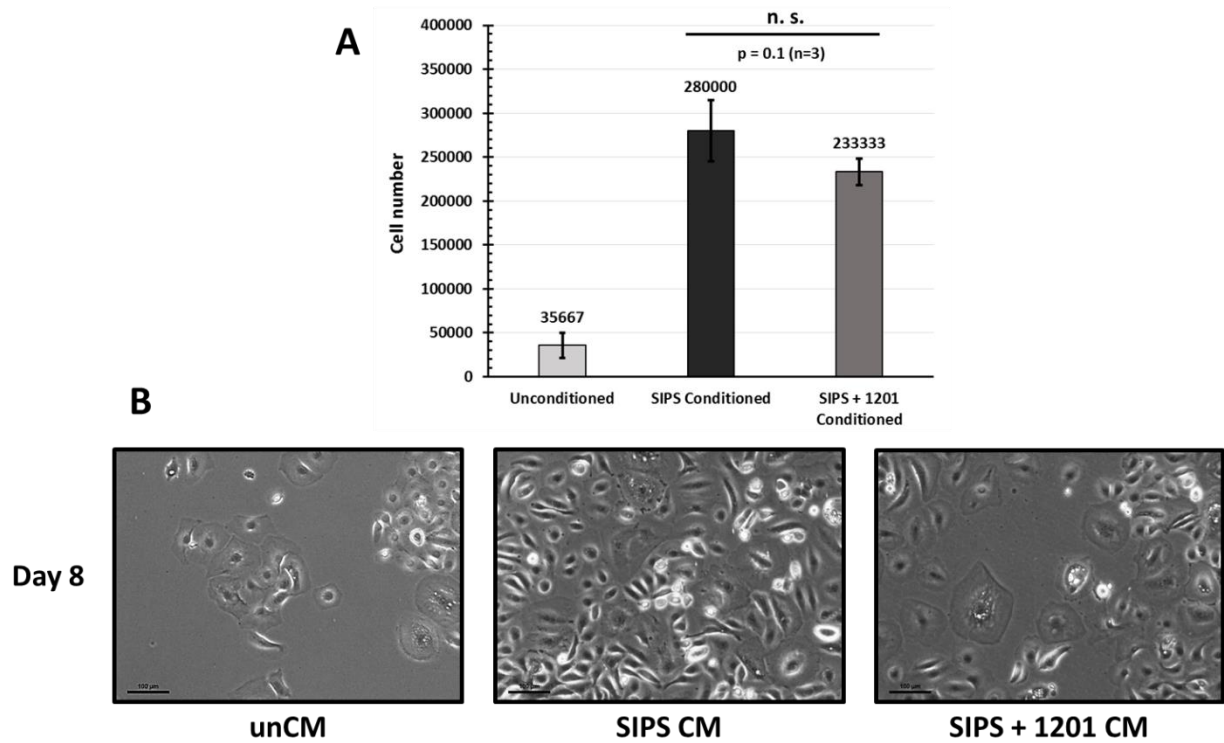


**Fig. 20** – (A) HaCaT growth cell numbers using conditioned media from donor 2 at PD 15. (B) Representative images of the HaCaT culture at P41 during day 8 under the three conditions for donor 2. (unCM) – Unconditioned Media. Data shown as mean  $\pm$  standard deviation. n.s.  $p > 0.05$ . Scale bar = 100  $\mu$ m.

Conditioned media from donor 1 promoted HaCaT proliferation, when compared to the unconditioned HaCaT cells (Fig. 19A). Cell growth was significantly reduced with 1201 treatment of conditioning fibroblasts. Treatment resulted in decreasing cell growth approximately to the level of unconditioned HaCaT cells. Microscopic visualization verified cell count results, displaying a greater number of HaCaT cells in wells cultured with conditioned media derived from premature senescent fibroblasts (Fig. 19B).

HaCaT cells that were cultured with conditioned media from donor 2 displayed a similar tendency as with the previous donor. Growth was substantially induced by conditioned media from premature senescent fibroblasts (Fig. 20A). Treatment with 1201 lowered the cell number, although not significantly. Visual inspection verified that non-treated conditioned media caused HaCaT cell confluence inside the well, limiting the cell number quantification by inhibiting proliferation through contact inhibition (Fig. 20B).

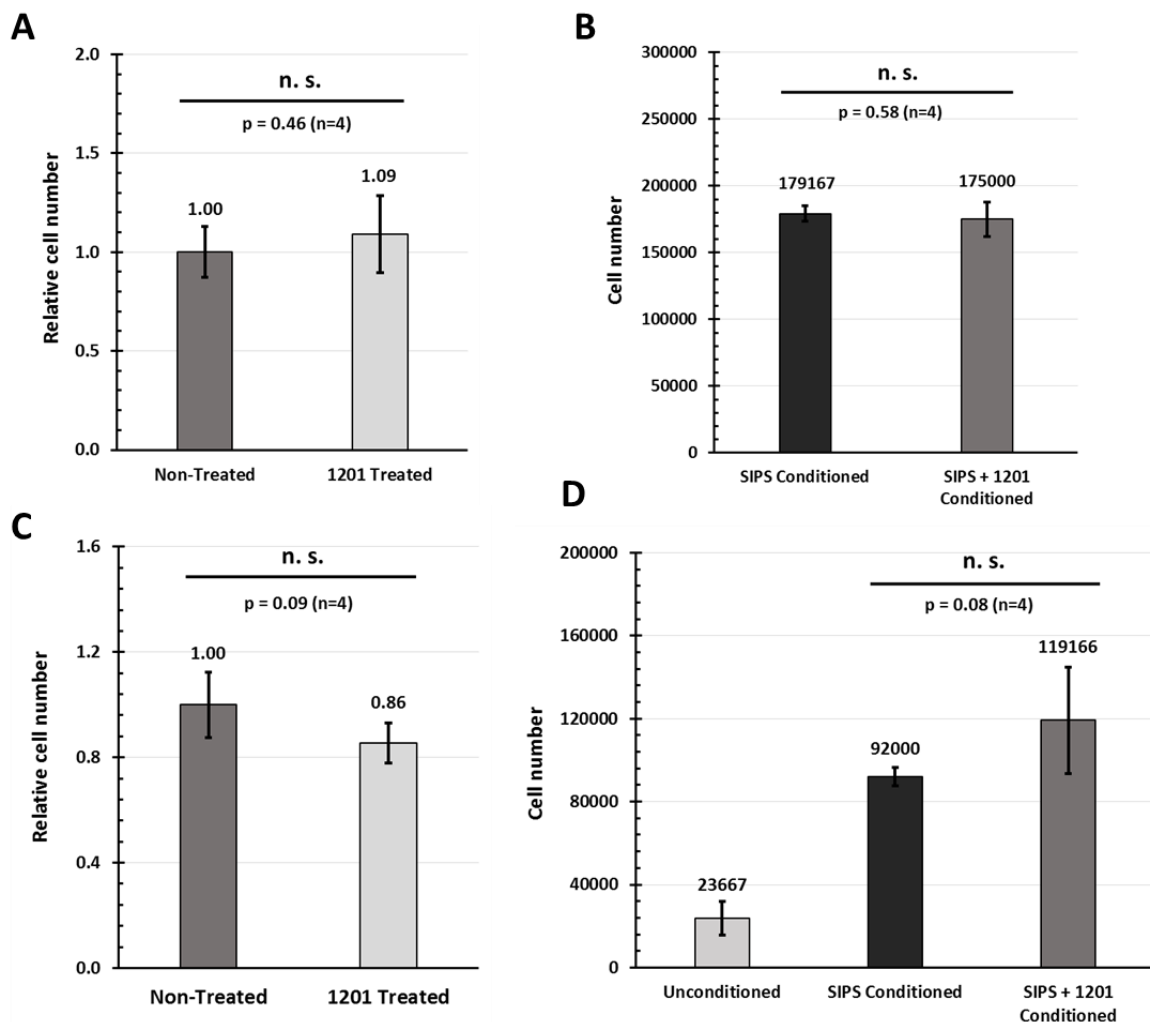


**Fig. 21** – Determination of fibroblast cell number from donor 2 after media conditioning for the first repetition (A) and the second (C). HaCaT cell numbers from the first repetition (B) and the second (D). Data shown as mean  $\pm$  standard deviation. n.s.  $p > 0.05$ .

The experiment for this donor was repeated two additional times with more biological replicates (Fig. 21). Additionally, after harnessing conditioned media, fibroblasts were counted. This measure served to exclude the possibility that any differences observed in HaCaT growth were due to more or less number of fibroblasts conditioning their respective media. In both cases, conditioning fibroblasts weren't significantly different in number. Furthermore, HaCaT population suffered the same growth promoting effect from conditioned media from both treated and non-treated senescent fibroblasts in both repetitions.

### 3.2.2. Unclear Modulation of Cytokine Secretion by 1201 Treatment

A chemotaxis assay was performed to discern 1201's action, specifically, towards cytokine release by premature senescent cells. Peripheral blood mononuclear cells were tracked in response to a cytokine gradient formed from two different and opposing fronts.

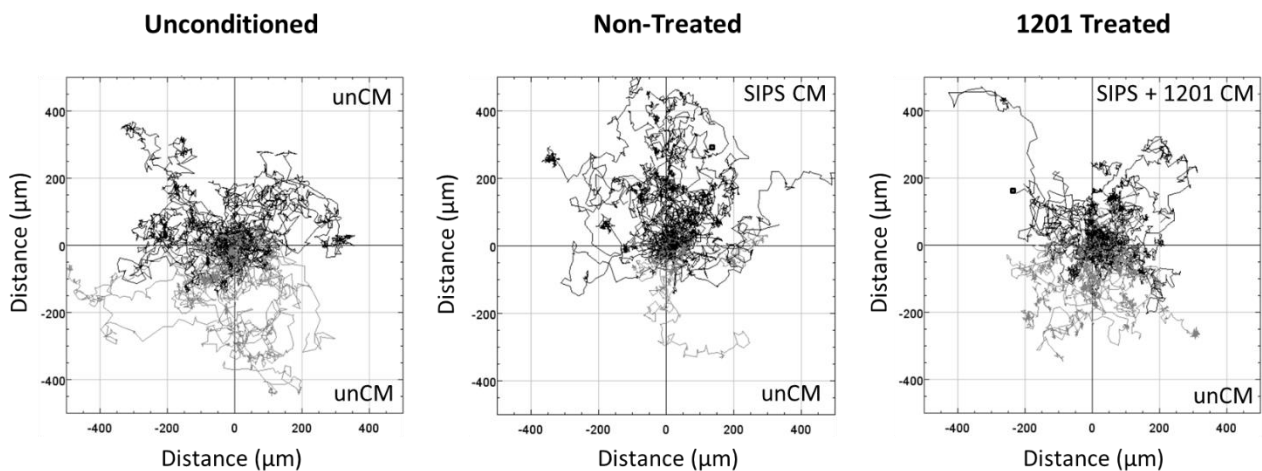


**Fig. 22** – Migration profile of three chemotaxis assays. (unCM) – Unconditioned Media (SIPS CM) – Conditioned media from non-treated senescent cells. (SIPS+1201 CM) – Conditioned media from 1201 treated senescent cells. Black paths correspond to cells whose migration ended in the top half of the graph, while grey paths display cells whose tracking finished in the lower half of the graph.

Conditioned media was produced from premature senescent fibroblasts from donor 1 at PD 23.5. Using unconditioned media on both sides of one channel, an even distribution of all tracked cell paths was observed. The calculated center of mass was localized near the origin of the axes (-31 μm, -7 μm). When non-treated conditioned media from senescent cells was used on one front, a significant migration response was observed. Most PBMCs ended their migration closer to the reservoir with the conditioned media, polarizing the distribution upwards. Thus, the corresponding center of mass was shifted (43 μm, 168 μm). 1201 treatment appeared to invert the migration profile closer towards what

was witnessed in the double unconditioned media assay (Fig. 22). A more compacted and evenly distributed migration was the result of 1201 treatment.

The assay was repeated two times in order to attain a total of 3 biological replicates (Appendix I). In contrast to the previous assay, only slight differences were observable between each condition tested for the second biological replicate. However, the shape of the migration profile changed amid conditions, from an expanded coil in the unconditioned/unconditioned assay to a compacted blob in the remaining two conditions which used conditioned media. Only horizontal variations of the center of mass were noticeable, while the vertical component maintained mostly constant.

The third replicate resembled the second in possessing small variations between conditions. A more opened and expanded shape belonged to the non-treated senescent conditioned media, while the other two were characterized by a compact globule.

### 3.2.3. Paracrine Senescence Wasn't Induced by SASP Conditioned Media

After discovering its effect on certain SASP factor groups, 1201's influence on a direct consequence of the SASP, bystander senescence, was determined. Being based on conditioned media, this experiment had a similar design as the previous. Cells from the first donor at PD 21 were subjected to SIPS treatment, giving rise to premature senescent cells. Half of the senescent fibroblasts were treated with 0.01% 1201 for 4 days. Besides the two senescent populations, a batch of proliferating cells at PD 26 was also cultured but not treated with 1201, to fulfill the role of negative control. Media conditioning was performed the day after, including media conditioned by proliferating cells. The three types of conditioned media were then transferred to wells previously seeded with 30 000 cells/well of fibroblasts from the same donor at PD 26. Cells were cultured with conditioned media during 5 days. BrdU incorporation was monitored to assess the percentage of dividing cells, whereas cell cycle analysis was performed through propidium iodide staining.

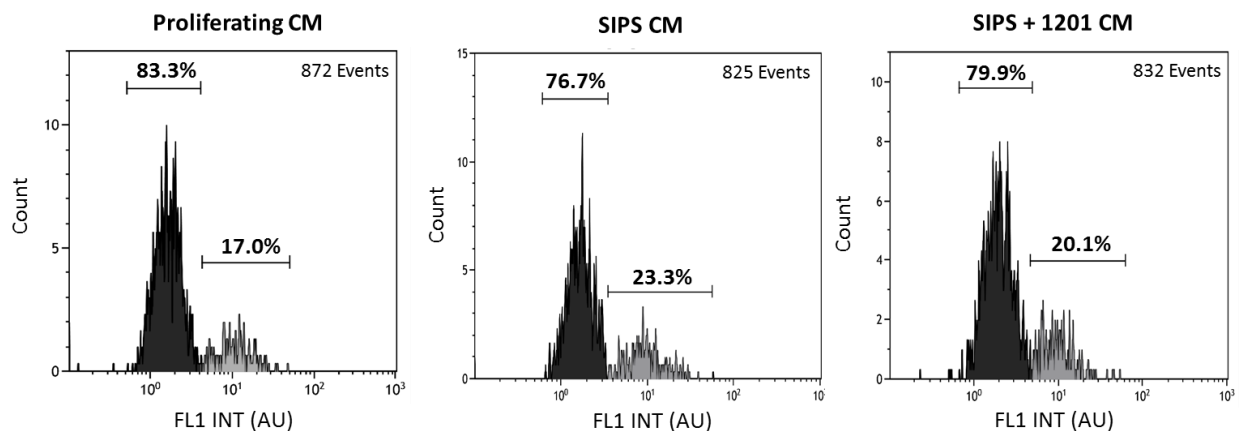


**Fig. 23** – Representative quantification of BrdU positive cells through flow cytometry. Dark cluster represents BrdU negative events, while grey is associated with BrdU positive events.

The same precaution was taken in determining the cell number of each senescent population which was responsible for media conditioning. No significant difference was observable between 1201 treated and non-treated cells (data not shown).

Comparable number of events were measured for all 3 conditions tested (Fig. 23). The fraction of BrdU positive cells for all types of conditioned media were comparable, with minor differences. Treatment with conditioned media wasn't able to promote growth arrest and thus a reduction of dividing cells wasn't seen. Therefore, bystander senescence wasn't established and cells were able to grow to confluence. 1201's influence over bystander senescence wasn't discernable, since this type of senescence wasn't observable with this experimental setup.

### 3.3. 1201 Demonstrates Signs of Senescence Eliminating Properties

The most promising approach in tackling senescence is eliminating senescent cells after their formation. A previously mentioned mouse model, capable of removing its p16-positive cells, showed the numerous improvements covering the whole body when their elimination was triggered. A whole group of drugs, termed senolytics, which try to achieve the SESC, holds much promise and is expanding. With all the previous results pointing to its interference with senescence, 1201 was therefore assayed for its possible SESC abilities.

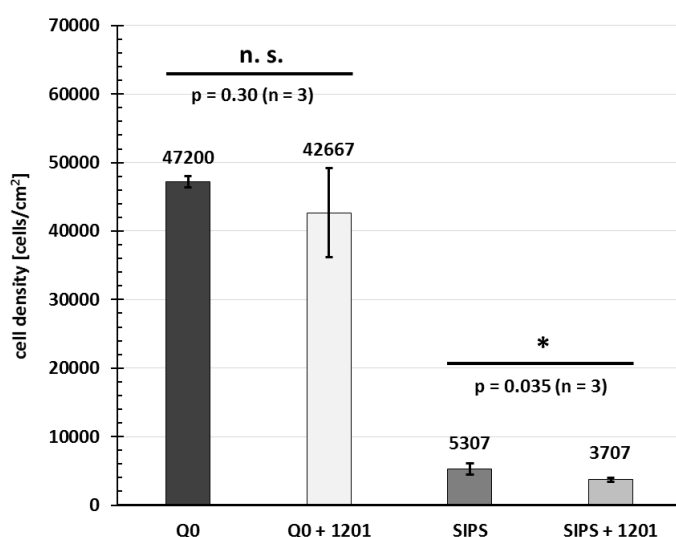


**Fig. 24** – Cell density levels of quiescent (Q0) and senescent (SIPS) cells from donor 1 with and without 1201 treatment. Data shown as mean  $\pm$  standard deviation. n.s.  $p > 0.05$ ; \* $p < 0.05$ .

Human dermal fibroblasts were seeded into T-25 flasks with an initial cell density of 3500 cells/cm<sup>2</sup>. After 24 hours, half of the fibroblasts were subjected to a two week SIPS treatment, to generate a pure population of senescent cells. Meanwhile the remaining cells were allowed to reach quiescence, through the two weeks, with corresponding media changes. With the SIPS treatment finished, a second stage of handling began, with 1201 treatment. Both senescent and quiescent

populations were split into two different subpopulations. One half's media was supplemented 1201, while the remaining half served as a negative control during 39 days. At the end, four distinct populations of fibroblasts existed, 1201 treated and non-treated senescent and quiescent cells. With the second phase completed, all fibroblasts were harvested and respectively counted, so as to determine their endpoint cell density. A photographic monitoring of the treatment was done. The entire experiment totalized in 50 days of cell culture, each population was represented by three biological replicates and was performed with two different fibroblast donors.

Premature senescent fibroblasts from donor 1 that were treated with 0.01% 1201 showed a significant decrease in cell density, compared to the non-treated senescent control (Fig. 24). The quiescent population showed no significant reaction to the long-term 1201 treatment, displaying a selective elimination behavior towards senescent cells. The efficacy of the SIPS treatment is observable, due to the discrepancy of cell densities between quiescent and senescent populations. Verifying the SESC property for this donor was previously completed work and was addressed here only to achieve an interdonor comparison.

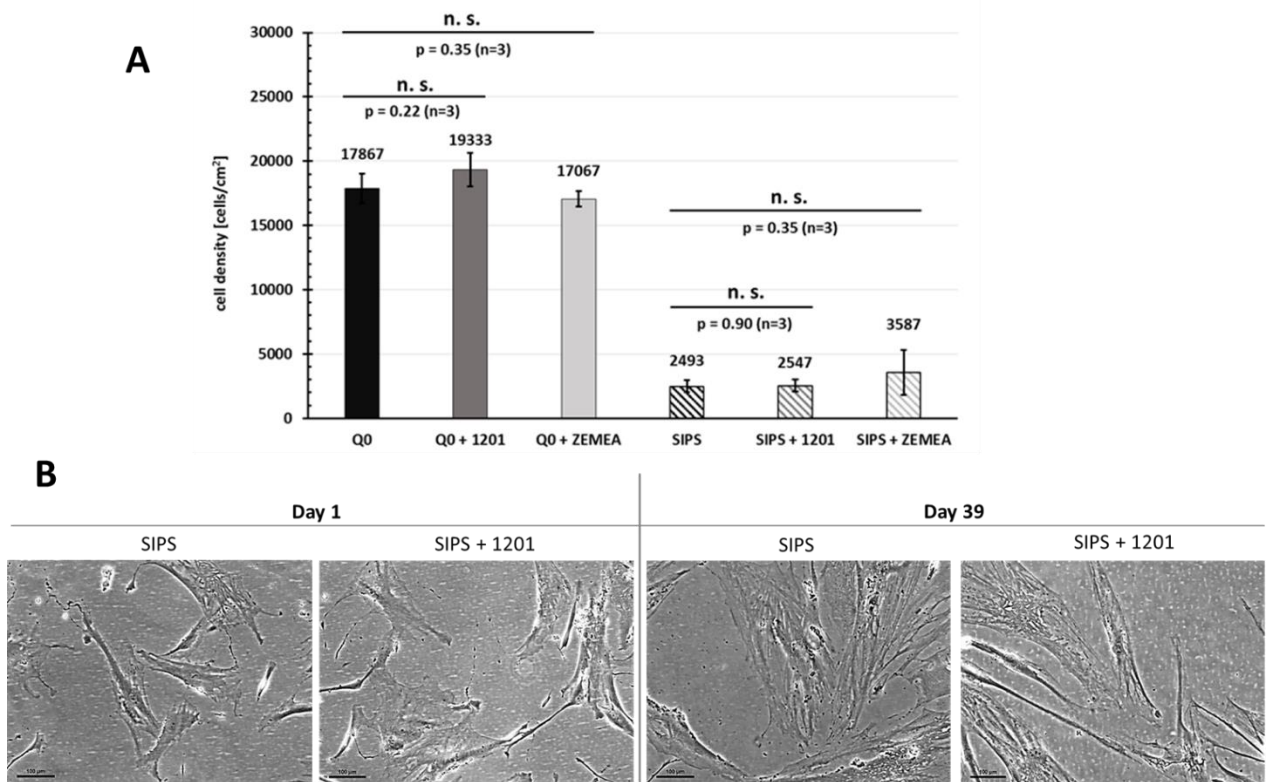


**Fig. 25 – (A)** Quantification of cellular density of quiescent (Q0) and senescent (SIPS) fibroblasts from donor 2 treated with 1201 and 1201's solvent, ZEMEA. **(B)** Representative depictions of the morphological cellular state of the various tested conditions. Data shown as mean  $\pm$  standard deviation. n.s. p > 0.05. Scale bar = 100  $\mu$ m.

Fibroblasts from donor 2 of PD 13 were chosen, when testing this donor. Although mostly repeating the experimental design for the second donor, changes were made. The exclusive role of 1201's solvent, propanediol, in influencing cells was additionally assessed and treatment with 1201 was

made with a concentration of 0.04%. No significant variations were observed between the conditions tested. While the SIPS treatment was reproducible among donors, no SESC capability was detected for this donor. Overall, smaller cell densities were measured, in comparison with the previous donor. Although the cell density didn't justify any existence of SESC abilities, morphological changes were observed. 1201 caused cells to elongate, thus pressuring them to alter their shape. This pressure usually resulted in cell death, a consequence which lacked for this donor.

Repetition of the experiment was accomplished with fibroblasts of slightly higher *in vitro* age, PD 15. A marginally different scenario was witnessed (Fig. 26A). Whilst, no reduction of the senescent population was observed, similar as beforehand, propanediol treatment caused a significantly higher cell density compared to the non-treated senescent cells. For the quiescent cells, the outcome was different. 1201 treatment significantly reduced the density by approximately 20%. Propanediol wasn't responsible for any changes, maintaining a similar cell density as the non-treated fibroblasts.

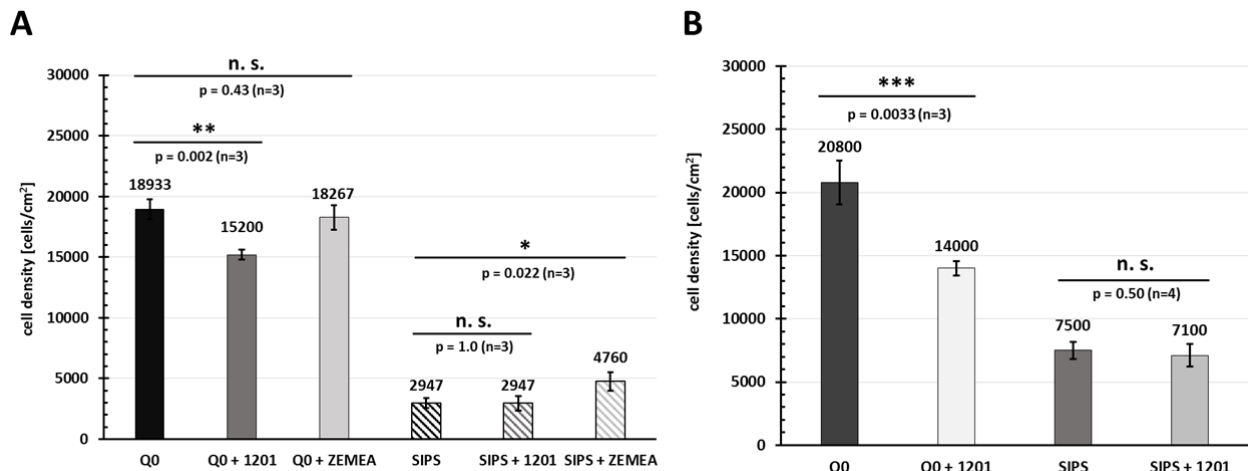


**Fig. 26** – Cell density of two repetition trials from quiescent (Q0) and senescent (SIPS) fibroblasts from donor 2 treated with 1201 and 1201's solvent, ZEMEA. Data shown as mean  $\pm$  standard deviation. n.s.  $p > 0.05$ ; \* $p < 0.05$ ; \*\* $p < 0.01$ ; \*\*\* $p < 0.001$ .

The third attempt to reproduce the properties found in the first donor brought more modifications to the experimental workflow. A concentration of 0.1% 1201 instead of the previous 0.04% was applied, while propanediol treated cells weren't included into the setup. Fibroblasts of PD 13 were seeded into larger T-75 flasks and 4 replicates of all the senescent populations were prepared. Once again, long-term treatment didn't show any significant alteration, even though a small reduction trend of the 1201 treated cells was visible (Fig. 26B). In contrast, 0.1% of 1201 treatment considerably reduced the quiescent population, close to 30%.

### **3.4. PRT Validation With Site-Matched Fibroblasts**

The human dermal fibroblast aging process is largely based on the papillary-to-reticular transition hypothesis. With the availability of site-matched papillary and reticular fibroblasts, the opportunity to verify this hypothesis couldn't be wasted. Thus, all PRT markers used were employed to confirm reported differences in gene expression between papillary and reticular fibroblasts. At the same time the reliability and robustness of the markers, throughout three different donors was determined. Also, proliferation rates and contact inhibition differences previously reported between both site-matched fibroblasts were attempted to be verified.

#### **3.4.1. Site-Matched Fibroblasts Display Distinct Marker Expression**

With site-matched fibroblasts from three different donors, the reliability of the papillary and reticular markers was judged. Also, senescence marker levels were obtained, in search of differentiated expression suspected by the papillary-to-reticular transition.

PDPN was significantly higher in reticular fibroblasts from two donors, A and B, while being significantly lower for donor C. NTN1 had a behavior worthy of a papillary marker, as through all three donors, NTN1 was very significantly increased in papillary samples compared to reticular. While PDPN showed some concerns as a papillary marker, NTN1 didn't display any doubt over its attributed role (Fig. 27A).

The reticular markers displayed great correlation between reticular and papillary fibroblasts. All donors exhibited increased A2M and PPP1R14A levels in their reticular samples (Fig. 27B). Considerable significance was observable for these two markers, solidifying them as consistent reticular markers.

SNEV expression profile was similar and stable between every donor. More SNEV expression was present in papillary samples and these differences were significant except in donor C. The other senescent marker, p21, had a mostly inverted behavior of SNEV, specifically observed in donor A and C. Levels for donor B weren't significantly different, unlike for the remaining donors (Fig. 27C).

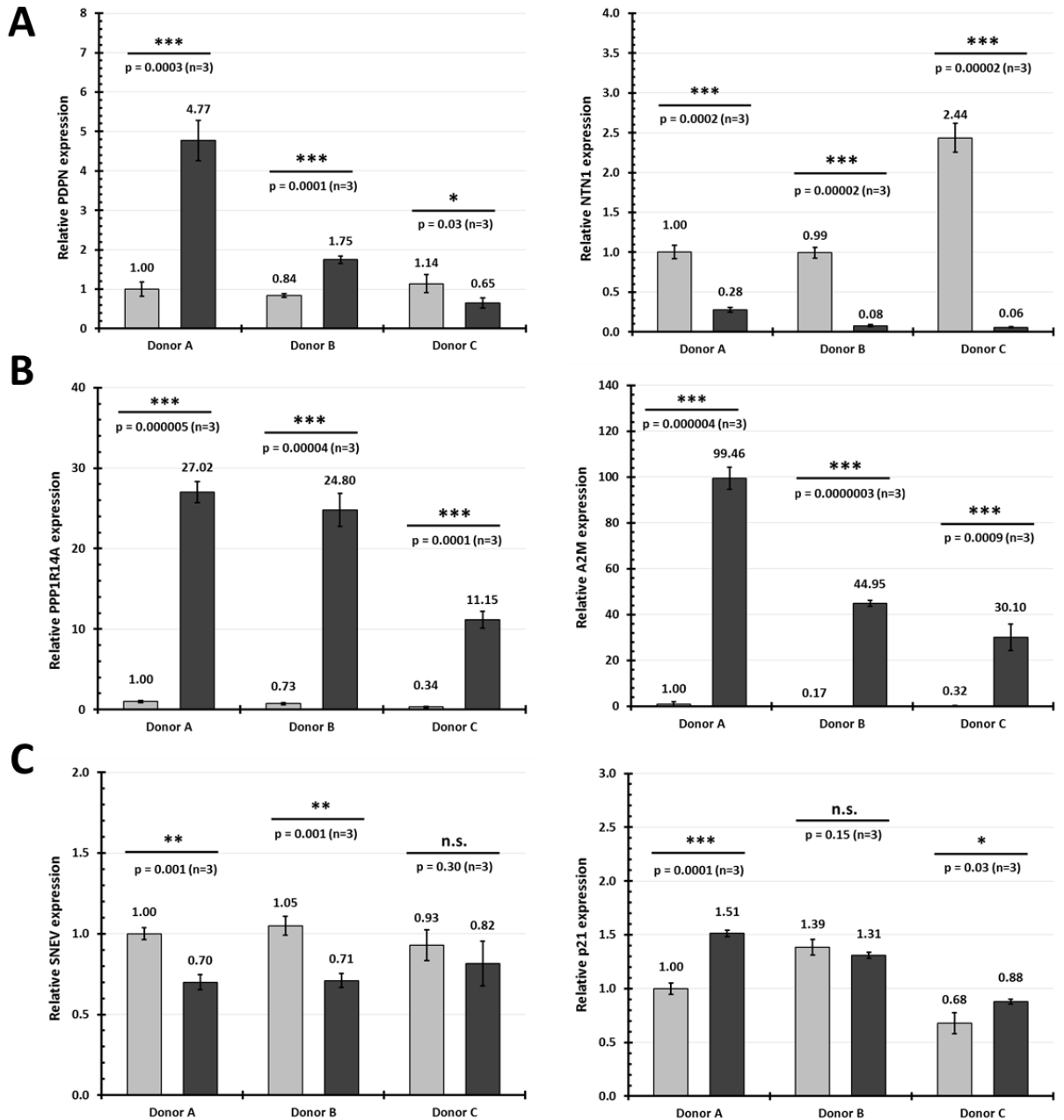


**Fig. 27** – Determination of mRNA expression levels of papillary (PDPN and NTN1) (A), reticular (PPP1R14A and A2M) (B) and senescent markers (SNEV and p21) (C). Site-matched papillary cell lines (◻) and reticular cell lines (■) from three donors were tested. All samples were normalized by donor A's papillary cell line levels. Data shown as mean ± standard deviation. n.s. p > 0.05; \*p < 0.05; \*\*p < 0.01; \*\*\*p < 0.001.

### 3.4.2. Papillary and Reticular Fibroblasts Differ in Their Contact Inhibition

Lifespan of every donor with site-matched fibroblast were carried out (Fig. 28). Reticular fibroblasts demonstrate different growth kinetics compared to papillary. Increased slopes are present in every papillary population compared to reticular, consequence of lower contact inhibition and higher

cell densities. One reticular fibroblast cell line that began their lifespan with a higher number of population doublings was rapidly surpassed by papillary cell lines that started with a lower value of PD. A widening gap is verified in every single donor between their papillary and reticular fibroblasts, confirming intrinsically diverse growth behavior amid papillary and reticular fibroblasts.

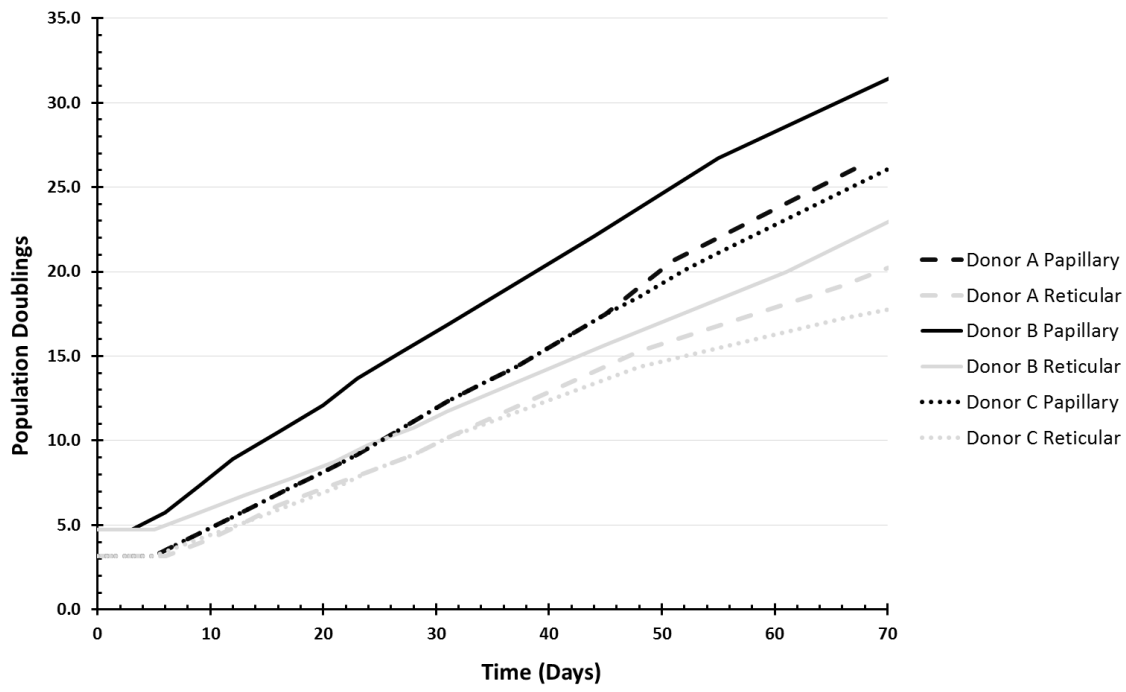


**Fig. 28** – Representation of growth curves from every site-matched donor, giving rise to six lifespans.



## 4. Discussion

Multiple assays were conducted to discern 1201's connection to senescence. Through every result, evidence has been uncovered in correlating this plant extract with senescence. Its action was seen to be wide and spread out in tackling senescence from multiple fronts.

### 4.1. Delaying Cellular Senescence

The papillary-to-reticular transition is hypothesized to be a fibroblast differentiation process associated with age, which ultimately ends in senescence. The possibility of being able to intervene on the PRT was assessed with several kinds of 1201 treatments.

#### 4.1.1. Thorough PRT Evaluation Shows 1201 Promotes Papillary Fitness

After initially identifying, to some extent, 1201's effects over the balance between papillary and reticular fibroblasts, a more thorough treatment regime was developed, to properly follow the PRT. An issue worth highlighting is the comparability of an engineered *in vitro* PRT with its *in vivo* situation. As with all *in vitro* studies, the struggle is assuring that knowledge gained is transferable to the *in vivo* reality. Nevertheless, these are simply the initial steps in describing 1201 and as such only *in vitro* studies were performed. Several assays were planned to recover the most from following treated and non-treated fibroblasts through 3-5 cell passages.

Photographic recording helped to detail the morphological changes observed in the initial screening. 1201's effect was cumulative over the course of the treatment, reaching a peak at the end time-point. Furthermore, heightened contrast, a new characteristic, was observable in 1201 treated cells, inferring a gain in cell height and compactness. These new features are also distinctive of papillary fibroblasts, hardening 1201's papillary promoting role. Increased contrast, joined with previously mentioned morphological changes, such as elongation and loss of cell width, constituted the visual consequences of 1201 treatment. Treatment of donor 2 was especially interesting, since an extended duration of exposure caused its fibroblasts to almost reach papillary-like states equivalent to donor 1. Thus, fibroblasts from donor 2 seem to be able to narrow, to certain extent, initial donor differences with enough amount or exposure duration of 1201. This observation is important, as it demonstrates that 1201's interdonor variability is due to the donors' different initial positions on the PRT pipeline. The closer fibroblasts from a specific donor are to becoming completely reticular, the more 1201 is needed to regain the same papillary-like morphological phenotype.

Information about contact inhibition, cell density and growth rate can be obtained from proliferation assays. Thus, caution is needed when examining results from this kind of assay. For both donors, an expected higher growth curve for replicative young compared to non-treated cells was visible. However, the growth curve created from 1201 treated cells had different behavior, based on the donor. While being flanked by the other two curves in donor 1, the 1201 treated growth curve was the

best performing of all three for donor 2. Thus, by observing the growth curve as a whole, it is possible to pinpoint 1201 treated cells' stage in comparison with the other populations, concerning proliferation characteristics. The situation for donor 2 was especial, since 1201 treated cells managed to overshoot replicative young cells. Young fibroblasts, the farthest away from reaching senescence, should detain the most growth capabilities. But besides being young, the ideal proliferative cell population would also need to consist of pure papillary fibroblasts, since reticular cells have a lower growth potential. However, the exact characterization of these two donors isn't available to discern the proportions of papillary and reticular populations. Therefore, if donor 2 were to possess a larger number of reticular cells, young fibroblasts from donor 2 might not be representative of the most proliferative cells. Considering the known effects of 1201 treatment, inducing a papillary-like state, treated cells in the proliferation assay may have increased the papillary ratio to a level even higher than the replicative young cells from donor 2.

The 1201 treated growth curve by itself has interesting features. Before reaching the growth-inhibited plateau in the end, treated cells tend, in a first stage, to trail non-treated with a lower proliferation rate. Afterwards, the slope drastically alters itself, causing treated cells to exceed non-treated cell number levels. This biphasic behavior is present in every donor.

Initial logic would describe higher or lower cell confluence as being simply dependent on the geometric shape of the cells. Nevertheless, cells also possess a mechanism to sense the presence and direct contact of cells, which lead cells to start growing in another direction to avoid growth collisions, termed contact inhibition. Therefore the final plateau is reached through a combination of both contact inhibition and maximum cell density confluency. Since reticular cells have at the same time a higher cell area and increased contact inhibition, any papillary inducing improvement through 1201 treatment causes a different plateau to appear. This manifested in every donor, showing how 1201 has a deeper effect than merely changing the shape.

Additionally, abnormal growth was never observed. This rested concerns over possible evasion of the senescence mechanism leading to cancer development. Thus, 1201 has a focus on extending the healthspan instead of cell immortalization.

From these proliferation assays, much information was retrieved related to cell growth and *in vitro* characteristics, such as confluency cell density, amount of contact inhibition and proliferation rates. These are the first indicators of functional change in 1201 treated cells.

Marker expression levels can dissipate any doubt over cell transformations. Two markers for each fibroblast cell state were chosen. Their selection as markers derived from the gene expression study performed in papillary and reticular fibroblasts and was not based on their intrinsic functions<sup>128</sup>. NTN1 corresponds to a laminin-related secreted protein, which has been described as an axon guidance factor, thus being responsible for neural development<sup>140</sup>. The other papillary marker, PDPN, is a transmembrane mucin-like protein, whose function has been linked to cytoskeleton reorganization through Ezrin/Radixin/Moesin (ERM) protein interaction, possibly having a role in promoting tumor aggressiveness. On the other hand, PPP1R14A as a reticular marker, possesses the role of a cytosolic inhibitor of protein phosphatase PP1-alpha catalytic subunit (PPP1CA), one of three sections of the

protein phosphatase 1 (PP1), an important cell cycle regulator<sup>141</sup>. Finally, A2M, also a secreted protein, is known as a multiple protease inhibitor through entrapment<sup>142</sup>.

Together, in both donors, 1201 treated cells exhibited higher papillary marker and lower reticular marker levels, with the exception of NTN1 for donor 2. Having such consistency is a considerable result, since the four markers seem to be independent between each other. Although NTN1 levels in donor 2 go against the remaining markers, this specific quantification was the result with the lowest statistical support. The choice of using two markers for each cell state becomes advantageous in these situations, where detection of debatable inconsistencies is facilitated. These markers, if not fully studied and understood, can in certain conditions offer controversial results. The assessment of marker levels corroborated previous assays in attributing 1201 a role in intervening in the PRT, specifically in promoting the papillary state.

The PRT begins with papillary fibroblasts, goes through the reticular state and in the end reaches senescence. As a cell population becomes more reticular, it also comes closer to senescence. Consequently, it became reasonable to assess senescence markers such as p21, SNEV and SA- $\beta$ -galactosidase activity.

The senescence markers had mirrored results for both donors. p21 levels remained constant and weren't affected by 1201 treatment. It may appear to go against previous SA- $\beta$ -galactosidase results, but p21 is a late senescence marker. As fibroblasts tested are still far away from a mature senescent state, the observed p21 expression profile was expected. However, changes in SNEV were noticeable and statistically significant. As SNEV overexpression has been reported to delay senescence and its inhibition to promote senescence, its expression levels infer inverse conclusions compared to p21. As SNEV is higher expressed in treated cells of both donors, 1201 gains more arguments of working against senescence.

Maintaining consistency with these marker results, SA- $\beta$ -galactosidase displayed a similar result. In both cases, from young fibroblasts to non-treated cells to 1201 treated, a bell-shaped tendency is present. 1201 was able to greatly reduce this marker, which came in line with previous results. In donor 1, almost all the gain in SA- $\beta$ -galactosidase in non-treated compared to young cells through replicative aging *in vitro*, with an increase of around 30 population doublings, was eliminated with 1201 treatment. In contrast, donor 2 seemed less affected in its SA- $\beta$ -galactosidase levels by replicative aging, demonstrating similar levels between non-treated and young cells. Nevertheless, once more, 1201 treated cells displayed better marker levels than its corresponding young fibroblasts. The same arguments arose from this observation as before, justifying the claim that in donor 2, 1201 is able to promote papillary-like phenotypes that surpass its replicative young cell state. Unexpectedly, overall percentages of positive cells were lower in this donor than donor 1. The reason for this discrepancy might be related with variability between staining procedures and therefore these results should not be used for direct interdonor comparisons. Nevertheless, they were direct results of 1201's action against senescence, while also confirming the connection between the papillary-to-reticular differentiation and cell senescence.

This multiple-assay experiment involving the papillary-to-reticular transition highlighted two main consequences of 1201 treatment. This plant extract can clearly manipulate the PRT, retarding its

usual progression and retaining the existing papillary fibroblasts. Also, signs of some degree of reversibility of the PRT are present with 1201, causing in some cases an improvement beyond the youngest representatives. While, interfering with the balance between papillary and reticular fibroblasts, 1201 also has an influence over senescence. If the assembly line towards reticular fibroblasts is slowed down, the path to senescence will suffer the same effect as both are components of the same PRT pipeline. Nevertheless, with these results 1201 has been elevated to a stature of being able to delay cellular senescence.

#### **4.1.2. Not Only Papillary, But Reticular Fibroblasts Are Targets of 1201**

Possessing a mixed fibroblast population with different growth kinetics can lead to an involuntary competitive selection. Papillary fibroblasts, with each cell passage, can gain more representation in the population, as reticular cells cannot keep up and could be eventually diluted out. Although 1201 was suspected to affect both papillary and reticular, it could not be assured since the existence of reticular cells after some cell passages couldn't be guaranteed. Therefore, donors with mixed population were exposed to a short and acute 1201 treatment. Thus, existing reticular cells still had, without doubt, a representative presence and could be observed for effects of 1201 exposure.

Both donors displayed similar morphological effects, fibroblasts from donor 2 seemed to trail its counterpart donor 1 in the amount of effect. However, donor 2 displays an intrinsically higher reticular-like behavior, inferring that donor 2 might be further ahead in the PRT differentiation pathway than donor 1. Therefore, 1201 could have had the same degree of effect, but was simply shifted due to divergent donor nature. Besides morphological monitoring, gene expression of several relevant markers was performed. These markers were determined to be able to distinguish papillary from reticular fibroblasts. Once more, already after 48 hours of 1201 treatment, signs of change in genomic expression were observable. While not every single marker responded in favor of a more papillary situation after 1201 treatment, a noticeable trend towards the presence of a papillary encouraging effect was verified. Evidence of this trend was corroborated by observing that the more statistically sound variations in marker expression pointed to an increased papillary state in 1201 treated cells.

This short-term treatment was responsible for proving that both papillary and reticular fibroblasts are influenced by 1201's ability in interfering the papillary-to-reticular transition, in favor of promoting the papillary state.

#### **4.1.3. Isolated Papillary and Reticular Fibroblasts Disperse any Doubt**

One considerable issue with these attempts at assessing PRT involvement of 1201 was the lack of knowledge over the precise distribution of papillary and reticular populations in the cell lines tested. This changed with the arrival of site-matched papillary and reticular fibroblasts. With a relatively

pure papillary and reticular population, the previous results were reassessed to explicitly validate their implications.

Reticular fibroblasts from donor A expressed, in terms of morphological characteristics, the same effects recorded before. However, with a considerably pure and replicative young papillary population, the influence of 1201 wasn't predictable as they represent the beginning of the PRT and this treatment regime could be insufficient to promote any visible *in vitro* aging. Visually, 1201 treated papillary fibroblasts managed to gain more contrast and become even more elongated and thinner than non-treated cells. Although only photographs were inspected, the cell density also seemed to increase with 1201 treatment. Even with such a solid papillary cell population to begin with, 1201 managed an enhancement of papillary morphology.

Proliferation assay made with reticular cells had similar growth curves as before. Biphasic behavior was also observed in this growth reassessment. Nevertheless, the papillary population obtained a different result. 1201 treated cells weren't able to compete with non-treated papillary cells. For the first time, non-treated cells exceeded 1201 treated cells' growth performance. Unlike the morphological changes, in terms of proliferation, 1201 might be unable to make a difference at such young replicative age and papillary state. After deciding to focus on 1201's properties on maintaining the papillary state, only reticular fibroblasts were put through the remaining assays.

Marker characterization was made with treatment of reticular cells, although papillary cells were also included as a comparison. For the papillary and reticular markers, the outcome of 1201 treatment mostly resembled previous results. A noticeable improvement was the compliance of all markers without exception to 1201 treatment. Both papillary markers were significantly increased for treated cells and reticular makers were reduced with 1201 treatment. Nevertheless, a surprising observation appeared. Young papillary fibroblasts displayed a lower amount of PDPN expression when compared to reticular fibroblasts, treated and non-treated. This contradicts quantifications of PDPN made previously, but, as stated before, markers can have peculiar and transient behaviors when their roles haven't been clearly identified. Even with fully differentiated reticular cells, 1201 can drastically improve marker levels comparable to those witnessed in young papillary cells. This gives strength to 1201's potency, as its treatment appears to be able to cover almost the whole gap between papillary and reticular fibroblasts in the PRT with just 5 cell passages.

SA- $\beta$ -galactosidase of reticular fibroblasts from donor A showed no difference in percentage of positive cells, while the values themselves were very low. This may be due to the replicative age of these cells. Although being reticular fibroblasts, thus supposedly further down the PRT, these cells were young in terms of *in vitro* aging. Therefore, the unchanging and low values of positive cells may be explained by a lack of replicative aging *in vitro*. With SA- $\beta$ -galactosidase activity being so small, it became hard to distinguish whether 1201 had an effect on the cells. Remaining senescence markers continued their consistency in displaying almost the same relation between treated and non-treated cells. However, with the presence of young papillary cells, the relative expression levels could be compared. Fitting into the logic of the PRT, more p21 exists in reticular cells compared to papillary. Even being a late senescence marker, the difference between the papillary state and the reticular is considerable, positioning reticular fibroblasts closer to the senescent state in the PRT pipeline.

Therefore, it is possible for papillary fibroblasts to possess less p21 than their reticular counterparts. SNEV expression profile bears a resemblance to any papillary marker, displaying an inverted bell-shaped distribution. The same rationale applied to the papillary markers is transposed to SNEV in relation with senescence.

These site-matched fibroblasts were important to solidify 1201 claim in delaying the PRT and senescence.

1201 was shown through three different, increasingly thorough treatment experiments to be able to refrain cells to reaching the senescence state. Intervening in the papillary-to-reticular transition was the key to achieve the delay of senescence for fibroblasts. With all these abilities confirmed, assessment of 1201 was transferred to determine its relationship with different senescence characteristics.

## 4.2. Mitigating Cellular Senescence

A significant part of senescence and its age-related consequences corresponds to the SASP. Its dangerous mixture of cytokines, chemokines and growth factors is responsible for multiple faces of age deterioration. 1201 influence over the SASP was tested with several different approaches.

### 4.2.1. Growth Factors Succumb to 1201's Sphere of Influence

An initial experiment was planned which involved HaCaT proliferation surveillance due to levels of SASP-belonging growth factors. The concept revolved around conditioned media. Studying the effects of conditioned media, direct mechanistic involvement could be assessed and indirect effects, such as aggregations between 1201 and secreted factors could be discarded. HaCaT cells are characterized as being a pre-malignant human keratinocyte cell line. Thus, the SASP's tumor-promoting ability through growth factor secretion was simulated *in vitro*.

Conditioned media derived from non-treated senescent cells from donor 1 stimulated HaCaT to grow more than unconditioned media, indicating a higher presence of secreted growth factors. A significant reduction in HaCaT growth stimulated by 1201 treated conditioned media implies an interference in the SASP pathways by 1201. Unconditioned media was only partly supplemented, to avoid the presence of intrinsic growth factors.

Conditioned media from fibroblasts of donor 2 showed a comparable trend to donor 1, but with important differences. A substantially higher growth was stimulated using both kinds of conditioned media compared to unconditioned media. Approximately three times more HaCaT cells grew from conditioned media from donor 2 than from donor 1. Consequently, the amount of growth factors secreted from senescent fibroblasts from donor 2 is much higher. This observation might help explain the reduction in HaCaT growth using 1201 treated conditioned media not being significant. If the growth factor level is very high, the corresponding HaCaT receptors might be completely saturated. Thus, while 1201 still reduces the absolute concentration of growth factors, they might still be above or close the saturation level. Therefore, the effect of 1201 might have been masked due to saturation.

More trials were made, while tuning some experiment variables, such as HaCaT culture time and conditioned media renewal. Unfortunately, no significant reduction was obtained with donor 2. Nevertheless, other external variables are suspected to have had a negative influence over the repeated experiments. The operator changed when performing the SIPS treatment for the first repetition, while HaCaT cells used for the second repetition might have still been still under thawing stress. An advantage of these repeated trials was the inclusion of the cell number determination of the treated and non-treated fibroblasts after media conditioning. There wasn't any significant change in cell number between both populations during the two repetitions. This made it possible to exclude the possibility of growth factor variations being caused by different number of cells secreting the factors, instead of 1201's influence.

1201 has been proven, through these assays, to be responsible in attenuating growth factor production of the SASP. Although conditioned media from donor 2 didn't follow the results from donor 1 completely, it seems to be a matter of tuning the experimental variables to avoid growth factor saturation to have 1201 also display a significant reduction in HaCaT proliferation.

#### **4.2.2. Restriction of Cytokine Secretion by 1201 is Uncertain**

As conditioned media based experiments have numerous advantages, another was planned to assess 1201's role relative to another group of SASP factors, cytokines. A chemotaxis assay was employed to ascertain immune cell migration modulated by conditioned media.

The initial round performed with conditioned media from donor 1 supported the idea that 1201's connection with the SASP wasn't restricted to growth factors. Filling a reservoir with conditioned media from non-treated senescent cells caused PMBCs to significantly displace themselves towards that same reservoir. With migration stimulated, 1201's effect was able to be witnessed. A recuperation of the even rounded distribution verified in the unconditioned/unconditioned channel, showed once more 1201's apparent capacity to directly influence the SASP.

Two more assays were completed to generalize the results onto biological triplicates. However, a different outcome was obtained. All the migration profiles were very similar in terms of not displaying any polarization or directionality towards any reservoir. Small variations were verified and highlighted, but there wasn't any attraction visible in general. Justifications for these inconsistent results may be related with the multi-factorial nature of the assay. The conditioned media, the isolated PBMCs and the 3D matrix can all be sources of variability. Although, nothing was reported during the assays that would account for the outcome of the chemotaxis trials, an optimization stage could be needed. Determining the most appropriate way to prepare the conditioned media, would be an important task. Not having the knowledge of cytokine concentration, the volume where cells conditioned their media could be too large, causing SASP factors to be much diluted. Consequently, with small concentrations, sensitivity to detect 1201 derived changes is lost. Without any migration in the non-treated conditioned media, 1201 can also not be assessed to confirm its initial cytokine inhibiting behavior.

Cytokine modulation by 1201 wasn't conclusive, although when migration was present, 1201 caused a suppression of the attraction visible with non-treated conditioned media. 1201 manages to

grasp the SASP to a certain extent and inhibit its activity causing an attenuation of a notorious component of cellular senescence.

#### 4.2.3 Lack of Paracrine Senescence Shrouds Possible 1201 Effect

Still concerning the SASP, the influence of 1201 over paracrine senescence was tested. As a consequence of this secreting phenotype, responsible for an adverse senescence promoting positive feedback loop, bystander senescence was confronted with 1201 treatment.

Contradicting reports concerning paracrine senescence have been put forward. The way it can be induced is under scrutiny. While, some studies state conditioned media from senescent cells is enough to induce senescence onto other healthy cells, others describe the need of cell-to-cell contact with the means of a coculture. Maintaining with the same experimental design, conditioned media from donor 1 was transferred onto proliferating fibroblasts. Visual inspection didn't demonstrate any signs of senescence, displaying complete cell confluence. However, BrdU incorporation was performed to quantify any possible senescence hidden from eyesight. A similar number of events, around 800, for each condition were passed through the cytometer, giving rise to the distribution of BrdU incorporation. This amount of events was small considering the available cell number before the fixating process. Considerable cells are suspected to have been lost in the preparation phase of the assay. The cluster associated with higher intensity and thus classified as positive for BrdU, was of similar size throughout all conditions. Paracrine senescence wasn't able to be induced through conditioned media. As a consequence, 1201 couldn't be evaluated over having an influence in bystander senescence.

This result triggered doubts over the concept of paracrine senescence and its respective experimental design. If with such a low culture time, it would have been possible to observe a considerable effect in causing senescence to neighboring cells, the senescence-inducing rate would be substantial. *In vivo* implications would be enormous as in a short period of time, once a single senescent cell had been formed, an exponential positive feedback loop would cause the whole organism to succumb to senescence. Every cell would be rapidly pushed into its senescent state, causing its adverse effects to proliferate. As this doesn't correlate with reports quantifying senescent cell population ratios, paracrine senescence's existence and triggers should be discussed and studied more deeply.

Several approaches were made to discern the relation between 1201 and the SASP. An effect from 1201 treatment can be observed, but lacked appropriate consolidation. Issues with positive controls and non-treated conditioned media, made it problematic to analyze 1201's role. Without observing the SASP, no effect over it by 1201 could be determined. Although, when non-treated conditioned media triggered a response, 1201 almost always mitigated its effect. Altogether, properties related with attenuating the SASP are suspected to be associated with 1201. If the SASP is inhibited and mechanistically disrupted to a certain degree due to 1201, it has a role in attenuating cellular senescence.

### **4.3. Eliminating Cellular Senescence**

One last angle to have been explored, was the possibility of 1201 being able to selectively eliminate senescent cells. Many compounds have been reported of having this property. Considering senescence as a whole, this ability seems to be the most preferable and attractive of them all, since it preserves the tumor-suppressive mechanism, while removing all the adverse effects sprouting from senescence.

The important aspect in this concept is selectivity. 1201 was tested to determine if it could remove senescent cells, while being harmless to the remaining cells. With fibroblasts from donor 1, 1201 was able to achieve that exact accomplishment. Fibroblasts over the 39 days of chronic treatment were seen to suffer conformational changes similar to what was observed for the PRT. Huge and spread out senescent cells were becoming ever more elongated and thinner. From a certain timepoint, these cells would then round up and suffer from cell death. Valuable SESC properties seem to be associated with 1201 treatment.

The same arrangements were made to assess the same in donor 2. One difference was the decision to include 1201's solvent as an additional condition. 1201 treatment for 39 days saw no change in both senescent and quiescent cell number. Interestingly, 1201's solvent displayed a slight non-significant increase in cell number. The assay was repeated two extra times, while trying to manipulate 1201's concentration to reach the desired balance between generally toxic and papillary promoting. Nevertheless, SESC wasn't able to be reproduced in donor 2. The third trial possessed a treatment concentration of 0.1%, which was without a doubt inside the toxic range, causing a deep reduction of cell number in quiescent cells.

Mixed observations make attributing 1201 a definitive SESC property not possible. However, donor 1 portrayed exactly such a SESC effect. What might be causing this discrepancy between donors is interdonor variability. A lot has been discussed over how diverse donor 1 and 2 are from each other. Chosen 1201 concentrations can work perfectly for one and have no effect on the other. One can hypothesize a need of optimizing 1201 amounts that would remove the doubts that remained from all assessments performed. Nonetheless, from observations made of donor 1 fibroblasts, 1201 can display a selective elimination of senescent cells.

### **4.4. Confirming Papillary and Reticular Differences**

With the availability of site-matched fibroblasts, the opportunity to reproduce and observe reported differences between these populations appeared. Solidifying the premises, which were based on to prepare the experiments, was a relevant task.

All markers used were tested on all three donors and their pure papillary and reticular fibroblasts. Papillary and reticular markers displayed great ability to clearly distinguish one populations from the other. However, PDPN as a reported papillary marker had contradicting results. Two donors, A and B, expressed more PD PN in reticular fibroblasts than in papillary. Only donor C confirmed PD PN's role as a papillary marker. This unexpected result for PD PN appears to be a manifestation of what was stated previously concerning markers. Biomarkers can have contradicting expressions in

certain conditions if its role isn't extensively studied. The reason that led PDPN to be more expressed in these reticular cells is currently not known. This peculiar effect should be looked into with more depth to assess if PDPN should be questioned as a papillary marker. Nonetheless, a considerable correlation between PDPN and the papillary state exists and so it is not probable that PDPN will be discredited in the future. Furthermore, its expression in the same donors displayed an expected behavior when determined with a different set of primers by Ghalbzouri, A. (data not shown), contradicting the previous result.

Senescence marker expression was also quantified for all site-matched donors. SNEV maintained its consistency with similar expression profile through all donors. It is the marker whose ratio between papillary and reticular fibroblasts remained the most constant, displaying low interdonor variability. p21 was mostly higher in reticular fibroblasts, inferring them to be further ahead in the senescence timeline, thus not going against the concept of PRT.

Lifespans with all three donors were initiated to verify distinct proliferative behavior from paired papillary and reticular fibroblasts. As reported, different growth characteristics seem apparent. A widening gap between each donor's site-matched populations was a consequence of different slopes in their respective growth curves, representing divergent contact inhibition. Reticular cells from donor C already display signs of growth stagnation after 60 days in culture.

These three donors, with their site-matched fibroblast subpopulations, do confirm diversity and heterogeneity in the dermal fibroblast population.

#### **4.5. 1201's Place as an Opponent of Senescence**

Tackling senescence may be achieved through multiple paths. Three main avenues in battling senescence were assessed and recognized with 1201 treatment. Delaying the arrival of the senescence phenotype, to postpone age-related deterioration was the first identified effect of 1201. Afterwards, 1201 displayed the ability of interfering directly and mechanistically with the main agent of senescence, namely the SASP. Finally, signs regarding SESC properties were noticeable through 1201 treatment. Therefore, this plant extract has shown capabilities in all three fronts. Although 1201 didn't have a certain and clear influence in all conditions and donors tested, its importance for fibroblast aging and senescence was proven.

## Bibliography

1. van Deursen, J. M. The Role of Senescent Cells in Ageing. *Nature* **509**, 439–446 (2014).
2. Childs, B. G., Durik, M., Baker, D. J. & Deursen, J. M. Van. Cellular senescence in aging and age-related disease: from mechanisms to therapy. *Nat. Med.* **21**, 1424–1435 (2015).
3. Giangreco, A., Goldie, S., Failla, V., Saintgny, G. & Watt, F. M. Human Skin Aging Is Associated with Reduced Expression of the Stem Cell Markers  $\beta$  1 Integrin and MCSP. *J. Invest. Dermatol.* **130**, 604–608 (2010).
4. Mine, S., Fortunel, N. O., Pageon, H. & Asselineau, D. Aging Alters Functionally Human Dermal Papillary Fibroblasts but Not Reticular Fibroblasts : A New View of Skin Morphogenesis and Aging. *PLoS One* **3**, 1–13 (2008).
5. Medvedev, Z. An Attempt at a Rational Classification of Theories of Ageing. *Biol. Rev.* **65**, 37–398 (1990).
6. Falandy, C., Bonnefoy, M., Freyer, G. & Gilson, E. Biology of Cancer and Aging : A Complex Association With Cellular Senescence. *J. Clin. Oncol.* **32**, 2604–2610 (2014).
7. Weismann, A. *Essays Upon Heredity And Kindred Biological Problems*. Oxford: Clarendon Press **1**, (1891).
8. Vijg, J. & Kennedy, K. The Essence of Aging. *Gerontology* **62**, 1–5 (2016).
9. Olsen, A., Vantipalli, M. C. & Lithgow, G. J. Using *Caenorhabditis elegans* as a Model for Aging and Age-Related Diseases. *Ann. N. Y. Acad. Sci.* **1067**, 120–128 (2006).
10. Longo, V. D., Mitteldorf, J. & Skulachev, V. P. Programmed and altruistic ageing. *Nature* **6**, 866–872 (2005).
11. Kirkwood, T. B. L. & Wellcome, H. Understanding the Odd Science of Aging. *Cell* **120**, 437–447 (2005).
12. Medawar, P. B. *An Unsolved Problem Of Biology.pdf*. (London:Lewis, 1952).
13. Harman, D. Aging: A Theory Based On Free Radical And Radiation Chemistry. *J. Gerontol.* **11**, 298–300 (1956).
14. Liochev, S. I. Reactive Oxygen Species And The Free Radical Theory of Aging. *Free Radic. Biol. Med.* **60**, 1–4 (2013).
15. Hekimi, S., Lapointe, J. & Wen, Y. Taking a “ Good ” Look at Free Radicals in the Aging Process. *Cell* **21**, 569–576 (2011).
16. Kirkwood, T. B. L. & Holliday, R. The Evolution of Ageing And Longevity. *Proc. R. Soc. B Biol. Sci.* **205**, 531–546 (1979).
17. Williams, G. C. Pleiotropy, Natural Selection, and the Evolution of Senescence. *Evolution (N. Y.)* **11**, 398–411 (1957).
18. Harley, C. B., Futcher, A. B. & Greider, C. W. Telomeres shorten during ageing of human fibroblasts.pdf.

- Nature* **345**, 458–460 (1990).
19. Counter, C. M. *et al.* Telomere shortening associated with chromosome instability is arrested in immortal cells which express telomerase activity. *EMBO J.* **11**, 1921–1929 (1992).
  20. López-Otín, C., Blasco, M. A., Partridge, L., Serrano, M. & Kroemer, G. The Hallmarks of Aging. *Cell* **153**, 1194–1217 (2013).
  21. Edgar, D. *et al.* Random Point Mutations with Major Effects on Protein-Coding Genes Are the Driving Force behind Premature Aging in mtDNA Mutator Mice. *Cell Metab.* **10**, 131–138 (2009).
  22. Kujoth, G. C. *et al.* Mitochondrial DNA Mutations, Oxidative Stress, and Apoptosis in Mammalian Aging. *Science (80-. ).* **309**, 481–484 (2005).
  23. Holzenberger, M. *et al.* IGF-1 receptor regulates lifespan and resistance to oxidative stress in mice. *Lett. to Nat.* **421**, 182–187 (2003).
  24. Morrow, G., Samson, M., Michaud, S. & Tanguay, R. M. Overexpression of the small mitochondrial Hsp22 extends Drosophila life span and increases resistance to oxidative stress 1. *FASEB J.* **18**, 598–599 (2004).
  25. Walker, G. A. & Lithgow, G. J. Lifespan extension in *C. elegans* by a molecular chaperone dependent upon insulin-like signals. *Aging Cell* **2**, 131–139 (2003).
  26. Rubinsztein, D. C., Mariño, G. & Kroemer, G. Autophagy and Aging. *Cell* **146**, 682–695 (2010).
  27. Tomaru, U. & Takahashi, S. Decreased Proteasomal Activity Causes Age-Related Phenotypes and Promotes the Development of Metabolic Abnormalities. *AJPA* **180**, 963–972 (2012).
  28. Garinis, G. A., Van Der Horst, G. T. J., Vijg, J. & Hoeijmakers, J. H. J. DNA damage and ageing: new-age ideas for an age-old problem. *Nat. Cell Biol.* **10**, 1241–1247 (2008).
  29. Pollex, R. L. & Hegele, R. A. Hutchinson – Gilford progeria syndrome. *Clin. Genet.* **66**, 375–381 (2004).
  30. Hardy, J. A. & Higgins, G. A. Alzheimer's Disease: The Amyloid Cascade Hypothesis. *Science* **256**, 184–185 (1992).
  31. Walker, F. O. Huntington's disease. *Lancet* **396**, 218–228 (2007).
  32. Hayflick, L. & Moorhead, P. S. The Serial Cultivation of Human Cell Strains'. *Exp. Cell Res.* **25**, 585–621 (1961).
  33. Carrel, A. On the permanent life of tissues of the organism. *J. Exp. Med.* **15**, 516–528 (1912).
  34. Sager, R. Senescence As a Mode of Tumor Suppression. *Environ. Health Perspect.* **93**, 59–62 (1991).
  35. Rodier, F. & Campisi, J. Four faces of cellular senescence. *J. Cell Biol.* **192**, 547–556 (2011).
  36. Campisi, J. Cellular senescence: when bad things happen to good cells. *Nat. Rev. Mol. Cell Biol.* **8**, 729–740 (2007).
  37. Bodnar, A. G. *et al.* Extension of Life-Span by Introduction of Telomerase into Normal Human Cells. *Science* **279**, 349–352 (1998).

38. O'Sullivan, R. J. & Karlseder, J. Telomeres: protecting chromosomes against genome instability. *Nat. Rev. Mol. Cell Biol.* **11**, 171–181 (2010).
39. Herbig, U., Jobling, W. A., Chen, B. P. C., Chen, D. J. & Sedivy, J. M. Telomere Shortening Triggers Senescence of Human Cells through a Pathway Involving ATM, p53, and p21 CIP1, but Not p16 INK4a. *Mol. Cell* **14**, 501–513 (2004).
40. di Fagagna, F. d'Adda *et al.* A DNA damage checkpoint response in telomere-initiated senescence. *Nature* **426**, 194–198 (2003).
41. Serrano, M. & Blasco, M. A. Putting the stress on senescence. *Curr. Opin. Cell Biol.* **13**, 748–753 (2001).
42. Di Leonardo, A., Linke, S. P., Clarkin, K. & Wahl, G. M. DNA damage triggers a prolonged p53-dependent G1 arrest and long-term induction of Cip1 in normal human fibroblasts. *Genes Dev.* **8**, 2540–2551 (1994).
43. Robles, S. J. & Adami, G. R. Agents that cause DNA double strand breaks lead to p16INK4a enrichment and the premature senescence of normal fibroblasts. *Oncogene* **16**, 1113–1123 (1998).
44. Campisi, J. Aging, Cellular Senescence, and Cancer. *Annu. Rev. Physiol.* **75**, 685–705 (2013).
45. Serrano, M., Lin, A. W., Mccurrach, M. E., Beach, D. & Lowe, S. W. Oncogenic ras Provokes Premature Cell Senescence Associated with Accumulation of p53 and p16INK4a. *Cell* **88**, 593–602 (1997).
46. Chen, Z. *et al.* Crucial role of p53-dependent cellular senescence in suppression of Pten-deficient tumorigenesis. *Nature* **436**, 725–730 (2005).
47. Lin, A. W. *et al.* Premature senescence involving p53 and p16 is activated in response to constitutive MEK/MAPK mitogenic signaling. *Genes Dev.* **12**, 3008–3019 (1998).
48. Campisi, J. Senescent Cells, Tumor Suppression, and Organismal Aging: Good Citizens, Bad Neighbors. *Cell* **120**, 513–522 (2005).
49. Juven-Gershon, T. & Oren, M. Mdm2 : The Ups and Downs. *Mol. Med.* **5**, 71–83 (1999).
50. Sherr, C. J. & McCormick, F. The RB and p53 pathways in cancer. *Cancer Cell* **2**, 103–112 (2002).
51. Sherr, C. J. The INK4a/ARF Network in Tumour Suppression. *Nat. Rev. Mol. Cell Biol.* **2**, 731–737 (2001).
52. Rodier, F., Campisi, J. & Bhaumik, D. Two faces of p53: aging and tumor suppression. *Nucleic Acids Res.* **35**, 7475–7484 (2007).
53. Xiong, Y., Hannon, G. J., Zhang, H., Casso, D. & Kobayashi, R. p21 is a universal inhibitor of cyclin kinases. *Nature* **366**, 701–704 (1993).
54. Campisi, J. Cellular senescence as a tumor-suppressor mechanism. *Trends Cell Biol.* **11**, 27–31 (2001).
55. Narita, M. *et al.* Rb-Mediated Heterochromatin Formation and Silencing of E2F Target Genes during Cellular Senescence State University of New York at Stony Brook. *Cell* **113**, 703–716 (2003).
56. Beauséjour, C. M. *et al.* Reversal of human cellular senescence : roles of the p53 and p16 pathways. *EMBO J.* **22**, 4212–4222 (2003).

57. Olsen, C. L., Gardie, B., Yaswen, P. & Stampfer, M. R. Raf-1-induced growth arrest in human mammary epithelial cells is p16-independent and is overcome in immortal cells during conversion p16-independent and is overcome in immortal cells during conversion. *Oncogene* **21**, 6328–6339 (2002).
58. Hayflick, L. The Limited In Vitro Lifetime Of Human Diploid Cell Strains. *Exp. Cell Res.* **37**, 614–636 (1965).
59. Cho, K. A. *et al.* Morphological Adjustment of Senescent Cells by Modulating Caveolin-1 Status. *J. Biol. Chem.* **279**, 42270–42278 (2004).
60. Childs, B. G., Baker, D. J., Kirkland, J. L., Campisi, J. & Deursen, J. M. Van. Senescence and apoptosis: dueling or complementary cell fates? *EMBO Rep.* **15**, 1139–1153 (2014).
61. Seluanov, A. *et al.* Change of the Death Pathway in Senescent Human Fibroblasts in Response to DNA Damage Is Caused by an Inability To Stabilize p53. *Mol. Cell. Biol.* **21**, 1552–1564 (2001).
62. Sanders, Y. Y. *et al.* Histone Modifications in Senescence-Associated Resistance to Apoptosis by Oxidative Stress. *Redox Biol.* **1**, 8–16 (2013).
63. Wang, E. Senescent Human Fibroblasts Resist Programmed Cell Death, and Failure to Suppress bcl2 Is Involved1. *Cancer Res.* **55**, 2284–2292 (1995).
64. Dimri, G. P. *et al.* A biomarker that identifies senescent human cells in culture and in aging skin in vivo. *Proc. Natl. Acad. Sci. U. S. A.* **92**, 9363–9367 (1995).
65. Itahana, K., Campisi, J. & Dimri, G. P. Methods to detect biomarkers of cellular senescence : the galactosidase assay. *Methods Mol. Biol.* **371**, 21–31 (2007).
66. Lee, B. Y. *et al.* Senescence-associated β-galactosidase is lysosomal β-galactosidase. *Aging Cell* **5**, 187–195 (2006).
67. Kopp, H., Hooper, A. T., Shmelkov, S. V & Rafii, S. β-Galactosidase staining on bone marrow . The osteoclast pitfall. *Histol. Histopathol.* **22**, 971–976 (2007).
68. Sharpless, N. E. & Sherr, C. J. Forging a signature of in vivo senescence. *Nat. Rev. Cancer* **15**, 397–408 (2015).
69. Mason, D. X., Jackson, T. J. & Lin, A. W. Molecular signature of oncogenic ras-induced senescence. *Oncogene* **23**, 9238–9246 (2004).
70. Kyung, I. *et al.* Exploration of replicative senescence-associated genes in human dermal fibroblasts by cDNA microarray technology. *Exp. Gerontol.* **39**, 1369–1378 (2004).
71. Coppé, J.-P. *et al.* Senescence-Associated Secretory Phenotypes Reveal Cell-Nonautonomous Functions of Oncogenic RAS and the p53 Tumor Suppressor. *PLoS Biol.* **6**, 2854–2868 (2008).
72. Kuilman, T. & Peepre, D. S. Senescence-messaging secretome: SMS-ing cellular stress. *Nat. Rev. Cancer* **9**, 81–94 (2009).
73. Coppé, J.-P., Desprez, P.-Y., Krtolica, A. & Campisi, J. The Senescence-Associated Secretory Phenotype: The Dark Side of Tumor Suppression. *Annu. Rev. Pathol.* **5**, 99–118 (2010).
74. Dávalos, A. R., Coppe, J., Campisi, J. & Desprez, P. Senescent cells as a source of inflammatory factors

- for tumor progression. *Cancer Metastasis Rev.* **29**, 273–283 (2010).
75. Kumar, S., Millis, A. J. T. & Baglioni, C. Expression of interleukin 1-inducible genes and production of interleukin 1 by aging human fibroblasts. *Proc. Natl. Acad. Sci. U. S. A.* **89**, 4683–4687 (1992).
76. Gabay, C., Lamacchia, C. & Palmer, G. IL-1 Pathways In Inflammation and Human Diseases. *Nat. Rev. Rheumatol.* **6**, 232–241 (2010).
77. Niu, J., Li, Z., Peng, B. & Chiao, P. J. Identification of an Autoregulatory Feedback Pathway Involving Interleukin-1 $\alpha$  in Induction of Constitutive NF- $\kappa$ B Activation in Pancreatic Cancer Cells. *J. Biol. Chem.* **279**, 16452–16462 (2004).
78. Orjalo, A. V., Bhaumik, D., Gengler, B. K., Scott, G. K. & Campisi, J. Cell surface-bound IL-1 is an upstream regulator of the senescence-associated IL-6/IL-8 cytokine network. *Proc. Natl. Acad. Sci.* **106**, 17031–17036 (2009).
79. Werb, Z. ECM and Cell Surface Proteolysis: Regulating Cellular Ecology. *Cell* **91**, 439–442 (1997).
80. West, M. D., Shay, J. W., Wright, W. E. & Linskens, M. H. K. Altered Expression of Plasminogen Activator and Plasminogen Activator Inhibitor During Cellular Senescence. *Exp. Gerontol.* **31**, 175–193 (1996).
81. Pankov, R. & Yamada, K. M. Fibronectin at a glance. *J. Cell Sci.* **115**, 3861–3863 (2002).
82. Kumazaki, T., Kobayashi, M. & Mitsui, Y. Enhanced Expression of Fibronectin During In Vivo Cellular Aging of Human Vascular Endothelial Cells and Skin Fibroblasts.pdf. *Exp. Cell Res.* **205**, 396–402 (1993).
83. Chien, Y. et al. Control of the senescence-associated secretory phenotype by NF-  $\kappa$ B promotes senescence and enhances chemosensitivity. *Genes Dev.* **25**, 2125–2136 (2011).
84. Kang, T. et al. Senescence surveillance of pre-malignant hepatocytes limits liver cancer development. *Nature* **479**, 547–551 (2011).
85. Krizhanovsky, V. et al. Senescence of Activated Stellate Cells Limits Liver Fibrosis. *Cell* **134**, 657–667 (2008).
86. McElhaney, J. E. & Effros, R. B. Immunosenescence: what does it mean to health outcomes in older adults? *Curr. Opin. Immunol.* **21**, 418–424 (2009).
87. Guo, S. & DiPietro, L. A. Factors Affecting Wound Healing. *J. Dent. Res.* **89**, 219–229 (2010).
88. Jun, J. & Lau, L. F. The matricellular protein CCN1 induces fibroblast senescence and restricts fibrosis in cutaneous wound healing. *Nat. Cell Biol.* **12**, 676–685 (2010).
89. Demaria, M. et al. An Essential Role for Senescent Cells in Optimal Wound Healing through Secretion of PDGF-AA. *Dev. Cell* **31**, 722–733 (2014).
90. Nelson, G. et al. A senescent cell bystander effect: senescence-induced senescence. *Aging Cell* **11**, 345–349 (2012).
91. Acosta, J. C. et al. A complex secretory program orchestrated by the inflammasome controls paracrine senescence. *Nat. Cell Biol.* **15**, 978–990 (2013).

92. Loukinova, E. *et al.* Growth regulated oncogene-alpha expression by murine squamous cell carcinoma promotes tumor growth , metastasis , leukocyte infiltration and angiogenesis by a host CXC Growth Regulated Oncogene- a expression by murine squamous cell carcinoma promotes tumo. *Oncogene* **19**, 3477–3486 (2000).
93. Krtolica, A., Parrinello, S., Lockett, S., Desprez, P. & Campisi, J. Senescent fibroblasts promote epithelial cell growth and tumorigenesis: A link between cancer and aging. *Proc. Natl. Acad. Sci.* **98**, 12072–12077 (2001).
94. Liu, D. & Hornsby, P. J. Senescent Human Fibroblasts Increase the Early Growth of Xenograft Tumors via Matrix Metalloproteinase Secretion. *Cancer Res.* **67**, 3117–3126 (2007).
95. Schneider, E. L. & Mitsui, Y. The relationship between in vitro cellular aging and in vivo human age. *Proc. Natl. Acad. Sci. U. S. A.* **73**, 3584–3588 (1976).
96. Bierman, E. L. The Effect of Donor Age on the in Vitro Life Span of Cultured Human Arterial Smooth-Muscle Cells. *In Vitro* **14**, 951–955 (1978).
97. Cristofalo, V. J., Allen, R. G., Pignolo, R. J., Martin, B. G. & Beck, J. C. Relationship between donor age and the replicative lifespan of human cells in culture: A reevaluation. *Proc. Natl. Acad. Sci. U. S. A.* **95**, 10614–10619 (1998).
98. Krishnamurthy, J. *et al.* Ink4a/Arf expression is a biomarker of aging. *J. Clin. Invest.* **114**, 1299–1307 (2004).
99. Jeyapalan, J. C., Ferreira, M., Sedivy, J. M. & Herbig, U. Accumulation of senescent cells in mitotic tissue of aging primates. *Mech. Ageing Dev.* **128**, 36–44 (2007).
100. Wang, C. *et al.* DNA damage response and cellular senescence in tissues of aging mice. *Aging Cell* **8**, 311–323 (2009).
101. Franceschi, C., Bonafè, M., Valensin, S. & Benedictis, G. D. E. Inflamm-aging. An Evolutionary Perspective on Immunosenescence. *Ann. N. Y. Acad. Sci.* **908**, 244–254 (2000).
102. Freund, A., Orjalo, A. V., Desprez, P.-Y. & Campisi, J. Inflammatory Networks During Cellular Senescence: Causes and Consequences. *Trends Mol. Med.* **16**, 238–246 (2010).
103. Maggio, M., Guralnik, J. M., Longo, D. L. & Ferrucci, L. Interleukin-6 in Aging and Chronic Disease: A Magnificent Pathway. *J. Gerontol. Med. Sci.* **61**, 575–584 (2006).
104. Franceschi, C. *et al.* Inflammaging and anti-inflammaging: A systemic perspective on aging and longevity emerged from studies in humans. *Mech. Ageing Dev.* **128**, 92–105 (2007).
105. Vasto, S. *et al.* Inflammatory networks in ageing, age-related diseases and longevity. *Mech. Ageing Dev.* **128**, 83–91 (2007).
106. Franceschi, C. & Campisi, J. Chronic Inflammation (Inflammaging) and Its Potential Contribution to Age-Associated Diseases. *Journals Gerontol. Biol. Sci.* **69**, 4–9 (2014).
107. Baker, D. J. *et al.* Opposing roles for p16Ink4a and p19Arf in senescence and ageing caused by BubR1 insufficiency. *Nat. Cell Biol.* **10**, 825–836 (2008).
108. Pajvani, U. B. *et al.* Fat apoptosis through targeted activation of caspase 8: a new mouse model of

- inducible and reversible lipoatrophy. *Nat. Med.* **11**, 797–803 (2005).
109. Baker, D. J. *et al.* Clearance of p16INK4a-positive senescent cells delays ageing-associated disorders. *Nature* **479**, 232–236 (2011).
110. Baker, D. J. *et al.* Naturally occurring p16INK4a-positive cells shorten healthy lifespan. *Nature* **530**, 184–189 (2016).
111. Naylor, R. M., Baker, D. J. & van Deursen, J. M. Senescent Cells: A Novel Therapeutic Target for Aging and Age-Related Diseases. *Clin. Pharmacol. Ther.* **93**, 105–116 (2013).
112. Ginn, S. L., Alexander, I. E., Edelstein, M. L., Abedi, M. R. & Wixon, J. Gene therapy clinical trials worldwide to 2012 – an update. *J. Gene Med.* **15**, 65–77 (2013).
113. Wang, C. *et al.* Adult-onset, short-term dietary restriction reduces cell senescence in mice. *Aging* **2**, 555–566 (2010).
114. Wang, A. M., Ma, C., Xie, Z. H. & Shen, F. Use of Carnosine as a Natural Anti-senescence Drug for Human Beings. *Biochemistry* **65**, 869–871 (2000).
115. Laberge, R. *et al.* Glucocorticoids Suppress Selected Components of the Senescence-Associated Secretory Phenotype. *Aging Cell* **11**, 569–578 (2012).
116. Tomimatsu, K. & Narita, M. Translating the effects of mTOR on secretory senescence. *Nat. Cell Biol.* **17**, 1230–1232 (2015).
117. Laberge, R.-M. *et al.* MTOR regulates the pro-tumorigenic senescence-associated secretory phenotype by promoting IL1A translation. *Nat. Cell Biol.* **17**, 1049–1061 (2015).
118. Walters, H. E., Hannemann, S. D. & Cox, L. S. Reversal of phenotypes of cellular senescence by pan-mTOR inhibition. *Aging* **8**, 231–243 (2016).
119. Liu, W. & Sharpless, N. E. Senescence-escape in melanoma. *Pigment Cell Melanoma Res.* **25**, 408–409 (2012).
120. Zhu, Y. *et al.* Identification of a novel senolytic agent, navitoclax, targeting the Bcl-2 family of anti-apoptotic factors. *Aging Cell* **15**, 428–435 (2016).
121. Zhu, Y. *et al.* The Achilles' heel of senescent cells: from transcriptome to senolytic drugs. *Aging Cell* **14**, 644–658 (2015).
122. Rook, A. *Rook's Textbook of Dermatology*. **1**, (Blackwell Publishing Ltd., 2010).
123. Ross, M. H. & Pawlina, W. *Histology: A Text and Atlas*. (Lippincott Williams & Wilkins, 2011).
124. Schafer, I. A., Pandy, M., Ferguson, R. & Davis, B. R. Comparative Observation of Fibroblasts Derived From the Papillary and Reticular Dermis of Infants and Adults: Growth Kinetics, Packing Density at Confluence and Surface Morphology. *Mech. Ageing Dev.* **31**, 275–293 (1985).
125. Harper, R. A. & Grove, G. Human Skin Fibroblasts Derived from Papillary and Reticular Dermis: Differences in Growth Potential in vitro. *Science* **204**, 526–527 (1979).
126. Sorrell, J. M., Baber, M. A. & Caplan, A. I. Site-Matched Papillary and Reticular Human Dermal Fibroblasts Differ in Their Release of Specific Growth Factors/Cytokines and in Their Interaction With

- Keratinocytes. *J. Cell. Physiol.* **200**, 134–145 (2004).
127. Schönherr, E., Beavan, L. A., Hausser, H., Kresse, H. & Culp, L. A. Differences in decorin expression by papillary and reticular fibroblasts in vivo and in vitro. *Biochem. J.* **290**, 893–899 (1993).
128. Janson, D. G., Saintigny, G., Adrichem, A. Van, Mahé, C. & Ghalbzouri, A. El. Different Gene Expression Patterns in Human Papillary and Reticular Fibroblasts. *J. Invest. Dermatol.* **132**, 2565–2572 (2012).
129. Lavker, R. M., Zheng, P. & Dong, G. Aged Skin: A Study by Light, Transmission Electron, and Scanning Electron Microscopy. *J. Invest. Dermatol.* **88**, 44–51 (1987).
130. Fenske, N. A. & Lober, C. W. Structural and Functional Changes of Normal Aging Skin. *J. Am. Acad. Dermatol.* **15**, 571–585 (1986).
131. Oh, J.-H. *et al.* Intrinsic aging- and photoaging-dependent level changes of glycosaminoglycans and their correlation with water content in human skin. *J. Dermatol. Sci.* **62**, 192–201 (2011).
132. Quan, T., He, T., Kang, S., Voorhees, J. J. & Fisher, G. J. Solar Ultraviolet Irradiation Reduces Collagen in Photoaged Human Skin by Blocking Transforming Growth Factor- $\beta$  Type II Receptor/Smad Signaling. *Am. J. Pathol.* **165**, 741–751 (2004).
133. Langton, A. K., Sherratt, M. J., Griffiths, C. E. M. & Watson, R. E. B. A new wrinkle on old skin: the role of elastic fibres in skin ageing. *Int. J. Cosmet. Sci.* **32**, 330–339 (2010).
134. Demaria, M., Desprez, P. Y., Campisi, J. & Velarde, M. C. Cell Autonomous and Non-Autonomous Effects of Senescent Cells in the Skin. *J. Invest. Dermatol.* **135**, 1722–1726 (2015).
135. Herbig, U., Ferreira, M., Condel, L., Carey, D. & Sedivy, J. M. Cellular Senescence in Aging Primates. *Science* **311**, 1257 (2006).
136. Janson, D., Mahe, C. & Ghalbzouri, A. El. Papillary fibroblasts differentiate into reticular fibroblasts after prolonged in vitro culture. *Exp. Dermatol.* **22**, 48–53 (2013).
137. Janson, D., Rietveld, M., Willemze, R. & Ghalbzouri, A. El. Effects of serially passaged fibroblasts on dermal and epidermal morphogenesis in human skin equivalents. *Biogerontology* **14**, 131–140 (2013).
138. Dellago, H. *et al.* ATM-dependent phosphorylation of SNEVhPrp19/hPso4 is involved in extending cellular life span and suppression of apoptosis. *Aging* **4**, (2012).
139. Monteforte, R. *et al.* SNEV Prp19/PSO4 deficiency increases PUVA-induced senescence in mouse skin. *Exp. Dermatol.* **25**, 212–217 (2016).
140. Serafini, T. *et al.* Netrin-1 Is Required for Commissural Axon Guidance in the Developing Vertebrate Nervous System. *Cell* **87**, 1001–1014 (1996).
141. Winkler, C. *et al.* The selective inhibition of protein phosphatase-1 results in mitotic catastrophe and impaired tumor growth. *J. Cell Sci.* **128**, 4526–4537 (2015).
142. Rehman, A. A., Ahsan, H. & Khan, F. H. Alpha-2-Macroglobulin: A Physiological Guardian. *J. Cell. Physiol.* **228**, 1665–1675 (2012).

## Appendix I

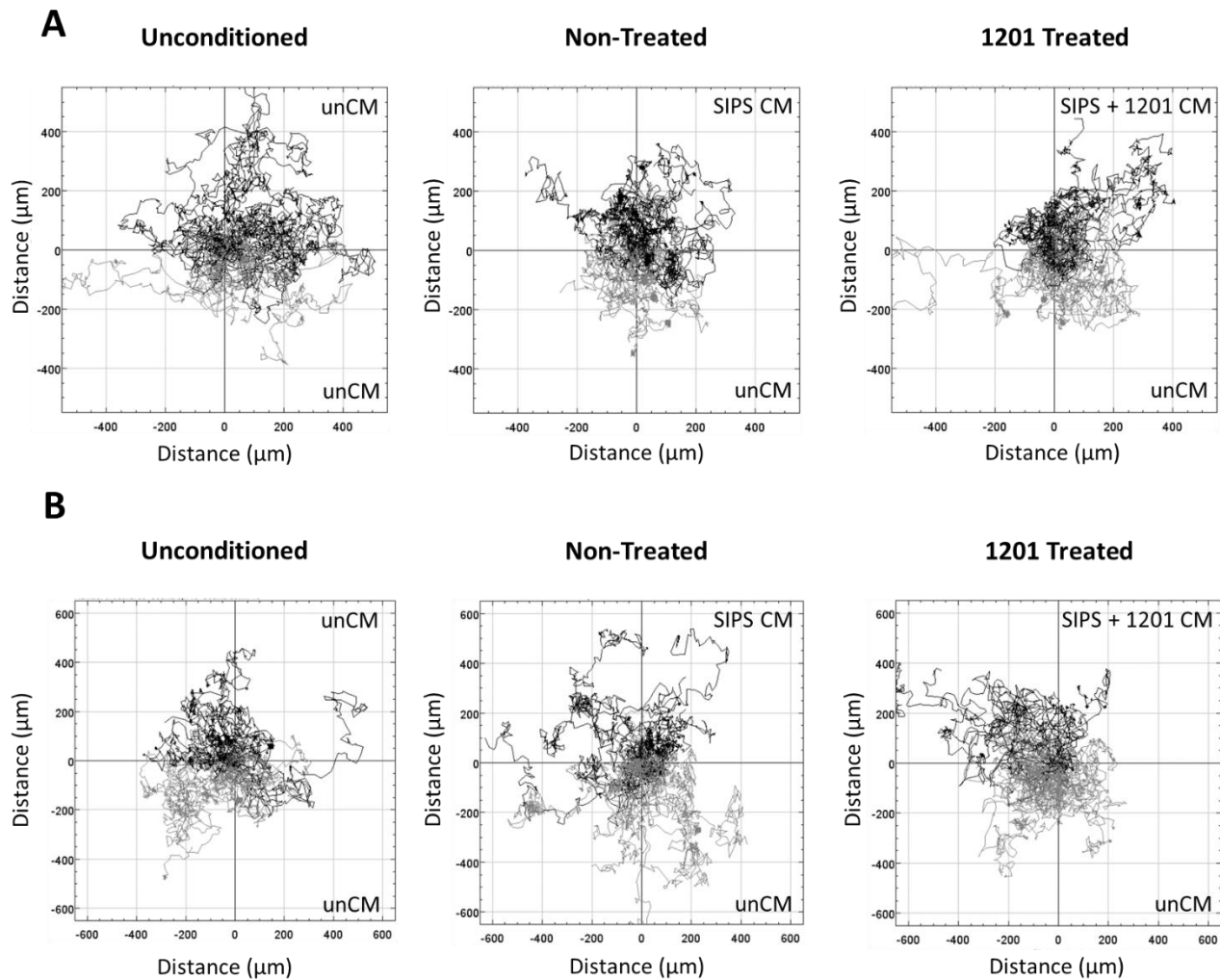


**Fig. 29** – Additional migration profiles from two other biological replicates. (unCM) – Unconditioned Media (SIPS CM) – Conditioned media from non-treated senescent cells. (SIPS+1201 CM) – Conditioned media from 1201 treated senescent cells.

## Appendix II

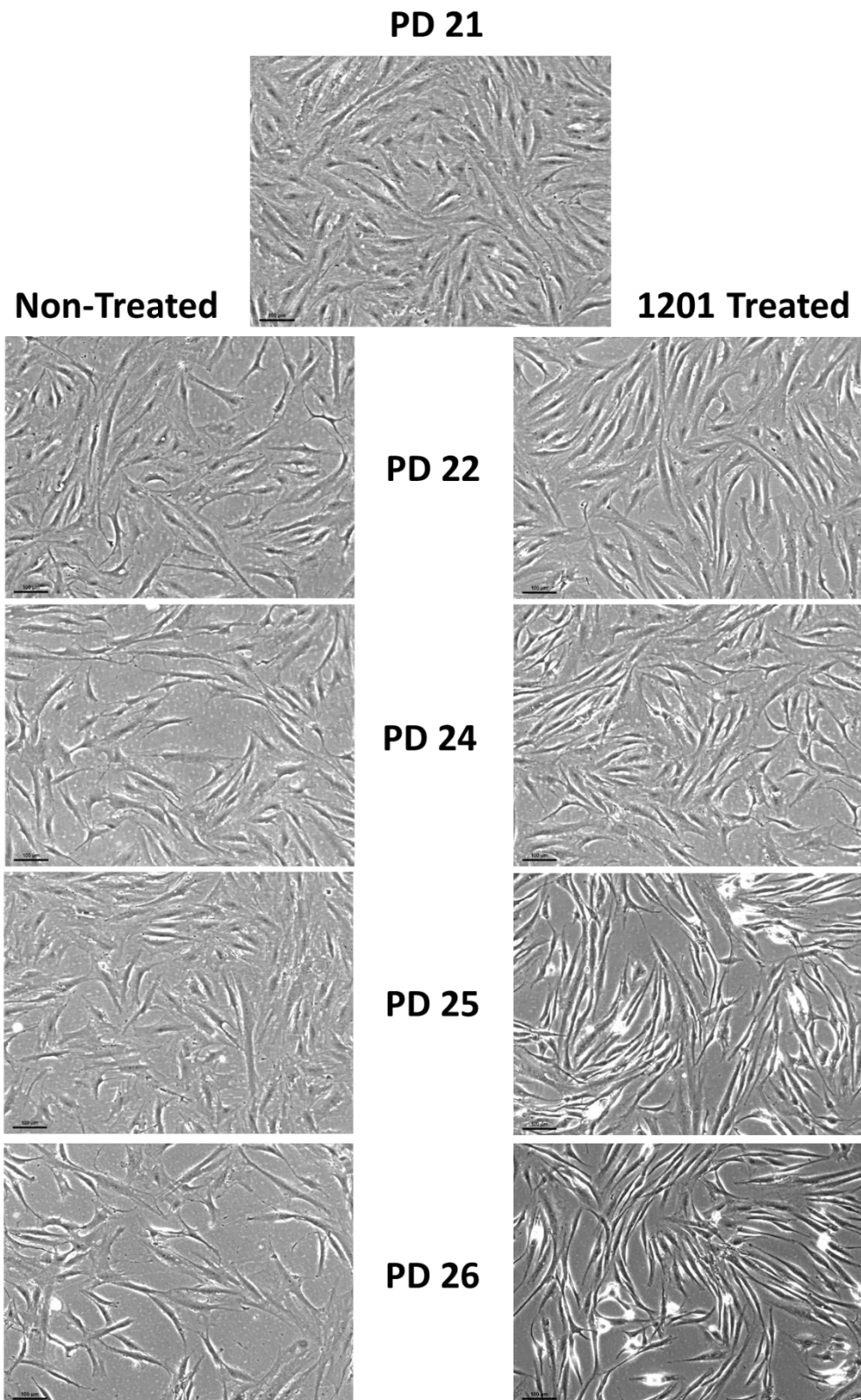


**Fig. 30 –** Gradual depicting of the morphological effect of 1201 on cells from donor 2 over 5 passages. Scale bar = 100  $\mu$ m.